2013-05-23

Real-Time Queue Length Estimation Using Probe Vehicles with Cumulative Input-Output Technique

Islam, Md Kamrul

UNIVERSITY OF CALGARY

Real-Time Queue Length Estimation Using Probe Vehicles with Cumulative Input-Output Technique

by

Md. Kamrul Islam

A THESIS

SUBMITTED TO THE FACULTY OF GRADUATE STUDIES

IN PARTIAL FULFILMENT OF THE REQUIREMENTS FOR THE

DEGREE OF MASTER OF SCIENCE

DEPARTMENT OF CIVIL ENGINEERING

CALGARY, ALBERTA

MAY, 2013

Abstract

Real-time vehicular queue length is an important parameter describing the temporal and spatial state of a traffic stream. A queue is the direct outcome of bottlenecks or roadway congestion, which causes longer travel times and delays and adversely impacts roadway performance. Therefore, in this thesis, two congestion scenarios, namely two roadway bottleneck cases (bottleneck over a roadway lane due to a merging lane/ramp and bottleneck due to a lane closure induced by an incident) and two signalized intersection cases (undersaturated and oversaturated) have been investigated to estimate the back of queue. The proposed methodology for real-time queue estimation is based on a GPS-based probe-vehicle trajectory data analysis obtained from a Paramics simulation environment applied in combination with an input-output technique. An extension of the queue estimation method of Lawson, Lovell and Daganzo (1996), based on a more realistic fundamental diagram of traffic flow, has also been proposed for bottleneck situations. Although the proposed methodologies maintain some strict assumptions, it has been found that the probe-based proposed methodology with a probe market share of around 30 percent is enough to outperform the theoretical Lawson et al. queue estimation model for all the case studies. Last, but not the least, this thesis should be considered as the first known contribution that focuses on the input-output technique and probe-vehicle information in the estimation of a real-time vehicular queue.

Acknowledgements

Completing my MSc degree has truly been a hard work, and I would not have been able to complete this journey without the aid and support of countless people over the past two and half years. I must first express my sincere gratitude toward my supervisor, **Dr. Lina Kattan**, and co-supervisor, **Dr. Babak Mehran**, for their relentless support and invaluable guidance toward the successful completion of my master's thesis. Collaborating with them has, indeed, been a nice experience with valuable lessons.

I also appreciate the financial assistance provided by **NSERC** and **GEOIDE,** without which my research could have not been undertaken.

I acknowledge the valuable suggestions, thoughtful ideas and encouragements from many of my fellow lab mates, which indeed helped me to reach my desired goal with enormous success.

Last, but not the least, I thank my dear wife, **Tazrina Alrazi**, and my parents, brothers and sisters for continuously boosting my confidence and supporting me during my hardships. I would also like to express my thanks to all those people who have provided me with encouragement and mental support to finish my thesis in due time.

Dedication

To My Beloved Parents

Table of Contents

List of Tables

List of Figures and Illustrations

List of Symbols and Abbreviations

Symbol	Definition
HCM	Highway Capacity Manual
MOE	Measures of Effectiveness
BOQ	Back of Queue
LOS	Level of Service
FIFO	First in First Out
VTL	Virtual Trip Line
ITS	Intelligent Transportation System
TTI	Texas Transportation Institute
FHWA	Federal Highway Administration
D(t)	Cumulative Departure Curve
A(t)	Cumulative Arrival Curve
V(t)	Cumulative Virtual Arrival Curve
B(t)	Cumulative Back of Queue Curve
μ	Service Flow Volume per hour per lane
GPS	Global Positioning System
GLONASS	Global Navigation Satellite System
I/O	Input-Output
v/c	Volume by capacity ratio

Chapter One: Introduction

1.1 Background

The management and control of urban transportation networks with intelligent transportation systems (ITSs) require reliable information on current traffic states, such as traffic volume, vehicular speed and lengths of the queues on freeways, ramps and signalized intersection approaches. Vehicular queues are natural occurrences of traffic accumulation along a roadway suffering from congestion and/or bottlenecks. In general, queues are created when traffic demand exceeds the road capacity.

The generic term bottleneck refers to any kind of interruption of regular flow of traffic that may be induced over freeway sections due to several factors, such as incidents, lane closures, merger of secondary lanes, weaving and slow moving vehicles. In an arterial network, the presence of traffic signals also causes traffic to be interrupted regularly, creating a queue on the approach facing a red traffic light. Under extreme conditions, delays due to queues can account for 90 percent or more of a motorist's total trip travel time (Mannering et al. 2007).

Information on real-time queue length is vital for several ITS applications, such as advanced traveller information, incidence management, adaptive signal control, adaptive ramp metering, variable speed limit and other advanced freeway control systems. For instance, accurate estimates of real-time queue lengths enable optimal control through the efficient allocation of the available capacity (i.e. green time), such that a defined performance metric can be optimized (e.g. minimize total delays or maximum queue lengths) (Comert et al., 2009).

The introduction of real-time traffic information into a transportation network makes it necessary to consider traffic flow and the development of queues as a dynamic process. In addition, real-time queue length can identify the exact time and location of queue spillback, which affects the performance of upstream intersections. Therefore, real-time estimation of queue length has attracted attention of many researchers.

Various queue-length estimation algorithms have been developed, with most of the approaches relying on intensive coverage of traffic detectors. Today's cellular phone tracking provides the most promising vehicle-probe methods for the production of reliable travel-time information (Cayford, Colson & Guthrie, 2008). The ubiquitous and location-enabled nature of mobile phones signifies that mobile phones have moved from pure communication tools to probe traffic sensors. Moreover, a high percentage of new vehicles are equipped with built-in GPS (Global Positioning System) units, adding to the existing probe vehicles equipped with mobile sensors and commercial GPS devices.

In addition to vehicular probes, most commercial fleets, such as taxis, carriers, busses and trucks, are tracked with GPS devices for commercial fleet management purposes. Even more probe data are expected to be present in the near future with the connected vehicle initiative moving into deployment. This research investigated the use of trajectory analysis from probe-vehicle data to get better estimates of queue lengths in real time.

1.2 Motivation for the Study

According to the Highway Capacity Manual (HCM, 2010), a queue is a line of vehicles waiting to be served by the system, where the flow rate from the front of the queue determines the

average speed within the queue. Slow-moving vehicles joining the rear of the queue are usually considered part of the queue. A faster moving line of vehicles is often referred to as a moving queue. HCM also defines the back of queue (BOQ) as the distance between the stop line of a signalized intersection and the farthest reach of an upstream queue, expressed as a number of vehicles. The vehicles previously stopped at the front of the queue are counted, even if they begin moving.

From the aforementioned definitions of queue, it is quite obvious that queue estimation must be undertaken dynamically with microscopic vehicle information in consideration. Loop detectors are one of the traditional ways of detecting vehicles. Several techniques have been developed to estimate queue length based on detector counts. However, these detectors are mainly capable of capturing point data; therefore, detector-based approaches alone are unable to accurately estimate the location, time and speed data of vehicles needed for queue estimation. Detectors at the stop line and at a point downstream of the intersection can only estimate the storage of vehicles inside the two detector points; and, if the upstream (advance) detector is not far enough from the stop line, the detector assembly fails to estimate the number of vehicles inside the link, let alone the vehicle queue.

The use of probe-vehicle data can, therefore, play an important role in better estimation of queue lengths; this is mainly due to the inherent characteristics of probe data being used to track microscopic trajectories. Most of the recent research studies on real-time queue-length estimation have been based on complicated and cumbersome models, which in most cases require data-hefty shockwave analysis to detect and estimate queues. A simple input-output technique of

queue estimation has also been used, although this technique is heavily dependent upon stationary point detector data and strict theoretical assumptions.

More sophisticated dynamic data, such as GPS-based probe trajectory data acquisition, in combination with necessary analyses are necessary to establish queuing criteria that can be eventually used to estimate the BOQ in real time using an input-output method. Since probe trajectory data reflect the speed profile of the probe vehicle, it can be used for queue estimation. If probe trajectory data are used in conjunction with an input-output technique, the estimation process is expected to yield better results. Moreover, as vehicle dynamics, such as acceleration and deceleration, can also be extracted from probe-vehicle data, slow-moving vehicles that join the upstream of a bottleneck can also be considered in the BOQ.

The above arguments motivated this research to be done in separate scenarios of queue accumulation with a simple, yet robust estimation framework fuelled by technologically advanced second-by-second (real-time) probe data and the use of an input-output technique.

1.3 Research Goals and Contributions

Based on the motivation of the research mentioned in the previous section, the ultimate goals of queue estimation are quite straightforward:

- Examination of how probe-vehicle trajectory data can be used to develop a BOQ estimation procedure,
- Investigation of the percentage of probe vehicles needed, and

- Estimation of the spatial and temporal evolution of the traffic queue length in the real-time upstream of a bottleneck and traffic signal.

The thesis makes the following contributions in the field of traffic engineering and ITS:

- Combination of real-time probe-vehicle data with an input-output technique to estimate the real-time BOQ,
- Estimation of queue overflows or spillbacks and cumulative arrivals without the need of upstream detectors,
- Extension of the theoretical model by Lawson et al. model through the incorporation of a more realistic fundamental diagram of traffic flow,
- Application of the approach developed in this thesis to several roadway case studies where queues develop, such as bottlenecks over a lane due to a merging lane/ramp, bottlenecks due to freeway lane closure, undersaturated and oversaturated signalized intersections and other roadway case studies where queue estimation is needed.
- Conducting of a sensitivity analysis to examine the performance of the proposed approach at different percentages of penetration rate for probe-vehicle data.

1.4 Organization of Thesis

The rest of this thesis has been put together in four main chapters, with several sections and subsections in each chapter. Necessary tables and figures are included.

Chapter 2 is a review of the literature related to the thesis topic. It has been a long time since the queue estimation topic has been a matter of great interest among researchers. However, due to

the topic's universal nature, various other disciplines of engineering, such as computer, geomatics and electrical engineering have focussed on various aspects of queue estimation, detection and prediction. Moreover, a detailed review has been undertaken of the Lawson et al. (1996) technique, since the method has been used as a benchmark for comparison of the proposed technique in Chapter 4.

Chapter 3 proposes methods of BOQ estimation for two main scenarios: 1) a bottleneck scenario, and 2) an isolated signalized intersection scenario with separate treatment for undersaturated and oversaturated conditions. The proposed methods depend on probe trajectory data and downstream stop line detector data, in combination with an input-output technique to estimate BOQs. An extended method of the Lawson et al. model is also proposed for queue estimation in bottleneck situations.

Chapter 4 describes the design of the simulation model and the acquisition of simulation data to be analyzed. Designing simulation model refers to the design of a simulation network, assignment of passenger car volumes, signal timing parameters, headway, driver behaviour in simulation environment, etc. To examine separate case studies, simulation runs with ten different random seeds were conducted to gather the necessary data for analysis. In this chapter, simulation data is also analyzed for different case studies, such as bottlenecks due to a lane merging and lane closures due to an accident for 15 minutes, and undersaturated and oversaturated signalized intersection scenarios. A relevant sensitivity analysis was also performed to determine the accuracy of the different estimation methods (i.e. proposed method,

Lawson et al. method, and methods extended from the Lawson et al. technique) with respect to different probe percentages.

Finally, Chapter 5 summarizes the entire research, and the main research contributions are identified. Further research based on this thesis is also suggested with proper direction and recommendations.

Chapter Two: Literature Review

2.1 Introduction

Vehicle queue length has long been considered as one of the performance measures of a signalized intersection for arterial road sections and as well as for freeways segments (Cheng, Qin, Ran and Anderson, 2011). If information on queue lengths can be acquired, a number of other performance measures can be estimated, such as freeway bottleneck delays, intersection delays, and level of service (Webster & Cobbe, 1966; Cronje, 1983a and 1983b; Balke et al., 2005). Information on vehicle queue can also be used for signal optimization (Webster, 1958; Gazis, 1964; Newell, 1965; Michalopoulos & Stephanopolos, 1977, 1981; Chang & Lin, 2000; Zou, N. 2007. To undertake a responsive process, signal control at each intersection requires the traffic demand on all approaches to respond accordingly.

Other intelligent transportation system (ITS) applications, such as freeway control including adaptive variable speed limit and adaptive ramp metering, require reliable online traffic data on the prevailing traffic conditions in order to formulate online control decisions. With adaptive ramp metering strategies, information on the dynamic evolution of the queue of vehicles waiting at the ramp is also important. This real-time information is needed to avoid queue spillback to upstream intersections and to provide good signal coordination along the corridor.

Queue length estimation can also be used to measure the overall performance of an arterial system. The average information on delays and vehicle speed can also be computed from information on the lengths and durations of queues on these signalized approaches. In addition,

real-time queue length is necessary to determine the advanced traffic control algorithms' performances and several level-of-service-based roadway measures (Yi, Xin & Zhao, 2001).

For the last 50 years or more, researchers from all over the world has been carrying out research investigations to get more accurate estimations of queue dynamics (i.e. the real-time formation and dissipation of queues) on different roadways, especially at signalized intersections and on ramps and freeway segments (Worthington 2009). Broadly, two types of queue estimation models have been developed for queue estimation algorithms, as mentioned by several researchers (e.g. Liu et al., 2009; Cheng et al., 2011). The two main techniques are as follows:

1. Input – Output Method
2. Shockwave based method

Several other queue estimation techniques have also been developed over the past few years. They are distinguished by their unique direction of queue estimation. These methodologies are listed below:

1. Kalman filtering,
2. Neural network methods for queue prediction,
3. Markov chain probabilistic queuing models,
4. Probe-vehicle-based positioning methods, and
5. Direct video-based measurements of queue.

Many researchers have combined and compared several algorithms. Evaluation and validation of results are done through one or more known and existing data sources, such as video data,

simulation dataset, NGSIM (next generation simulation) dataset and GPS (Global Positioning System) logger dataset (Liu et al., 2009; Cheng et al., 2011, Ban & Hao, 2011)

2.2 Input-Output Models

Input-output models focus on the accumulation of vehicles before the intersection or freeway bottleneck. Such cumulative traffic input and output was first devised by Webster (1958) to estimate queue length on a signalized intersection approach and was later extended and improved by a number of researchers (Newell, 1965; Robertson, 1969; Gazis, 1974 ;Catling, 1977; Akçelik, 1999; Strong, 2006; Sharma et al., 2007; Vigos et al., 2008). Data necessary for such models are mainly collected by sensors/detectors installed on the roadway at the stop line and several metres away from the stop line (also known as advance detectors).

Most of the early models are steady-state models, which assume that after sufficient time has elapsed, the flow conditions last indefinitely and the state of the system becomes essentially independent of the initial state and elapsed time (Webster, 1958, Miller, 1968). Time-dependent expressions are to be derived from steady-state expressions using a well-known coordinate transformation technique developed by Kimber and Hollis (1979) and Akçelik (1988). A steady-state model is valid only for demand flow rates below capacity (saturation ratio up to about 0.95).

Table 2.1 summarizes various traffic models based on the input-output technique that were developed to estimate queue length, e.g. PASSER II-90, SIGNAL 94, Highway Capacity Manual (HCM 2000),SIDRA, SYNCHRO3 and TRANSYT-7F. The outputs of these models tend to give different results, due to their different computational approaches and different queue definitions,

as shown in Table 2.2 (Sadegh et al., 1987). For example, PASSER II-90 and SIGNAL 94 can only estimate the maximum queue, which is the maximum number of vehicles in the queue at the start of the green period; whereas SIDRA and HCM 2000 considers the maximum back of queue (BOQ), which is the number of vehicles (cumulative) in a queue, including the vehicles that join the queue after the beginning of green and also the average maximum queue.

Some models assume the arrival and departure distribution as uniform and consider no residual queue at the start of the green time. Moreover, in an effort to standardize the methodology for queue-length estimation, the U.S. Transportation Research Board (TRB) committee on highway capacity and quality of service has proposed a specific queue-length model for HCM (2000, 2010), which is mainly based on the model developed by Akçelik (1999). As mentioned earlier, the queue-length definition for the HCM 2000 and 2010 queue model is the BOQ length, rather than the cycle-average queue. The BOQ measure is useful for identifying spillback conditions, i.e. the blockage of available queue storage distance.

The SCOOT system is another adaptive traffic control system that is widely used in over 200 congested urban traffic networks worldwide. SCOOT is based on input-output methodology. SCOOT 3.1 stores and manages the automatic SCOOT traffic information database (ASTRID), which includes flow and delay occupancy data gathered from the detectors. It uses this data for queue estimation and managing traffic signal timing to minimize delay (SCOOT, 2013)

Table 2.1: Models Reviewed (Mystkowski et al., 1999)

Model	Method / Assumption	Estimate Provided
CORSIM (Version 4.01)	Microscopic, stochastic simulation models queue left over from previous cycle	Average and maximum queue
HCM 2000 / SIDRA	Microscopic, stochastic simulation models queue left over from previous cycle	Average and maximum BOQ (back of queue). Higher queue expansion factor
PASSER II-90 (Version 2.0)	No initial queue (default)	Maximum queue
SIGNAL 94 (Version 1.22)	Uniform arrivals on red, no initial queue, adjustment factor of 2 is used to provide a 90th percentile randomness factor	Maximum queue
SYNCHRO3 (Version 3.0)	No initial queue for v/c < 1 For v/c < 1 considers queues for one previous cycle	Maximum BOQ 50% and 95% queue length estimates
TRANSYT-7F (Version 7.0)	Macroscopic simulation models platoon progression, no initial queue, no adjustments	Maximum BOQ

Table 2.2: Different Queue Definitions (Mystkowski et al., 1999)

	Definition
Maximum Queue Length	Number of vehicles in queue at the beginning of the green light
Average Queue Length	Average length of queue based on an estimate of queue every time interval or a time-based average
Average Maximum Queue	Average of the maximum queue length every cycle
Maximum Back of Queue	Number of vehicles (cumulative) in queue, including the vehicles that join the queue after beginning of the green light

The HCM 2000 queue model is applicable for both pre-timed and actuated signals using different, but consistent model parameters. The equations developed are time-dependent expressions, i.e. the queue length predicted by this expression depends on the duration of the analysis period (non-steady-state condition). This queue model allows for an initial residual queue at the start of the flow period. Equations with no residual queue are also given. The queue length model is expressed in the form of traditional two-term equations. The first-term queue expression represents non-random BOQ values, and all randomness and oversaturation effects are accounted for in the second term. Moreover, the HCM model is based on individual lanes. To apply the method to lane groups, an average queue length per lane has to be calculated. (Akçelik, 2001)

Viloria et al. (2000) also provided conversion factors for translating the various model outputs to their HCM 2000 equivalent. HCM 2000 and its parent model from SIDRA and CORSIM are,

therefore, superior, as they try to overcome the limitations of the other models (e.g. TRANSYT-7F and SYNCHRO3) by taking into consideration the presence of a residual queue at the beginning of the analysis period.

In a simple and straightforward input-output queue estimation technique, as shown in Figure 2.1, advance detector actuations measure the arrival flow profile for the current cycle length. Stop line detector actuations along with the signal phase change data are used to develop a discharge flow profile. The two flow profiles are combined together in a queue polygon (arrival profile – discharge profile) to determine if there is a queue accumulation on the intersection approach. Maximum queue length is estimated once for each signal cycle (Felsburg Holt & Ullevig, 2008).

Similar work was done by Sharma et al. (2007), who presented a hybrid input-output queue estimation technique that can measure queue and delay in real time. If full queue discharge failure occurs in the current cycle, the residual queue is taken into consideration at the arrival pattern module. Their results showed that hybrid technique is not too much better than the input-output technique, due to the presence of noise of the stop line detectors. Therefore, the detection of vehicles through nonintrusive detectors/sensors (such as video imaging technology) can be an option to be implemented in conjunction with input-output queue models.

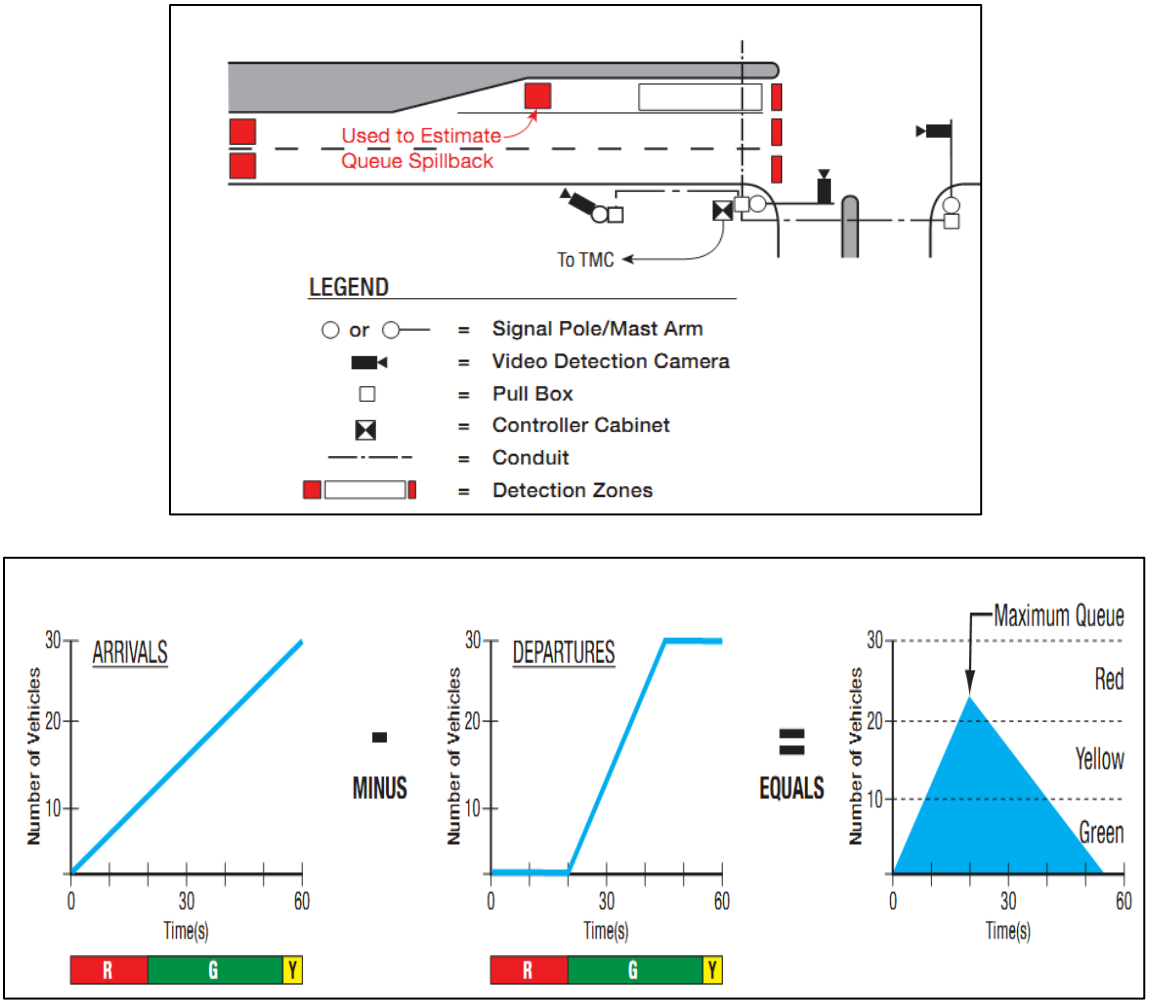

Figure 2.1: Input-Output Queue Estimation Technique (Felsburg, Holt & Ullevig, 2008)

The Lawson et al. model (1996), which is thoroughly reviewed in Section 2.8, is a simple graphical method based on an input-output diagram that can theoretically determine the spatial and temporal extents of a queue upstream of a bottleneck. The technique was applied to three cases: a simple case of a constant departure rate from a bottleneck; a bottleneck that changed once; and, an undersaturated signalized intersection. The macro parameters needed for the model were supplied from a basic triangular flow-density relationship. Due to its ease of construction and analysis an alternate approach (cumulative input-output diagrams) was used for determining

the time and distance of the queue, instead of using a time-space (t-x) diagram. Several assumptions (i.e. instantaneous speed change from non-queued to queued state, undersaturated condition, first in first out (FIFO) and one lane link situation) limit the applicability of this theoretical method in practical situations. Nevertheless, this versatile simple technique allows for possible extensions.

Although the above-reviewed input-output models are capable of successfully describing the queuing process, they lack the ability to estimate the spatiotemporal evolution of queue lengths in real time, which make them static queue estimation approaches. Moreover, cumulative input-output techniques developed using the advance detector data can only work when the BOQ does not exceed the vehicle detector, meaning that the models cannot handle long queues that accumulate beyond the advance detector. There is also the possibility of detector failure. Therefore, although the input-output models developed so far provide useful insight and firsthand knowledge of the queuing process, the application of such techniques has always remained limited in real-time applications.

To overcome some limitations of the input-output technique, Muck (2002) proposed a model for real-time estimation of queue length based on an input-output technique of vehicle counts from detectors located close to the stop line and signal timing information. This model could estimate a queue from the advance detector that was 5-10 times longer than the distance between the stop line and the advance detector. The advance detector was placed at 30 m from the stop line, which was considered a normal measurement position.

The method was mainly based on the linear regression relationship between the "fill-up" time (the time passed from the starting of red time until the continuous occupancy of vehicle on a detector) and queue sizes. If congestion occur in signalized intersection that was not cleared after the end of the green-light period, the vehicles that could not leave, backed up faster behind the stop line than they would have if they had been in free flow. In such cases, the fill-up time fell significantly short of a certain reference period (dt_0), which depended upon the distance between the stop line and the detector. Hence, the comparison of the fill-up times against a threshold (dt_0) provided a queue parameter, known as congestion characteristics, with a value (δ) between 0 and 1. A short fill-up time was a sign of congestion (i.e. $\delta = 1$). With the aid of manually retrieved data, a correlation calculation could then be determined between δ and the length of queue (Ln).

Muck's approach considers the arrival flow of traffic to be constant within a phase/cycle, thereby making the approach limited to mainly steady-state cases and unreliable for those cases where traffic flow fluctuation occurs. This technique also requires an educated guess on the selection of a reference period (dt_0) to identify congestion characteristics, making the method heuristic in nature. The development of this method was done using a Kalman filtering (KF) algorithm.

Further improvement on input-output models includes the provision of queue length in small time stamps based on vehicle arrival and departure profiles, which was first applied in TRANSYT software. This approach was later extended and named as the incremental queue accumulation (IQA) method (Rouphail et al., 2006).

Stochastic analysis has also been introduced to address the stochastic and dynamic nature of arterial traffic (Akcelik, 1988).

2.3 Kalman Filtering Technique

Kalman filtering is a mathematical time series method that uses measurements observed over time, containing noise (random variations) and other inaccuracies, and produces values that tend to be close to the true values of the measurements and their associated calculated values. The KF technique implements a predictor – a corrector type estimator that is optimal in the sense that it minimizes the estimated error covariance – when some presumed conditions are met. It consists of two sets of equations: state and measurement equations. State equations can project forward the current state and error covariance estimates to obtain the estimate for the next time step. The measurement equations are used for the feedback, incorporating a new measurement into the estimate to obtain an improved estimate (Welch & Bishop, 1995).

In an extension of the Muck method discussed in the previous section, Freidrich et al. (2003) also demonstrated that, in cases of high and varying degrees of saturation, a fusion of Muck's estimation module with the KF technique stabilizes and improves the queue estimation. However, at lower saturations (saturation <= 0.5), the combination of methods does not work well, as the Muck method assumes a zero queue at lower saturations.

Pecherkova et al. (2008) devised various estimation and identification techniques that were applied for three types of roads and micro-regions, i.e. a city ring road, a peripheral road and a city centre. For estimation of directly immeasurable queue lengths, the necessary unknown parameters were derived with the application of the KF algorithm. It was shown that the KF is

suitable for micro-regions with rather smooth traffic flow, where all the important roads are equipped with detectors.

Vigos et al. (2006) and Wu et al. (2008) developed queue estimation models based on a KF algorithm for a signalized ramp link. The Vigos et al. model depended on the presence of three detectors: one at the stop line, one in the middle and one at the end of the link. The authors produced reliable estimates of the queue using a KF algorithm based on real-time measurements of flow and occupancy readings provided by the three detectors.

Wu et al (2008) also provided estimations using concepts of linear occupancy similar to those developed by Muck in 2002 and the HCM BOQ with necessary comparisons with field observed queue data.

2.4 Markov Chain Process

Several recent studies formulated traffic queuing as a Markov Chain renewal process (Friedrich et al. 2003; Geroliminis & Skabardonis, 2005; Viti & van Zulen, 2004; Wang et al., 2008). A Markov chain is a mathematical system that undergoes transitions from one state to another (from a finite or countable number of possible states) in a chainlike manner. It is characterized as a random process, since the next state depends only on the current state and not on the entire past (Wikipedia, 2013).

Usually, a Markov chain is defined for a discrete set of times, but in explaining queuing theories, a continuous-time version of the Markov process is considered. As a simple example, imagine a first-come ,first-served queue with average service time μ and Poisson arrival rate λ. The number

of vehicles in the queue is a continuous-time Markov process on the non-negative integers. The transition rate from one number to the next (meaning a new vehicle arrives within the next instant) is λ, and the transition rate to the next lowest number (meaning a vehicle is already served) is $1 / \mu$. Various queuing systems or service patterns, such as the M/M/1 queue, M/M/1/K Queue – Finite Capacity, M/M/c system and M/M/∞ queuing systems, have been adopted based on the Markov Chain renewal process. For instance, the number of vehicles, N(t), in an M/M/1 system is a continuous-time Markov chain, where the queue length is estimated based on the condition of previous time steps (Noble, 2009).

Constantin (2011) introduced several general queuing processes and found the steady-state solution to the M/M/1 queue, which is also a Markov chain probabilistic queuing model. Viti et al. (2010) worked on a probabilistic queuing model that can explain the dynamic and stochastic behaviours of queues at fixed controlled signals. The probabilistic approach allows for the capture of the temporal behaviour of queues and for the measurement of the uncertainty of a queue state prediction by computing the evolution of its probability in time. They extended the classic discrete-time Markov Chain model for the calculation of overflow queues at fixed-time controls to a continuous-time formulation by developing a model for the within-cycle process. Their research found that their probabilistic model gave a better understanding of what really causes random delays, i.e. the effect of the probability distribution for queue lengths that is limited to non-negative values.

Although computationally challenging, the probabilistic Markov Chain approach has enormous potential as a modelling tool for several transportation areas, such as urban state estimation and

prediction (i.e. queue and delay estimation, travel-time estimation), and planning and design problems.

2.5 Shockwave Theory Based Models

One of the most promising queue estimation techniques is based upon the principle of shockwave theory originally developed by Lighthill and Whitham (1955) and Richards (1956), and the model is most often called the LWR shockwave model. The main working principle of the model is the estimation of queue lengths by tracing the trajectory of shockwaves based on the continuum traffic flow theory. Tracing the shockwave trajectory means identifying the critical points over the shockwave moving upstream creating vehicle queues (Liu et al. 2009). Continuum traffic flow theory considers traffic stream as a one-dimensional compressible fluid that leads to two basic assumptions: 1) traffic flow is conserved, and 2) there is a one-to-one relationship between speed and density or between flow and density. A simple continuum model consists of conservation equation and speed-density or flow-density relationships. These are solved to trace different shockwaves (such as queue formation or dissipation shockwaves) at different flow-density conditions.

The shockwave queue estimation approaches that have been developed by different researchers can be categorized into approaches that do not use probe data and approaches based on probe data. In this section, only the non-probe based shockwave techniques are reviewed.

After the development of the LWR shockwave model, Stephanopoulos et al. (1979) investigated the dynamics of queue formation and dissipation at isolated signalized intersections by analyzing the vehicle conservation equation along the street. The paper examined the effects of the control

variables (cycle length, green and red intervals) and system parameters (arrival rates, capacity) on the length of the stop line queue. A solution to the conservation equation was then obtained by the method of characteristics for general initial and boundary conditions.

Michalopoulos et al. (1981) further analyzed the dynamics of traffic downstream of a signalized intersection and on the links between adjacent intersections. Their approach was macroscopic in nature and treated traffic as a continuum fluid. They also demonstrated the existence and behaviour of shockwaves generated periodically downstream of a traffic signal and derived an analytical expression for describing their propagation along the road.

Messer et al. (1973) developed a framework to estimate delays caused by a freeway incident using shockwave analysis. In their study, various traffic states related to incidents were first defined in terms of the fundamental traffic variables, i.e. flow and density. The shockwaves created by traffic incidents were then identified, and related velocities were estimated using Greenshields' linear traffic flow model.

Wirasinghe (1978) also used shockwave theory to calculate individual and total delays upstream of incidents. The formulas developed through this work were based on areas and densities of regions representing different traffic conditions (mainly congested and capacity regions) that were formed by shockwaves in a time-space plot.

A widely used framework based on shockwave theory was developed by Al-Deek et al. (1995), which extended the analytical method of Morales (1986), where instead of using deterministic

flow-density relationship; densities were estimated using the ratio of the measured flow to the measured speed departure curves. The cumulative vehicle hours of incident delay are eventually calculated.

Ping Yi et al. (2000) developed a macroscopic model based on the continuum principle. This method could describe the queue formation and dissipation based on a general speed-density relationship, which led to the development of a general mathematical formulation for the determination of intersection queue length. Due to the strength of its analytical formulation, the model can adapt to the changing traffic demand, signals and other geometric and environmental factors. Both undersaturation and oversaturation traffic conditions can be considered in this method for queue estimation, provided that the right speed-density model is chosen to match the prevailing conditions on the roadway.

Another shockwave-based method incorporated with high-resolution second-by-second event-based traffic signal data queue estimation was developed by Liu et al. (2009). This technique can provide real-time estimation of queues. It can also estimate queues way beyond the advance detector. Using shockwave theory's break points, traffic flow pattern changes can be identified. These points have important physical meaning in terms of traffic shockwave and contribute greatly toward the estimation of long queues. The model assumes an undersaturated condition, no queue overflows, a known vehicle arrival pattern and constant effective vehicle length of 25 ft. Moreover, a time gap between vehicles of 2.5 seconds is assumed, in order to identify that the end of queue is propagated forward, indicating a change in traffic state.

Among the inherent limitations of the model, its incapability of addressing oversaturated traffic conditions and identifying break points, frequent platoon arrivals (eliminated by an expansion model) and detector errors (which can be reduced by a KF technique) are worth mentioning. The model was evaluated by comparing the estimated queue with observed field data. The model requires improvements to include more complex geometries for turning movements of vehicle queues and large-sized vehicles and more testing for application in real-world situations.

Shockwave theory successfully describes the complex queuing process in both temporal and spatial dimensions, but these theoretical models have limitations in practical applications, as they require perfect information and huge amounts of input data. These models assume known vehicle arrivals, which cannot be satisfied for most situations. Vehicle arrivals cannot be measured when the roadway detector is occupied, which is usually the case with congested arterials. Without arrival information, the existing shockwave models cannot be utilized to accurately estimate intersection queue lengths.

2.6 Probe-Based Approaches

With today's wide deployment of ITS and positioning technologies, floating data derived from mobile sensors (e.g. smart phones, navigation devices and, in the future, connected vehicles) are able to track vehicle trajectory and position, helping to acquire perfect input information required for shockwave analysis. Future deployment of the connected vehicles initiative, which combines GPS navigation, advanced vehicle sensors, on-board computer processing and vehicle-to-vehicle (V2V), vehicle-to-infrastructure (V2I) and infrastructure-to-vehicle (I2V) communication, can provide accurate network and traffic data required for real-time shockwave analysis (Smith, B. L et al., 2011).

Comert et al. (2007 & 2009), Hao et al. (2010, 2011) and Cheng et al. (2011) have outlined the possibility of probe-vehicle use and related simulation studies to establish techniques for real-time queue estimation. Comert et al. (2009) mainly focussed on the last probe-vehicle position and the last probe time stamp when it joins the BOQ to estimate queue length. The research showed that, in the queue, neither the total number nor the location of other probe vehicles is necessary for estimating the queue length.

Analytical models have also been developed to assess how queue length estimation is influenced by the percentage of probe vehicles in the traffic stream. Generally, accuracy depends upon the percentage of the penetration rate of vehicle probes (Figure 2.2). Another important finding of Comert et al. (2009) is that a higher position of the last probe vehicle in the queue results in the expected queue length more closely matching the length from the stop line to the last probe location, regardless of the penetration rate of probes in the queue (Figure 2.2). As an initial research effort, the study assumed a steady-state condition, isolated and undersaturated intersections, a Poisson's distribution for arrivals, constant departures from the stop line and fixed signal timing. Unfortunately, no real-world data could validate the results of this model rather than the empirical study that generated data from microsimulations to account for various scenarios and percentage of probes.

Hao et al. (2011, 2010) developed a probe-based queue estimation method based on kinematic wave theory that describes queue formation and dissipation. The main theme was the estimation of the queue length by the estimation of queue full-discharge time (QFDT) from the delay pattern sampled probe vehicle. Signal timing derivation was also done using the delay

measurements by upstream and downstream virtual trip line (VTL) technology based on GPS-equipped cell phones from the queuing delay. Using sampled travel times, they found that a 40% penetration rate of probe vehicles was needed in order to obtain reliable signal timing detection (incorporation of shockwave theory reduces the percentage significantly as described by Cheng et al. 2011). Testing of the model using microsimulation and field data was also done, but the method was only tested at an isolated intersection assuming uniform arrivals. As a future research, fusing loop detector data and mobile sensor data can be taken into consideration.

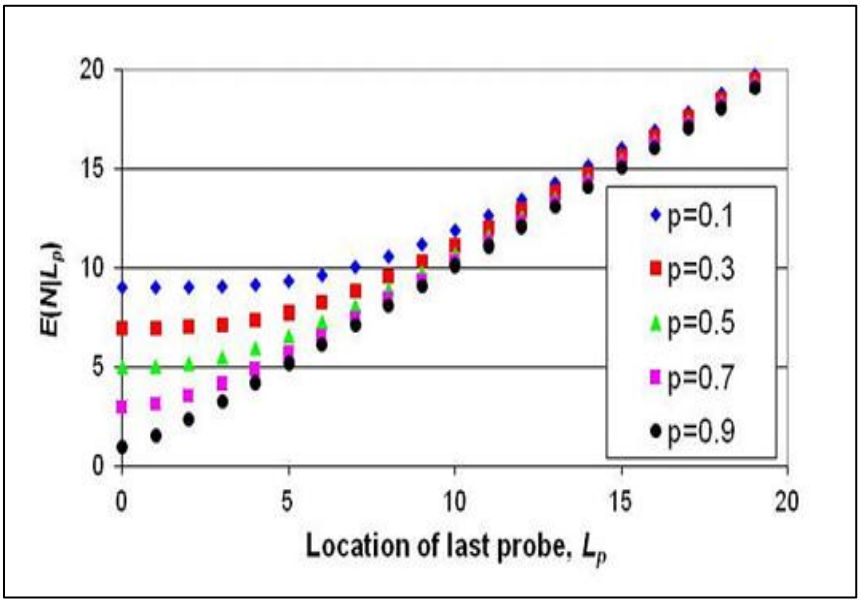

Figure 2.2: Expected Queue Length vs. Location of Last Probe at Different Probe Penetration Rates (Comert et al. 2009)

A recent research by Cheng et al. (2011) proposed cycle-by-cycle queue length estimation for signalized intersections using sampled trajectory data of probe vehicles. The study was also based upon critical point identification (Figure 2.3) from shockwave analysis to estimate the queue length, similar to the research done by Liu et al. (2009). For shockwave analysis, the

research concentrated on sample probe-vehicle trajectory data as the only input in the analysis. The study also considered a separate determination approach for isolated and non-isolated intersections. Isolated intersections were assumed to have a constant arrival rate, which causes the queue length to grow at a constant rate. However, for non-isolated intersection with varying arrival patterns, the queue was considered to increase as a piecewise linear line. Moreover, lower and upper bound queue length estimations could also be taken into consideration with the use of critical points.

Another feature of the model (Cheng et al., 2011) was that, if only offline trajectory data were available, this method could potentially be used in the prediction of queue length as the input for the optimization of a traffic control system. For the sake of performance evaluation and validation, several data sets, such as simulation data sets under different flow and signal timing conditions, were used.

Kong et al. (2009) developed a data-fusion-based approach (fusion of underground loop detector data and GPS-equipped probe-vehicle data for the estimation of urban-traffic states. Three parts of the algorithms were developed for fusion computing and the data processing of loop detectors and GPS probe vehicles. First, a fusion algorithm integrating a federated KF algorithm was proposed for the fusion of multi-sensor data. A novel algorithm based on the traffic wave theory was then employed to estimate the link mean speed using single-loop detectors buried at the end of links. With the GPS data, a series of technologies were combined with a GIS-T (geographic information system for transportation) map to compute another link mean speed. These two speeds were taken as the inputs of the proposed fusion platform. Finally, tests on the accuracy,

conflict resistance, robustness and operation speed by real-world traffic data illustrated that the proposed approach could be used in urban traffic applications on a large scale. Although this fusion methodology has some limitations in its application, further research can be conducted to strengthen the algorithm.

In recent years, several travel-time estimation methods have also been proposed using probe-vehicle data, e.g. Hellinga et al. (2000), Kwong et al. (2009) and Herring et al. (2010). Further research on traffic-state estimation processes using probe vehicles and shockwave analysis is expected to increase the credibility of these methods for application in real-time queue length estimation in the near future.

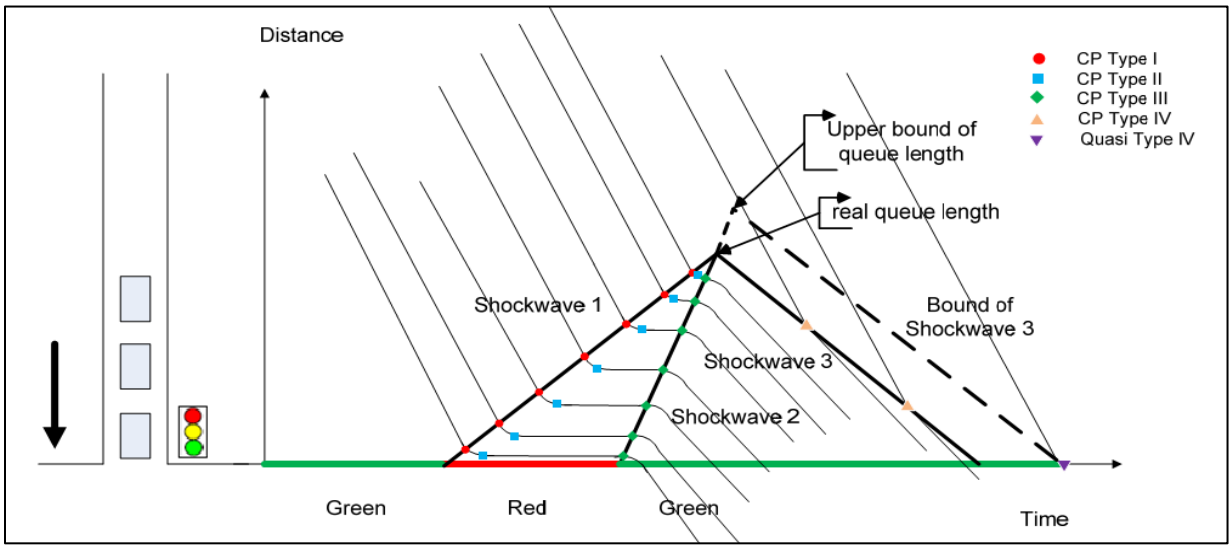

Figure 2.3: Critical Point Identification from Shockwave Analysis Using Probe Trajectories (Cheng et al. 2011)

2.7 Direct Queue Measurement Methods

It is to be noted that more direct measurements of queue length are becoming possible with the employment of video detection systems, which are non-intrusive in nature and can detect maximum queues during each cycle (Figure 2.4). These systems have mainly been used in the calibration and validation of existing queue estimation algorithms, such as an algorithm developed by Texas Transportation Institute (TTI), and also helped in the development of a queuing algorithm, such as the one developed by Cheek, M. T. (2007)

Cheek, M. T. (2007) concurrently collected signal phase data and video data of vehicle queues. Figure 2.5 shows the video image detection of a vehicle in a queue. They used a video imaging and vehicle detection system (VIVDS) for queue length estimation in real time with the KF technique for error minimization. The direct measurement of queues using video detection and the queue-by-queue estimation algorithm were compared; and, for almost 86 percent of cases of different lengths of queues, both the actual and predicted lengths matched with one another.

Video imaging methods can easily overcome the errors of loop detectors (mainly used in input-output queue estimation methods), eliminating the need for the installation of these detectors on heavy volume roadways. These methods can accurately measure queue lengths up to 400 ft. Queues beyond this length need extra attention and may cause errors beyond acceptable limits. Merging of the vehicle detection lines (the black lines in Figure 2.5) in a longer queue makes it impossible to detect individual vehicles beyond 400 ft. Also video imaging technology does raise privacy concerns for drivers and passengers. Nevertheless, the incorporation of video imaging to detect queues in input-output techniques of queue estimation does appear to be very promising.

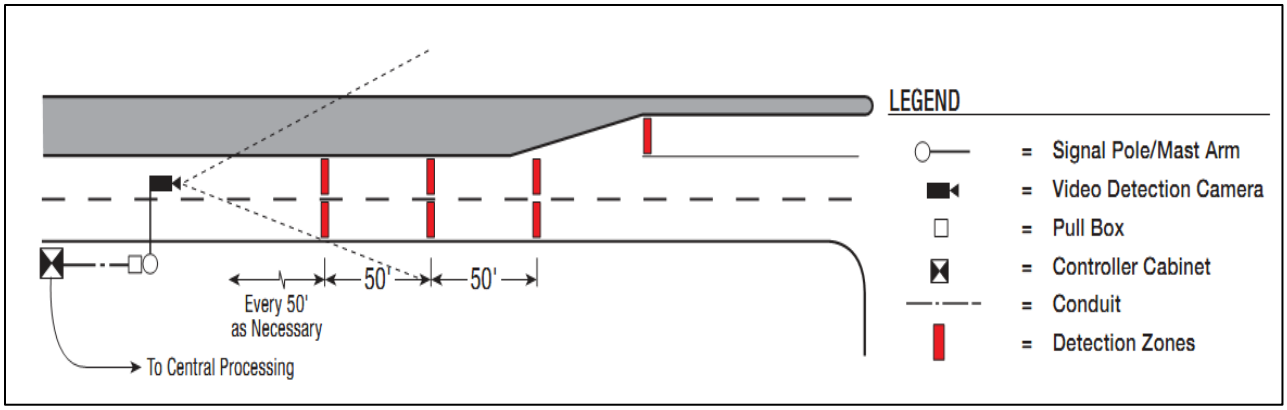

Figure 2.4: Non-Intrusive Video Imaging Technique of Queue Estimation (Felsburg Holt & Ullevig, 2008)

Figure 2.5: Typical Setup for VIVDS Data Collection (Cheek, M. T. (2007)

2.8 Detailed Review of the Lawson Lovell and Daganzo Technique

This section focuses on reviewing the Lawson et al. (1996) BOQ estimation technique in detail, since this technique is used as a benchmark for comparing the proposed techniques.

The method of Lawson et al. (1996) mainly considered three scenarios of queue accumulation: 1) a simple case of a constant departure rate from a bottleneck; 2) a bottleneck departure that changes once; and, 3) an undersaturated signalized intersection. Each of these scenarios is discussed separately in this section. In their methodology, the authors also assumed that the traffic stream maintained a triangular flow-density (q-k) relationship similar to the one shown in Figure 2.6, where k_j and V_f refer to jam density and free-flow speed, respectively, and V_μ refers to the queued speed when the bottleneck departure rate is μ.

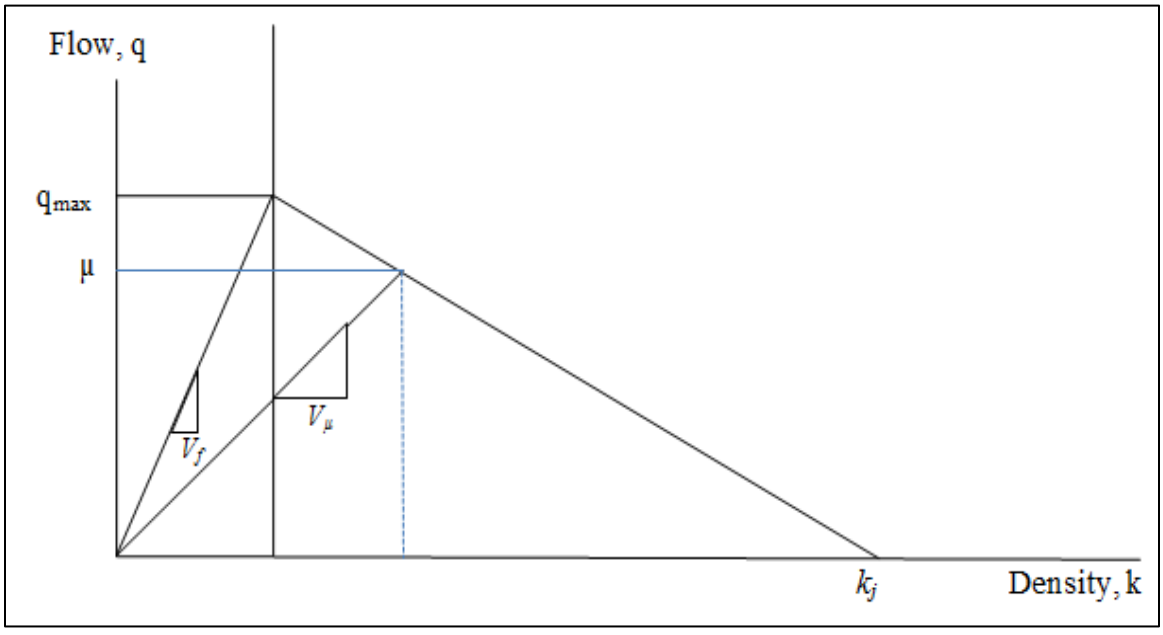

Figure 2.6: Basic Triangular Flow-Density (q-k) Diagram

It must be pointed out that the queue length estimated using this method is expressed in the number of vehicles instead of the physical numerical queue length in metres or kilometres. This is due to the proposed queue definition, which implies that queue length is the accumulation of vehicles (slow moving, stop and go or stopped vehicles) which face delays due to a certain bottleneck condition.

2.8.1 Constant Departure Bottleneck Scenario

2.8.1.1 Assumptions

The technique is quite theoretical in nature; therefore, it assumes one lane link where a bottleneck is created. Furthermore, it is assumes that the departure rate from the bottleneck is uniform and maintains a maximum service flow rate, μ . The flow regime for all vehicles in the road segment is considered to maintain an uncongested free-flow condition with a velocity of v_f, except in the queued portion where congested flow with a velocity of v_μ is maintained. It is assumed that speed changes occur instantaneously and that there is no inflow or outflow of vehicles while they are in the queue. The traffic stream is also assumed to be composed of standard passenger cars, maintaining FIFO (first in first out) queuing characteristics.

2.8.1.2 Working Principle

The theoretical time-space diagram shown in Figure 2.7 demonstrates the vehicle dynamics as assumed in the Lawson et al. (1996) method, where vehicles are considered to be at a constant free-flow speed, v_f, when it is not queued. Again, the queued vehicles are considered to be at a congested speed of v_μ before they depart from the bottleneck at a constant service flow rate, μ.

The curved dashed line in Figure 2.7 represents the BOQ trajectory. A vehicle, *N*, shown as a bold trajectory line, reaches the BOQ prior to the bottleneck. The bold dashed line is the desired trajectory of the vehicle if there was no bottleneck. Figure 2.8 is a reproduction of Figure 2.7 that shows more precisely the actual and desired trajectories of vehicle *N*. The vehicle's actual trajectory within the queue has a speed (i.e. slope) of v_μ as shown, whereas the desired trajectory's speed is v_f. The delay, *w*, the time spent in the queue, t_q (> *w*), and the distance traveled in the queue, d_q, are clearly shown in the figure, and the relationships among these three variables are discussed below.

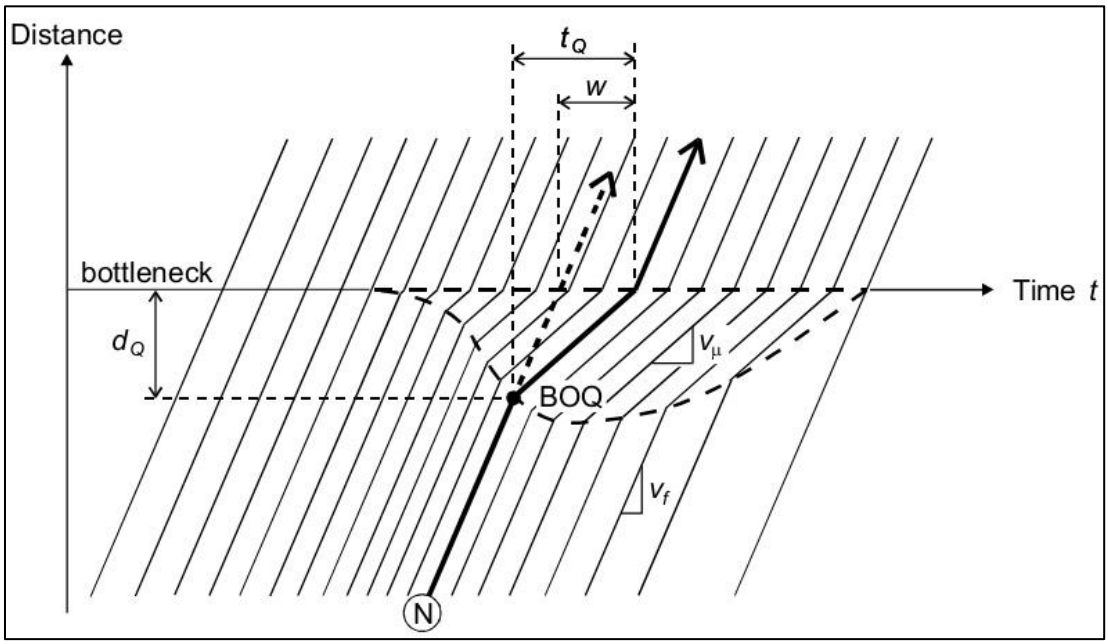

Figure 2.7: Time-Space Diagram (Lawson, Lovell & Daganzo, 1996)

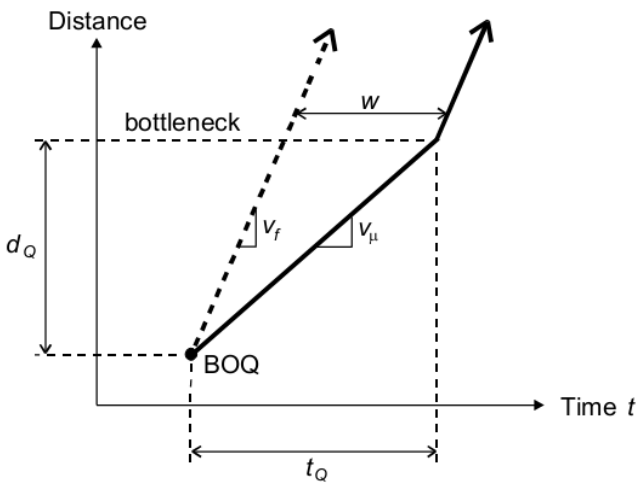

Figure 2.8: Actual and Desired Trajectories of Vehicle *N* (Lawson, Lovell & Daganzo, 1996)

From the geometry of Figure 2.8, it can be shown that

$$w = \left(\frac{1}{v_\mu} - \frac{1}{v_f}\right) d_q \quad \text{……..} \quad (1)$$

And since $t_q = d_q / v_\mu$, we can write

$$t_q = \frac{w}{1-\frac{v_\mu}{v_f}} \quad \text{……..} \quad (2)$$

In the original method of Lawson et al. (1996), it is assumed that the arrival profile, *A(t)*, is known (Figure 2.9). Translation of the *A(t)* curve to the right by the use of a free-flow travel time, t_f , which is fixed for any vehicle in the traffic stream on that link, allows for the desired or virtual arrival curve to the bottleneck, *V(t),* to be constructed. The departure curve, *D(t),* which defines the time that each vehicle departs the bottleneck, can then be constructed using a

service flow rate, μ. For a given vehicle number, n, the horizontal separation between $V(t)$ and $D(t)$ represents the delay for that vehicle and is denoted by w.

Using equation 2 for each and every vehicle, the input-output diagram of Figure 2.9 can be modified to include a $B(t)$ curve, which represents the number of vehicles to reach the BOQ by time t or, equivalently, the times that each vehicle reachs the BOQ. We can determine the time that each vehicle joined the BOQ by extending the delay of each vehicle, w, to the left by the factor in equation 2, which equals to t_q. The locus of these points for all vehicles represents the BOQ curve, $B(t)$, which can now be constructed on the input-output diagram, as shown in Figure 2.10. The number of vehicles in a queue at any time t, $Q(t)$, can then be found as the vertical separation between the $B(t)$ and $D(t)$ curves .

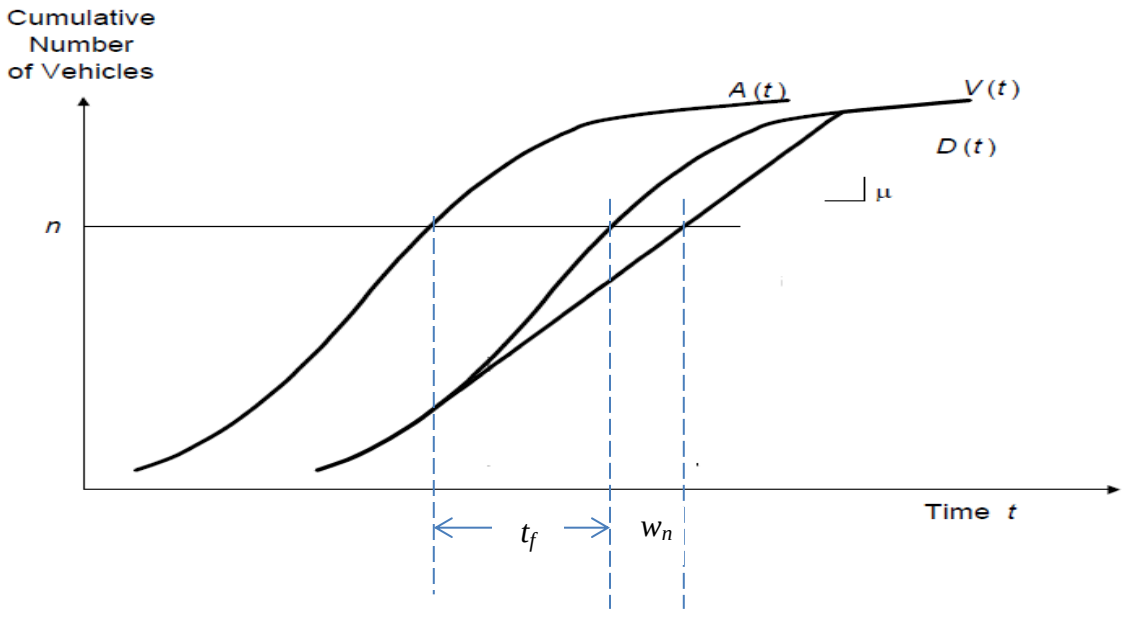

Figure 2.9: Input-Output Diagram (Lawson et al., 1996)

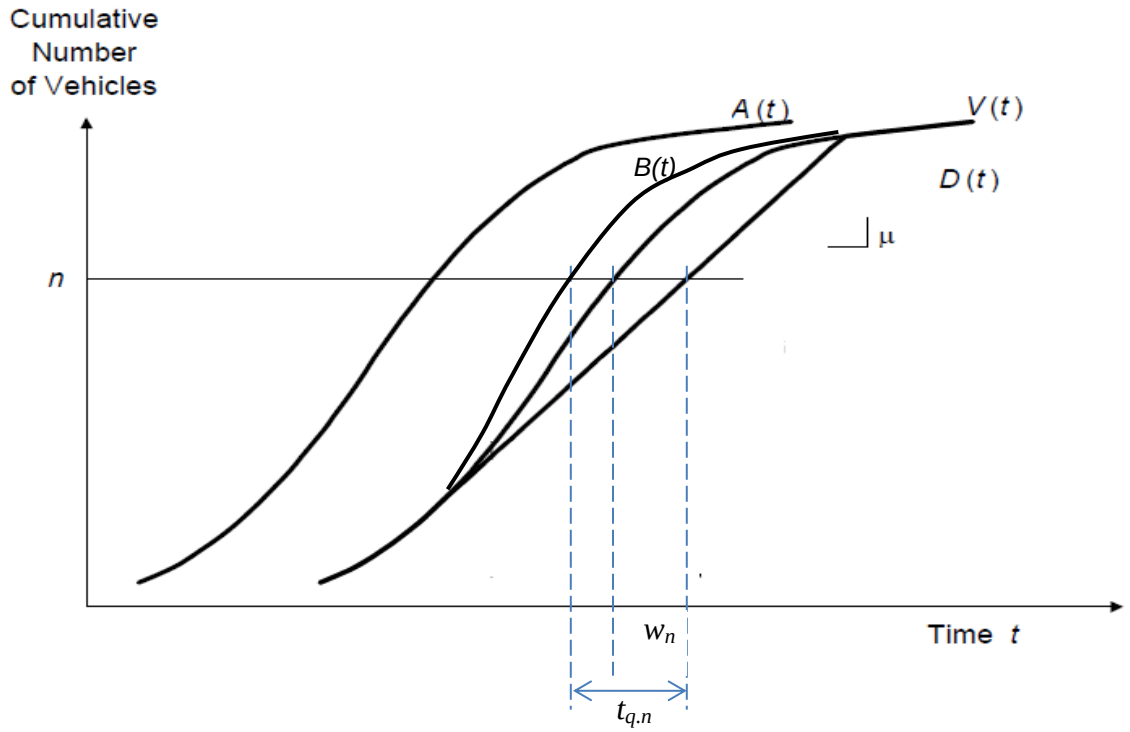

Figure 2.10: Locating the Back of Queue Curve, *B(t)*, for a Constant Departure Rate (Lawson et al., 1996)

2.8.1.3 Limitations

Although the input-output technique of Lawson et al. (1996) explains, in a simple way, the spatial and temporal extents of a queue upstream of a bottleneck, it has some major limitations and, therefore, cannot be used directly for queue or delay estimation in real-life situations or in a simulation environment. The main limitations are:

- Consideration of a triangular fundamental diagram to estimate free-flow speed v_f and queued vehicle speed v_μ . However, several recent research studies, such as Brilon et al. (2008) and Dervisoglu et al. (2009), prove that a capacity drop exists for a fundamental flow-density diagram in case of a bottleneck or congested roadway section.

- A constant maximum service flow rate is assumed out of the bottleneck to construct *D(t)*, which is not always true.
- Consideration of a simultaneous speed change from free-flow speed to the queued speed as the only criteria for a vehicle to reach the BOQ.
- Arrival profile *A(t)* is assumed to be known.
- All vehicle data seems to be required, which is quite unrealistic.

Based on the above limitations of the theoretical model of Lawson et al. (1996), a few suggestions can be made to estimate the BOQ :

- Use of probe vehicles to know the temporal and spatial aspect of the BOQ,
- Development of a BOQ criteria using probe trajectory data analysis that can determine when a probe vehicle reaches the BOQ,
- Use of detector counts to estimate the real-time departure rate of the bottleneck, and
- Use of a fundamental flow-density diagram that considers a capacity drop.

2.8.2 Bottleneck Departure Rate that Changes Once

2.8.2.1 Assumptions

Lawson et al. (1996) also proposed a theoretical model where they extended the previous constant departure bottleneck scenario to a time-dependent bottleneck scenario, where the departure rate changes only once. In a real-life situation, this phenomenon may occur in the case of a lane closure due to an incident which lasts for some time and then again gains the usual flow.

It is assumed that the flow and density of the bottleneck road section maintains a triangular relationship (Figure 2.11) and can easily be defined by free-flow speed, maximum flow and jam density. Again, FIFO traffic flow conditions and known arrivals of all vehicles are assumed to be maintained throughout the entire analysis period.

2.8.2.2 Working Principle

Referring to Figure 2.12, it can be seen that the bottleneck can discharge at a maximum rate of μ_1 until time t_j and at a maximum rate, μ_2. This departure curve, *D(t)*, can be easily computed using known arrivals, i.e. a known virtual arrival curve, V(t). To construct the BOQ curve, *B(t)*, in the cumulative diagram, it is necessary to recognize three types of vehicles, which are distinguished by the characteristics of the queue when the vehicles join it and by the bottleneck departure rate when the vehicles pass the bottleneck.

The first type of vehicle (n_L to n_j) in the cumulative diagram of Figure 2.12 passes out of the bottleneck without being impacted by the changing bottleneck capacity; therefore, $B_1(t)$ for these vehicles is constructed in a similar way as is mentioned in Section 2.8.1. The second group of vehicles joins the queue at a time before the information about the change in the bottleneck departure rate has had time to reach the BOQ. To construct the BOQ curve for these vehicles, it is assumed that the discharge rate never changed (μ_1 is continued from *J* point, which is extrapolated as the $D'_1(t)$ departure curve; and, a BOQ curve is constructed, which is actually an extension of $B_1(t)$.

Departure curve $D_2(t)$ with a discharge rate μ_2 is used for the same type of vehicles (n_j to n_m) to construct another BOQ curve, $B_2(t)$. These two BOQ curves intersect at point *K* and the

corresponding vehicle, n_k, is considered to be the last vehicle that is impacted by both of the discharge scenarios. The segment of $B_1(t)$ to the left of this intersection point combined with the segment of $B_2(t)$ to the right of the K point yield the desired curve, $B(t)$. The number of vehicles inside the queue in number of vehicles at any time t is found from the vertical separation between the $B(t)$ and $D_1(t)$ and $D_2(t)$ curves.

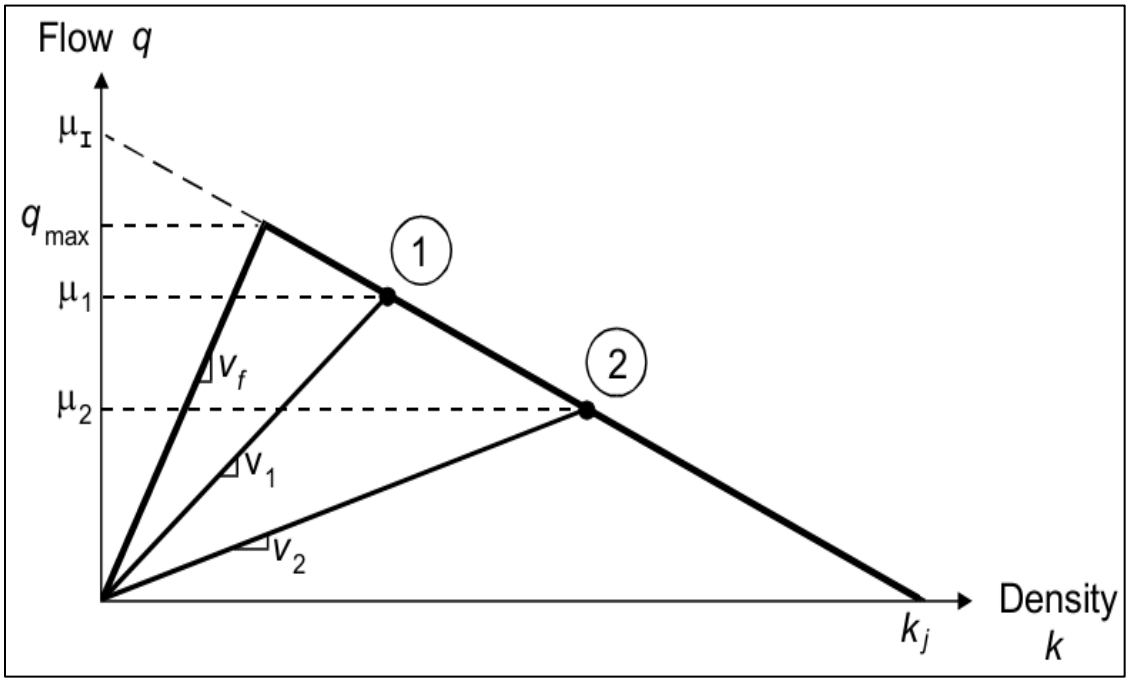

2.11: Flow-Density Relationship (Lawson et al., 1996)

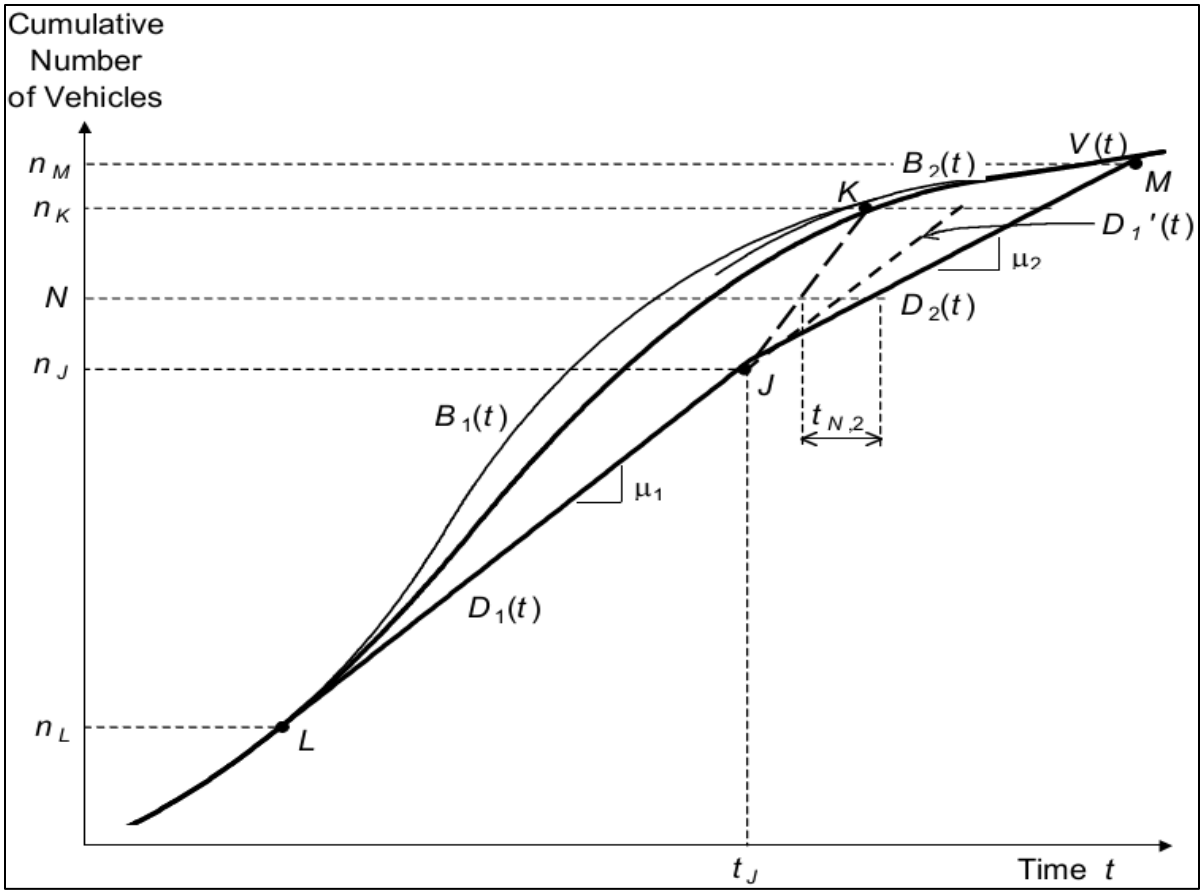

Figure 2.12: Locating the Back of Queue Curve, *B(t)*, for a Departure Rate that Changes Once (Lawson et al., 1996)

2.8.2.3 Limitations

The main limitation of this method is that it assumes bottleneck departures change just once, which is not realistic. In an accident scenario, although it is possible to encounter such a situation where the bottleneck capacity drastically changes just once, it is too restrictive to think that the bottleneck discharge would change only once during the entire queue estimation period. Moreover, this method relies on a simple triangular flow-density relationship; and, the required cumulative diagrams are plotted based on this relationship. Therefore, it is quite obvious that this method is prone to certain inaccuracies.

In Chapter 4, a case study of an accident scenario is investigated applying this method and compared with the much more advanced methodology proposed in Chapter 3, which uses probe-vehicle data as input incorporating the input-output technique. An extension is also proposed that uses a realistic fundamental flow-density diagram for queue estimation.

2.8.3 Undersaturated Isolated Signalized Intersection Scenario

2.8.3.1 Assumptions

The theoretical method of Lawson et al. (1996) discussed in the previous sections is also applicable for the estimation of queues in signalized intersections. For this, the authors assumed an undersaturated traffic signal, which by definition means situations where the entire queue clears during the green phase (no residual vehicle for the next cycle). Certain other assumptions are also considered, such as fixed signal timing, FIFO conditions, one lane link and no queue spillback into upstream intersection. Again, the traffic stream is assumed to be composed of standard passenger cars only. It is also assumed that the speed changes occur instantaneously and that there is no inflow or outflow of vehicles while the traffic stream is in queue

2.8.3.2 Working Principle

The conventional time-space diagram in Figure 2.13 demonstrates a purely theoretical case of vehicles queued at a traffic signal. Two states have to be defined; state 1 is the time a vehicle remains inside the queue with a queued speed, v_μ, of 0; and, state 2 is the time period from when the vehicle leaves state 1 until it departs from the intersection at free-flow speed v_f.

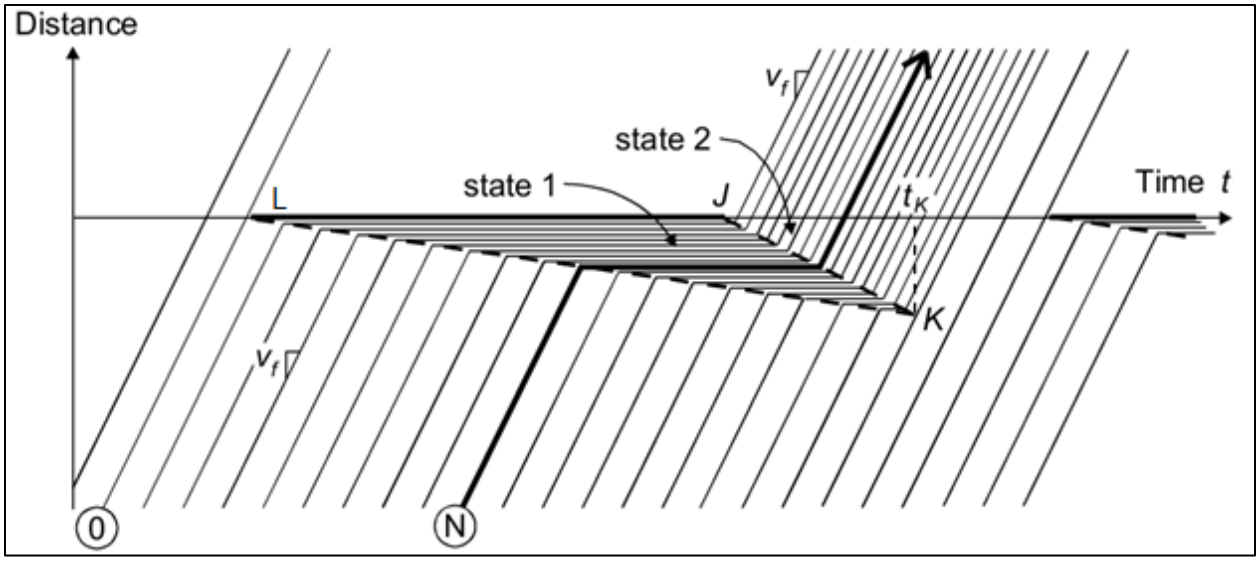

Figure 2.13: Time-Space Diagram of a Signalized Intersection (Lawson et al., 1996)

Unlike the bottleneck situation where a constant service flow rate departure (μ) is assumed, the technique in case of a signalized intersection breaks down for $\mu = \mu_r = 0$ or $\mu = \mu_g = q_{max}$= saturation flow rate, where the velocities of vehicles are $v_\mu = v_r = 0$ and $v_f = v_g$, respectively. The flow rates at the red and green phases of the traffic signal are defined by μ_r and μ_g, respectively. As the ratio $1/ v_\mu$ in equation 1 [$w = \left(\frac{1}{v_\mu} - \frac{1}{v_f}\right) d_q$] is not defined in this case of a signalized intersection, a limiting case has been introduced by Lawson et al. (1996) to alternatively explain the current situation. This was done by relating *B(t)* to the virtual arrival curve, *V(t)* instead of *D(t).*

For vehicle *N* in Figure 2.14, the additional time spent in queue is defined by ΔN ($= t_{q.N} - w_N$) and is related to delay w_n by

$$\Delta N = w_n \frac{v_\mu}{v_f - v_\mu} \quad \text{…….. (3)}$$

This quantity represents the horizontal separation between $V(t)$ and $B(t)$ for vehicle N. For a very small departure rate ($\mu = 0$) or a near-zero departure rate (i.e. $V_\mu \rightarrow 0$), equation 3 reduces to $\Delta N = w_n \frac{v_\mu}{v_f}$. Again ,for very small V_μ, $w_n \approx \frac{N}{v_\mu k_j}$; therefore, ΔN can be rewritten as:

$$\Delta N = \frac{N}{v_\mu k_j} \text{ for } \mu \rightarrow 0 \text{ ..... (4)}$$

From equation 4, it can be also stated that, as $\mu \rightarrow q_{max}$ = saturation flow rate, ΔN becomes extremely large and, therefore, a horizontal straight line. All these features are shown in Figure 2.14.

The straight line *JK* in Figure 2.14 (also in Figure 2.13) indicates the time when the information concerning the change in capacity at the bottleneck reaches vehicles. In other words, this line identifies the time when a vehicle goes from congested state 1 to uncongested state 2. This line has a constant slope, because the information travels backward toward the end of the queue at a constant wave velocity. This line is also important in the identification of the extent of the queue (i.e. the last vehicle that enters into the queue).

Based on the above approach, BOQ curves $B_1(t)$ and $B_2(t)$ and departure curves $D_1(t)$ and $D_2(t)$, pertaining to the limiting cases of $\mu = \mu_r = 0$ *and* $\mu = \mu_g = q_{max}$= saturation flow rate, are plotted in a cumulative input-output diagram, as shown in Figure 2.14. $B_1(t)$ diverges from $V(t)$ at a constant rate with an increasing number of vehicles (equation 4). $B_2(t)$ is a horizontal line representing only the last queued vehicle. This line is drawn from the intersection point of virtual arrival curve $V(t)$ and $D(t)$. Now the vertical separation (red vertical lines in Figure 2.14) between the lines *MKL* and *MJ* represents the instantaneous queue $Q(t)$ in number of vehicles.

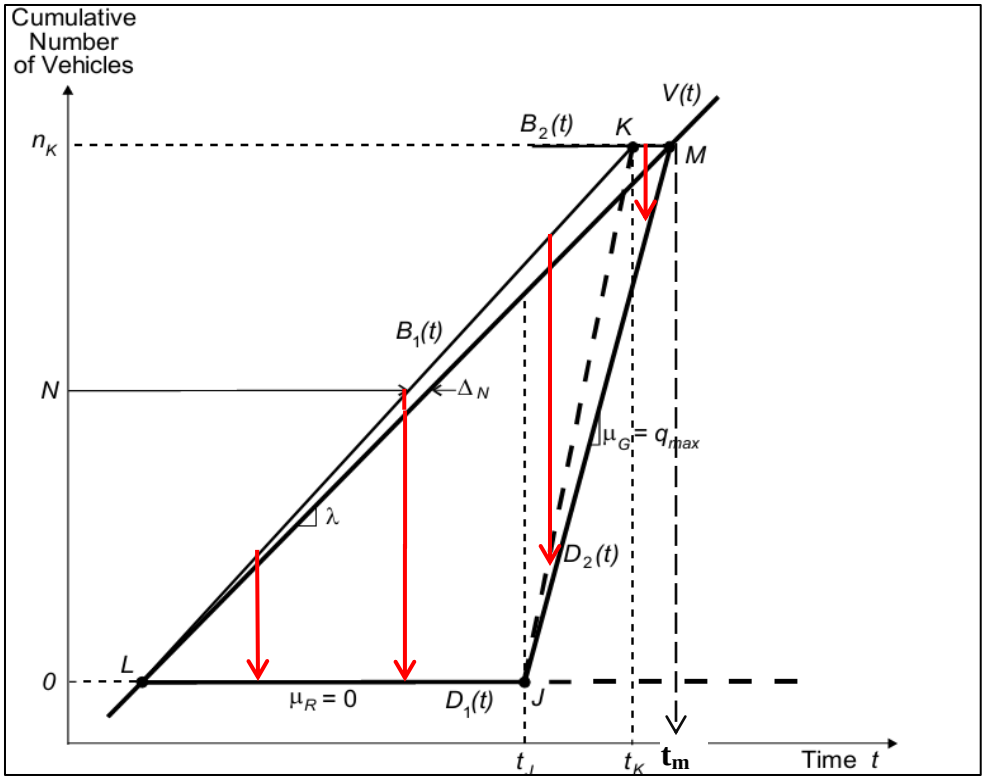

Figure 2.14: Locating the Back of Queue Curve, *B(t)*, for a Traffic Signal Case

2.8.3.3 Limitations

The method explained above can successfully state the flow conditions during red and green phases at the intersection. However, it still has a few limitations or drawbacks:

- Instantaneous speed changes (free-flow speed v_f to queued speed v_μ or vice versa);
- Queued vehicle speed v_μ and the speed at the BOQ are assumed to be zero;
- Instantaneous speed change from v_f to $v_\mu = 0$ is considered to be the only criterion for a vehicle to enter queued state 1 represented by line *LK* (as seen on Figures 2.13 and 2.14);
- Instantaneous speed change from $v_\mu = 0$ to v_f is considered to be the criterion for a vehicle to leave the queued state 1 and enter into the free-flow state represented by line *JK* (as seen in Figures 2.13 and 2.14);

- All vehicle data is available, which is quite unrealistic; and,
- There is no direction toward successful interpretation for oversaturation conditions.

Based on the above drawbacks or limitations, the following suggestions to overcome the inaccuracies of BOQ estimation in the case of an isolated signalized intersection can be proposed:

- Data availability: probe data from simulation trials that represent real-world situations;
- Determination of the free-flow speed (v_f) based on probe-vehicle data;
- Consideration of the actual vehicle trajectory and analyzing it to determine the BOQ line *KL* and the backward information flow line *JK*. Actual vehicle trajectory simply ignores the instantaneous speed changes from v_f to queued speed and vice versa, as opposed to the theoretical model of Lawson et al.; and,
- Inclusion of a vehicle into queued state 1 based on its deceleration phenomenon caused by the queue in front of it, even though its speed is not zero ($v_\mu \neq 0$). In other words, V_f to $V_\mu = 0$ is not the only criterion to determine if a vehicle is in queued state or not.

2.9 Discussion and Conclusion

This chapter introduces several queue estimation techniques. Of these methods, significant efforts have been given to the input-output technique, although technological challenges have left these techniques mostly as theory. A theoretical methodology developed by Lawson, Lovell and Daganzo in 1996 for the determination of the spatial and temporal extents of a queue upstream of a bottleneck is largely based on input-output technique. However, this theoretical methodology cannot be used in real-world situations, due to its strict assumptions and its

dependency on all vehicle data. Nonetheless, this methodology clarifies the understanding of queue estimation or, more precisely, the back of queues from the cumulative input-output diagrams.

Based on this methodology as described in this chapter for two different roadway conditions, efforts have been put in the development of techniques for the estimation of queues in these two roadway scenarios – the bottleneck scenario on a roadway and a signalized intersection, which are discussed Chapters 3 and 4. Relevant comparisons with the proposed methodologies developed in Chapter 3 are also described.

Table 2.3 provides a summary of the main queue estimation methods reviewed in this chapter. It is quite notable that the analysis and implementation of successful queue estimations in freeway bottleneck situations has not been widely investigated. In the case of signalized intersection scenarios, although the queue estimation using shockwave analysis seems to be very elegant in nature, in real-life situations, shockwaves are difficult to examine and analyze with accuracy. Most of the techniques developed using shockwave analyses are theoretical in nature. They require huge amounts of data for analysis. Moreover, if shockwaves are used as the basis of measuring queues, for a situation with no shockwave (i.e. mainly during off-peak periods), it is more likely that the models of queue estimation are going to show erratic, inaccurate results. Most shockwave analyses also require a known arrival profile and a definition of shockwave speeds based on a flow-density diagram, which is a macro feature of traffic movement; whereas a probe-based input-output technique only requires readily available vehicular speed, time and location data to be analyzed for queue length estimation.

This thesis proposes a method that uses an input-output technique in conjunction with probe-vehicle trajectory to estimate queue lengths in real time. Efforts have also been made to implement the theoretical input-output technique developed by Lawson et al. into a simulation environment to estimate queues. Sensitivity analysis was conducted to examine the performance of the algorithm for several percentages of probe-vehicle penetration rates.

The proposed methodology is the first attempt of detailed research that uses GPS-based probe-vehicle data as the main inputs and also employs an input-output technique to construct the necessary cumulative plots for queue estimation. In addition, the technique can be easily applied in real-world traffic conditions, especially during peak hour periods when the traffic condition is assumed to remain constant. Analysis during the peak period is important, as several roadway measures of effectiveness, such as vehicle travel times, delays and congestion, are mainly affected during that time.

Critical point identification (Cheng et al. 2011) for the estimation of queues requires shockwave analysis with probe trajectory data. However, the proposed approach shows that probe trajectory data analysis is enough to reflect when and where a vehicle goes into a queue and also departs from the queue, i.e. is somewhat similar to critical points found using shockwave analysis. In such a way, the design and implementation of the proposed technique is quite straightforward and requires less computational effort to estimate bottleneck queues or signalized intersection cycle-by-cycle queues than other probe-based shockwave approaches.

Explicit definition and estimation of the back of queues at any time *t* with the proposed technique reduces confusion arising from several queue definitions used by different authors (i.e. average queue, maximum queue, cycle average, cycle maximum and minimum queue). Nevertheless, the technique is deterministic in nature and cannot be transferred from peak period to non-peak period traffic state estimation without model recalibration.

Table 2.3: Summary of Previous Studies on the Main Queue Estimation Methods

Method	Contributing Authors and Traffic systems	Main Features	Point/Physical Queue	Application	Disadvantages
Input-Output Models	Webster, Newell, Robertson, Gazis, ,Catling, Akcelik, Strong, Lawson et al., Sharma et al., Vigos et al. and many more. Traffic systems: SCOOT, Syncrho,TRANSYT-7F SYNCHRO3 SIGNAL94 PASSER II-90 HCM 2000/ SIDRA CORSIM	- Detector-based vehicle detection upstream from the intersection. - Mainly undersaturated flow regime considered - Steady-state flow condition assumed - Development of traffic systems that employ queue estimation as a basis of delay minimization	- Mainly stacked/point queues are considered - Physical queues are possible when vision processing is incorporated (as a future scope of SCOOT systems)	Mainly signalized intersections. Freeways are also considered in a few studies.	- Detector errors - Steady-state flow condition cannot describe sudden fluctuation of flow - Inability to estimate queues beyond the upstream detector
Shockwave-based Models	Liu et al. (2009)	- Incorporation of high-resolution traffic signal data and advance detector data based on shockwave theory - Break points (where traffic state changes)	- Physical extent of shockwaves are identified and as is the queue.	Signalized intersection	- Detector errors - Cannot deal with Oversaturation and platooned arrivals
	Hao et al. (2010)	Samples travel times from probe vehicle to estimate queuing delay and queue length	- Physical extent of shockwaves.	Isolated intersection	- Minimum 40 percent probe penetration rate needed for better estimates of queue - Vehicle acceleration and deceleration has been ignored
	Cheng et al. (2011)	Shockwave theory based critical point identification for sampled trajectory data to estimate queues	- Physical queue length	Signalized intersection and further research for freeways	- Perfect input data necessary for shockwave analysis - Threshold for critical Point (CP) extraction are not well known

Method	Contributing Authors and Traffic systems	Main Features	Point/Physical Queue	Application	Disadvantages
Direct Estimation Methods	Cheek, M. T. (2007)	- Non-intrusive video imaging technique to detect vehicles - Inclusion of Kalman filtering to minimize error	Physical queue estimation	Freeway and signalized intersection	- Maximum 400 ft queue can be measured - Costly setup for video capture
Conditional Probability Distribution of Probe Vehicles	Cetin et al. (2007)	- An analytical formulation based on conditional probability distributions is developed for estimating the expected queue length based on probe-vehicle location and sample size	Physical queue estimation	Isolated Signalized intersection cases. Freeway scenario can be incorporated with further research effort	- Actual Probe percentages must have to be known -

Chapter Three: Proposed Back of Queue Length Estimation Approaches

3.1 Introduction

The thesis proposes a new dynamic approach to estimate the back of queue (BOQ) lengths based on combining information from probe-vehicle trajectory with an input-output (I/O) diagram. Instead of relying on theoretical free flow and shockwave speed magnitude, this approach extracts the spatial and temporal information of a BOQ directly from probe-vehicle trajectory data, which enables the estimation of the cumulative BOQ curve, *B(t)*, and the cumulative arrival curve, *A(t)*, based on departure rate data from detectors and the trajectory of probe vehicles. This approach is applied for several cases: a fixed bottleneck, a bottleneck induced by an incident, undersaturated and oversaturated signalized intersections.

Moreover, efforts are made to extend the approach of Lawson et al. (1996), based on a more realistic fundamental diagram for the bottleneck cases.

According to the Highway Capacity Manual (HCM, 2010), back of queue (BOQ) is the distance between the stop line of a signalized intersection and the farthest reach (the most distant point of a queue) of an upstream queue, expressed by the number of vehicles. Therefore, in case of a bottleneck queue estimation, we redefine the BOQ by a location further upstream of a queue, where a vehicle experiences significant deceleration (greater than or equal to 3 m/s^2), due to the presence of stopped or very slow-moving vehicle(s) in front of it. In other words, the proposed probe-based approach of BOQ estimation considers stopped, slow-moving and decelerating vehicles as being in the queue.

3.2 Proposed Approaches for a Fixed Bottleneck (Case Study 1a)

3.2.1 Proposed Extension of the Method of Lawson et al.

Several research efforts, such as Brilon et al. (2008), Dervisoglu et al. (2009) and Cassidy et al. (1999), confirm that the capacity of a roadway with a bottleneck can be 2 to 24 % lower than the capacity measured prior to the congestion or with no congestion. Therefore, it is expected that rather than using a basic triangular fundamental diagram as used by Lawson et al. in their research, a more realistic fundamental diagram, such as the one shown in Figure 3.1, that considers a capacity drop can be used to do the necessary analysis of queue estimation. The free-flow speed, v_f, remains the same, but the departure rate from the queue, μ, and the queued speed, v_μ, are more realistic.

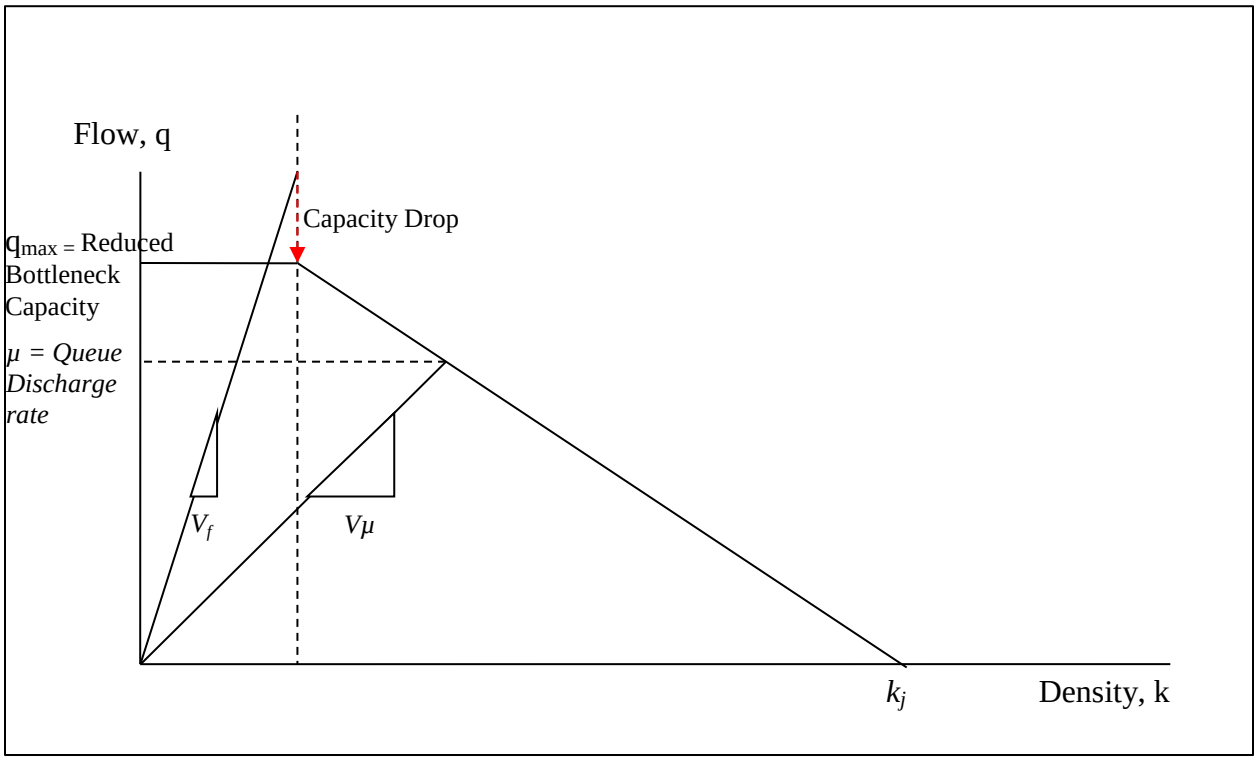

Figure 3.1: Fundamental Diagram for the Extended Lawson et al. Method

3.2.2 Proposed Approach to Dynamically Estimate the Back of Queue using Probes in Combination with an I/O diagram

Consider a long, one lane road segment, *i*, with traffic arriving upstream of the link with an unknown arrival rate, *A(t)*. Assume that a bottleneck exists downstream of this link. Based on deterministic queuing theory, for a queue to form, the departure rate is lower than the vehicle arrival rate. Figure 3.2 shows the cumulative inflow and outflow on link *i*. As illustrated in Figure 3.2, the departure rate is assumed to be constant and is equal to μ. In this figure, the cumulative counts of the vehicle departure rate downstream of link *i* are plotted against time and denoted as *D(t)*. The true cumulative arrival rate upstream of the link is unknown and is denoted as *A(t)*.

The horizontal distance between curves *A(t)* and *D(t)* represents the total travel time of the last vehicle that entered the road segment at time *t*; and, the vertical difference between *A(t)* and *D(t)* represents the storage of vehicles at time *t*. If vehicle trajectories are obtained and if the departure curve is known, the cumulative BOQ and cumulative arrival curve *A(t)* can be estimated without any additional data. The accuracy of the estimation would depend on the percentage penetration rate of probe vehicles.

As shown in Figure 3.3, with the presence of probe vehicles, the trajectory of probe vehicles can be obtained and can be traced on a time-space diagram. From the trajectory data, the deceleration of probes vehicles can be extracted to indicate the time when and location where the probe vehicles join the BOQ. By tracking the trajectories of other probe vehicles exhibiting similar behaviour, the back propagating shockwave speed can also be extracted (dotted blue line in Figure 3.3).

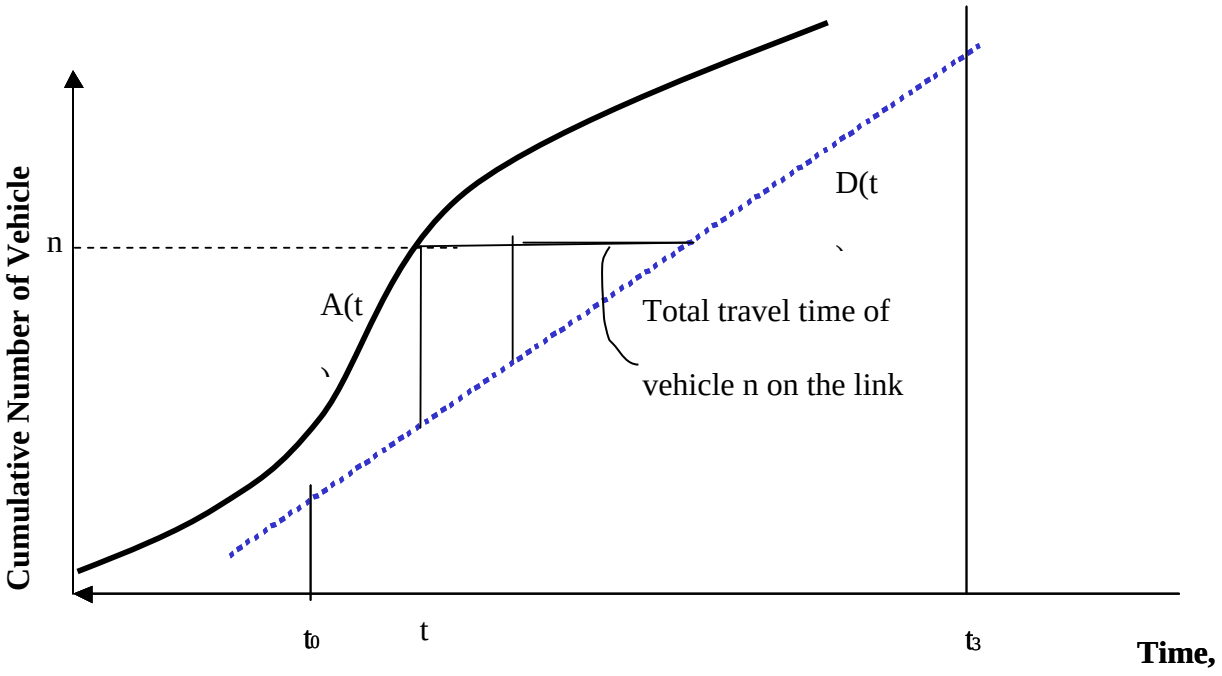

Figure 3.2: Basic Cumulative Input-Output Diagram

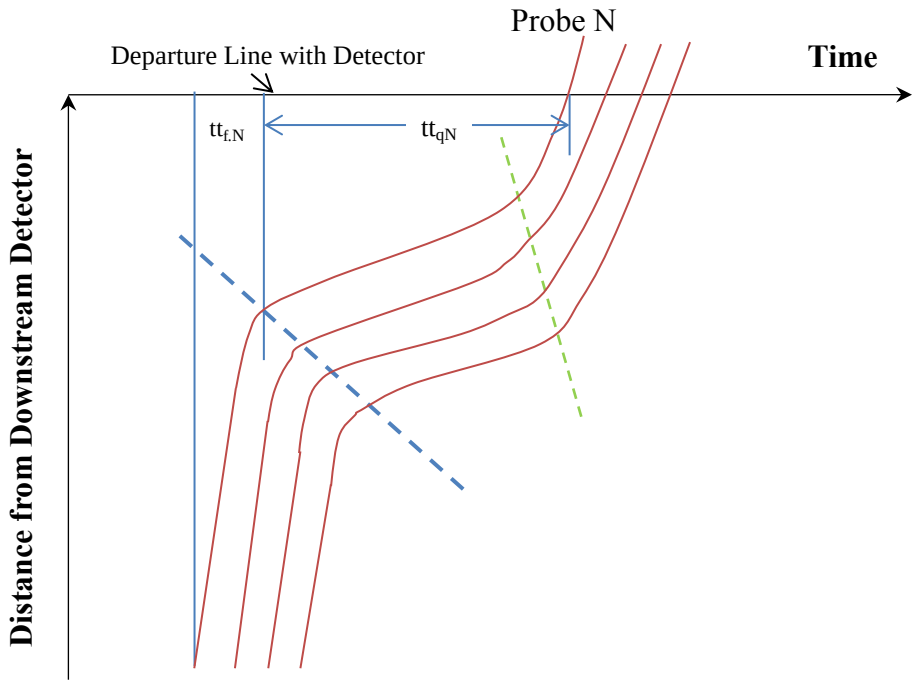

Figure 3.3: Sample Probe Trajectory in Link *i*

The travel time on link *i* can be distinguished into two types: the free-flow travel time, tt_f; and, travel time in the queue, tt_q. The tt_f and tt_q values can be directly extracted from individual probe vehicles. If this information is combined with a known bottleneck departure rate, one can work backward on the cumulative input-output diagram to determine the dynamic evolution of the BOQ and cumulative arrival.

The proposed methodology to estimate the BOQ and cumulative arrival rate can be summarized as shown in Figure 3.4. The cumulative service curve, *D(t)*, which represents the cumulative number of vehicles that have departed from the system (i.e. the cumulative number of vehicles that are able to leave a bottleneck downstream of a link), can be estimated using downstream detector counts. In a bottleneck downstream of link *i*, probe vehicle *N* entering the link at time t_1 will join the BOQ at time t_2 and will leave the bottleneck at time t_3.

Since a probe vehicle can identify its position at a frequent interval, the travel time for the probe vehicles on the link can be obtained from the vehicle trajectory (similar to the one in Figure 3.3). This travel time can be distinguished as tt_f and tt_q and can accordingly be identified in Figure 3.4. Time t_3, when that probe vehicle *N* leaves the bottleneck, can also be stamped and identified on the cumulative departure curve. Working backward to the left tt_q from the point of intersection of a vertical line at t_3 and the cumulative departure curve, the BOQ at time interval t_2 can be identified. The tt_q of that particular vehicle can be determined from the time-space diagram (Figure 3.3). The new point corresponds to the BOQ at time interval t_2. By moving backward to the left from that latter point by tt_f, the cumulative arrival can be identified similarly. As long as the bottleneck is active, this process can be repeated for every probe vehicle. Consequently, the

cumulative arrival curve, *A(t)*, and the BOQ curve, *B(t)*, can be reconstructed by linear regression fitting of consecutive estimated points.

The strength of this approach is that same procedure can be used for any departure rate, even if the departure is not constant. However, in the case of a changing departure rate, the departures rate should be counted by a detector. A similar procedure can be used for the case of a pulsed departure rate, such as in the case of a signalized intersection, as discussed in Section 3.4.

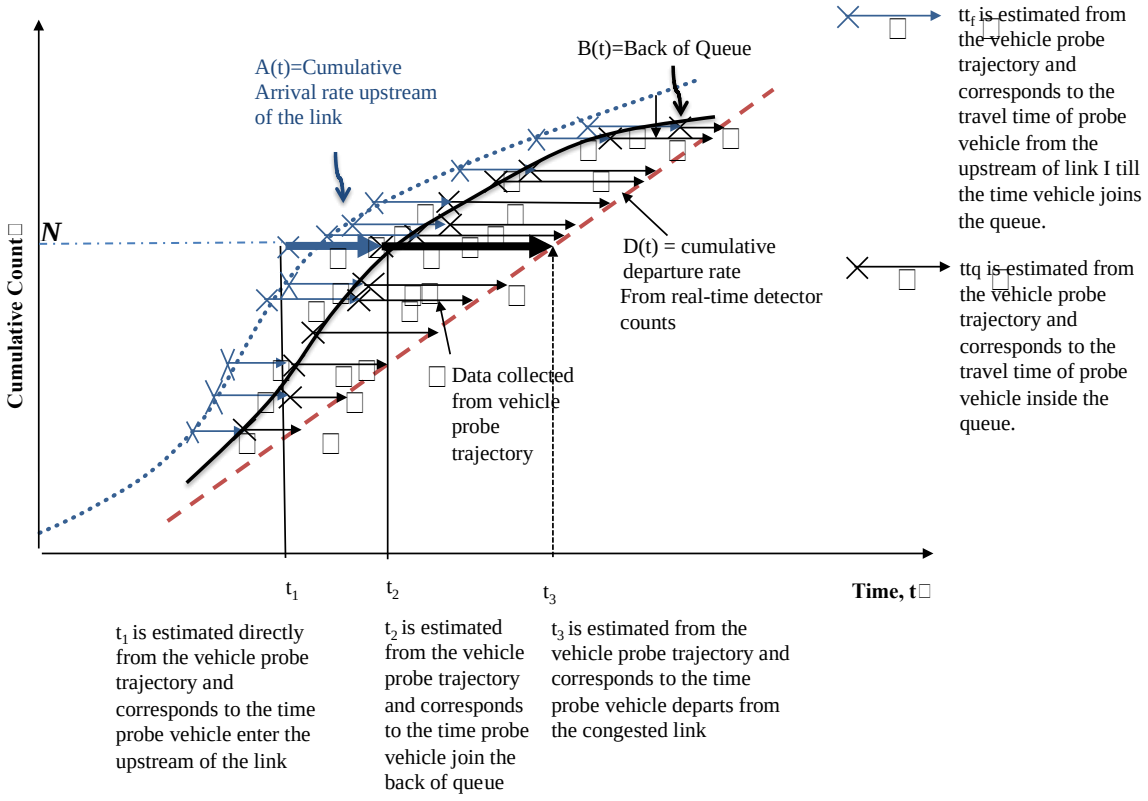

Figure 3.4: Estimation of Dynamic Back of Queue and Cumulative Count for a Bottleneck from Probe-Vehicle Trajectory and Input-Output Diagram

3.2.3 Conclusion

The proposed methodologies have been discussed in Sections 3.2.1 and 3.2.2 for the fixed bottleneck scenario, i.e Case Study 1a. The flowchart in Figure 3.5 illustrates the generalized steps of the queue estimation procedure for both of the methods. The proposed extension of the Lawson et al. method discussed in Section 3.2.1 mainly reconstructs a fundamental diagram based on the sampled simulation data obtained from Paramics simulation software; and, the probe-based method uses trajectory analysis and combines it with an input-output technique.

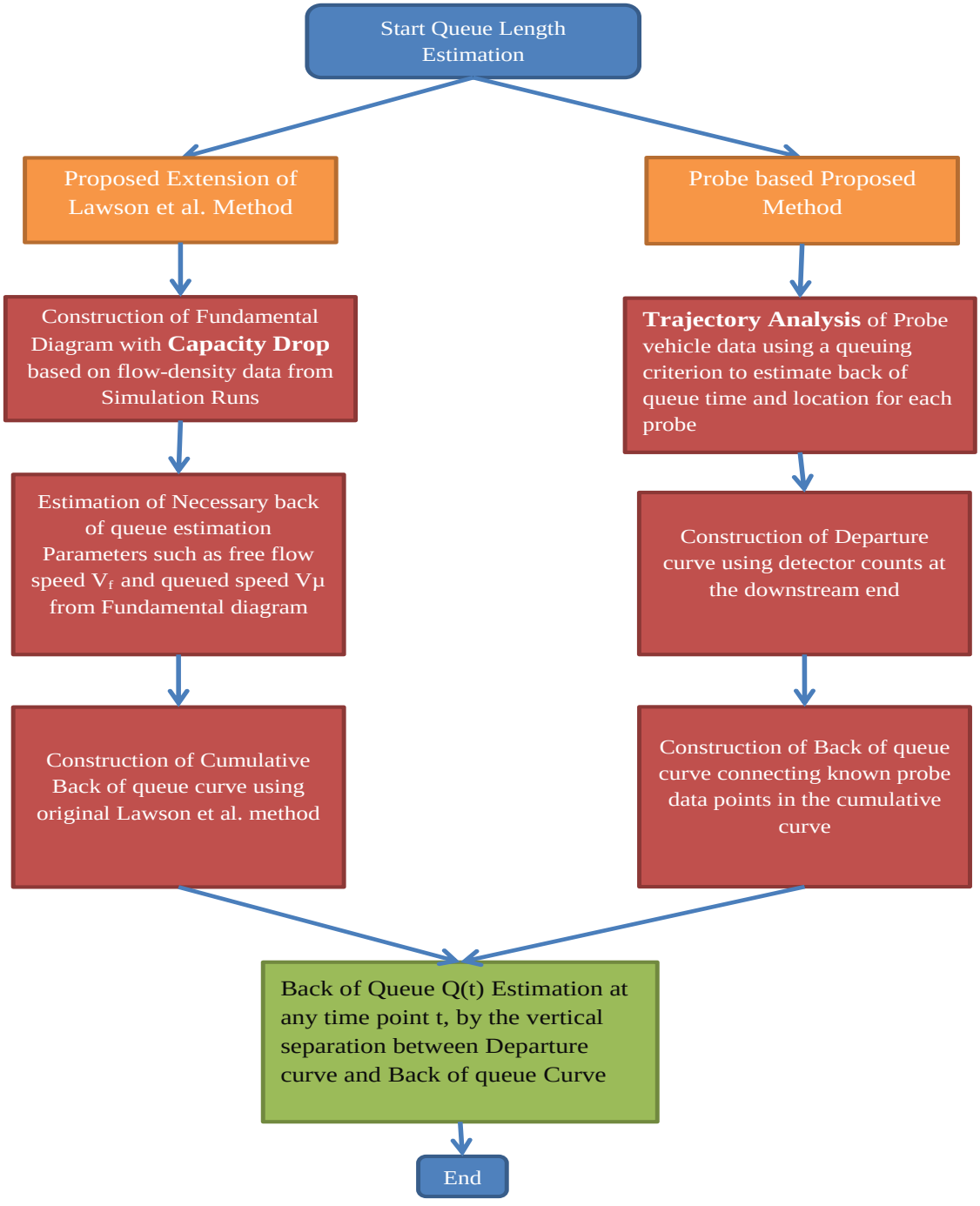

Figure 3.5: Proposed Methodical Flowchart for Case Study 1a (Fixed Bottleneck)

3.3 Proposed Approaches for a Bottleneck due to an Incident (Case Study 1b)

Two approaches similar to the ones mentioned in Sections 3.2.1 and 3.2.2 are proposed for a bottleneck due to an incident (Case Study 1b). In an incident scenario, suppose for a two-lane roadway, a lane is closed for a certain time due to an accident, during which it is assumed that each lane flow has been equally halved. After the accident lane is opened again, the flow goes back to the normal flow situation. Therefore, in this case, the queue estimation methodology of Lawson et al. (1996) discussed in Section 2.8.2 can be applied (departure rate changing once) to estimate queues on each lane separately. An extension of the Lawson et al. method can be proposed, considering a similar bottleneck capacity drop as discussed in Section 3.2.1 with the methodology almost similar to that of Lawson et al.

The proposed method using probe data and detector counts in conjunction with I/O diagram for this incident case is also quite straightforward and similar to the methodology discussed in Section 3.2.2. The basic difference with the methodology mentioned in Section 3.2.2 is that the departure rate during the lane closure is assumed to be equally halved between two lanes and that each lane is analyzed separately for BOQ estimation. It is also assumed that vehicles only change lanes just before the accident site to pass the bottleneck, maintaining FIFO (first in first out) flow characteristics. A simple methodical flowchart for the proposed techniques for this case study is shown in Figure 3.6.

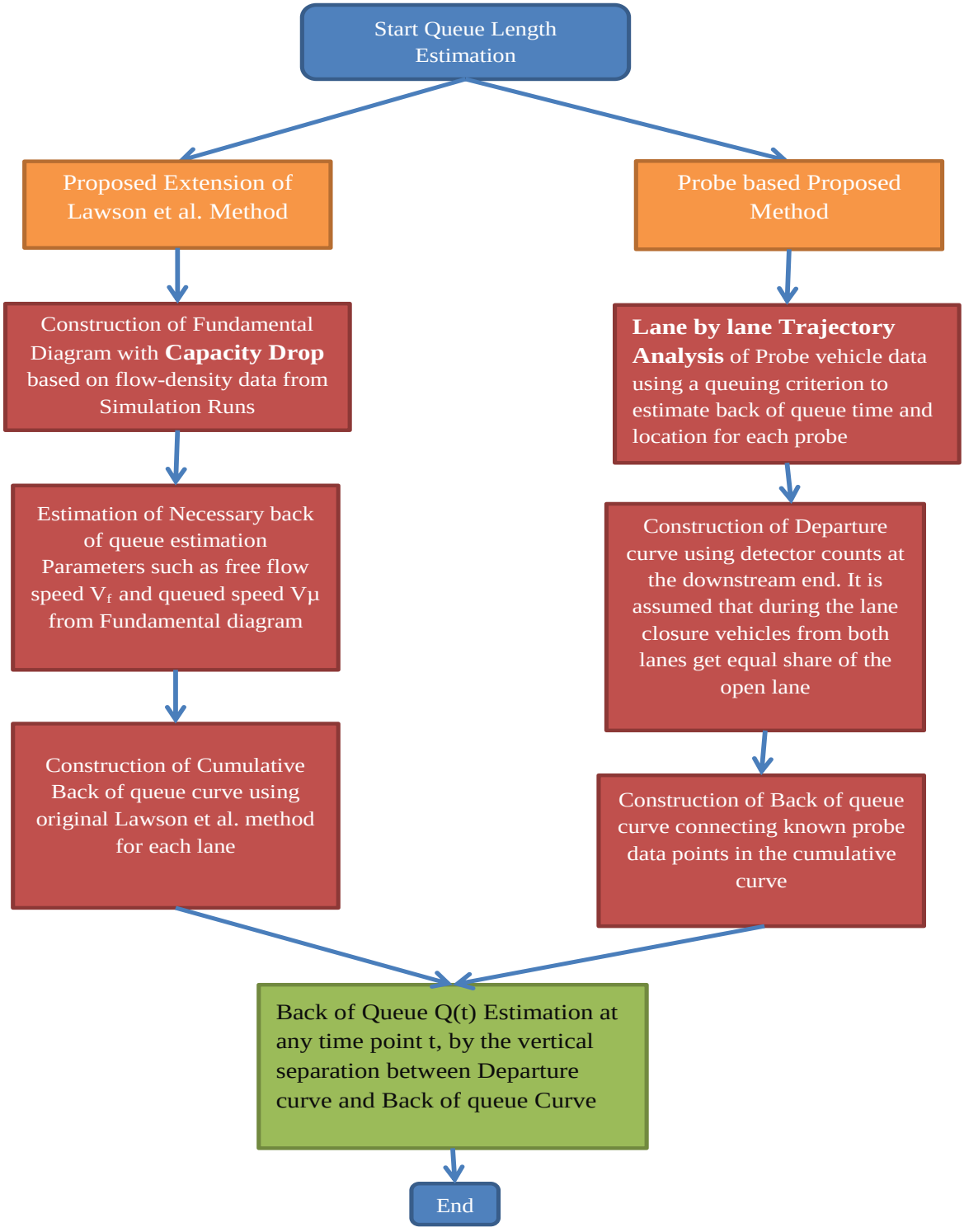

Figure 3.6: Proposed Methodical Flowchart for Case Study 1b (Incident Case)

3.4 Proposed Approaches for Signalized Intersections

3.4.1 Undersaturated Signalized Intersection (Case Study 2a)

The approach of queue estimation proposed in the previous section can also be used to estimate queues in an undersaturated intersection scenario. By undersaturation we mean that all vehicles stranded in a cycle of traffic signal can successfully clear themselves from the intersection during the green interval of that cycle. Similar to the previous section of proposed methodology, this method also relies on detector counts at the downstream stop line and true trajectory data of probes to estimate the BOQ location and time for probes and consequently the BOQ curve, *B(t).*

From the trajectory plot shown in Figure 3.7, the deceleration of probe vehicles is shown and can indicate the time and location the probe vehicles join the BOQ. This can also be used to estimate the back propagating shockwave, shown by line *LK*. The acceleration time points and corresponding locations of probes after being in the queue can also be found from the trajectory data (line *JK*). The utility of line *JK* lies in the estimation of point *K*, which is the intersection point of two known lines, *JK* and *LK*. Point *K* denotes the cessation of queue accumulation and also suggests that any vehicle coming after time point t_k is not counted as being in the queue in the cumulative input-output diagram. The quality of the queue estimation for signalized intersections is largely based on successfully estimating point *K*.

The free-flow travel time, tt_f, and travel time in the queue, tt_q, for any probe can also be found from the trajectory data, as shown in Figure 3.7. If these data are combined with a known bottleneck departure rate, one can work on the cumulative input-output diagram to determine the dynamic evolution of the *B(t)* curve and the cumulative arrival curve, *A(t).*

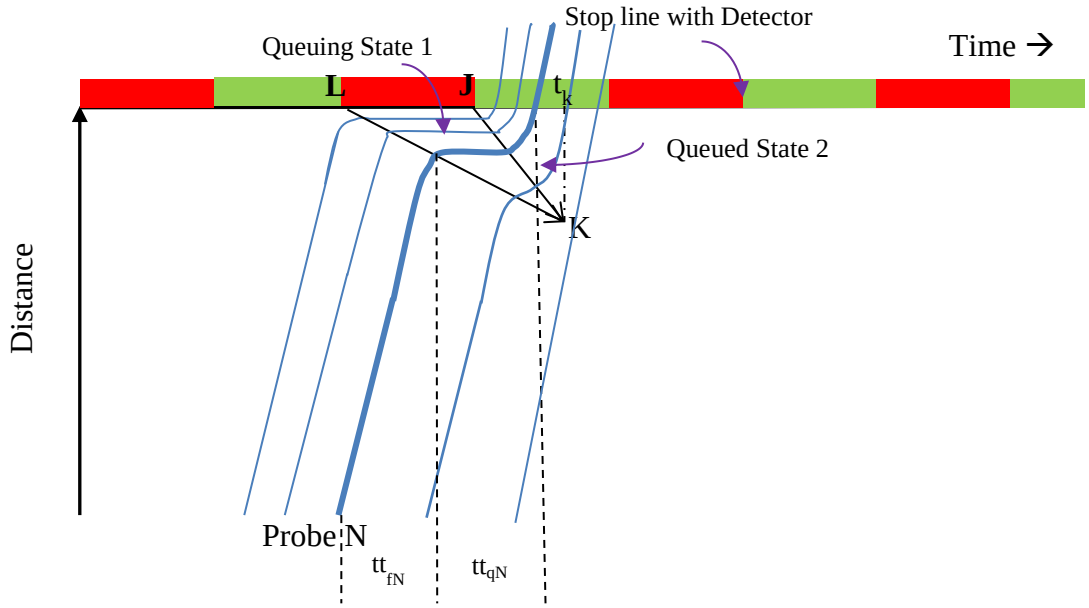

Figure 3.7: Theoretical Time-Space diagram (Undersaturated Condition)

Figure 3.8 illustrates the queue estimation process on a cumulative diagram. With a known departure time of each vehicle (detector data), it is possible to draw the departure curve, *D(t)*. The known free-flow travel time, tt_f , and travel time in the queue, tt_q, for probe *N* found using probe trajectory data analysis helps to determine the BOQ and arrival point for that probe. This process should be repeated for every probe vehicle as long as point *K* is reached in the cumulative diagram. Point *K* and its corresponding time point, t_k, are plotted in Figure 3.8 with the help of probe trajectory data. *K* denotes the last queued vehicle; and, beyond time t_k, queue accumulation ceases, and new vehicles arriving beyond time t_k are not included in the queue calculation. Consequently, the cumulative arrival curve, *A(t)*, and *B(t)* curve can easily be constructed using linear regression fitting of the estimated points. A simple methodical flow chart in Figure 3.9 illustrates the general methodology explained above.

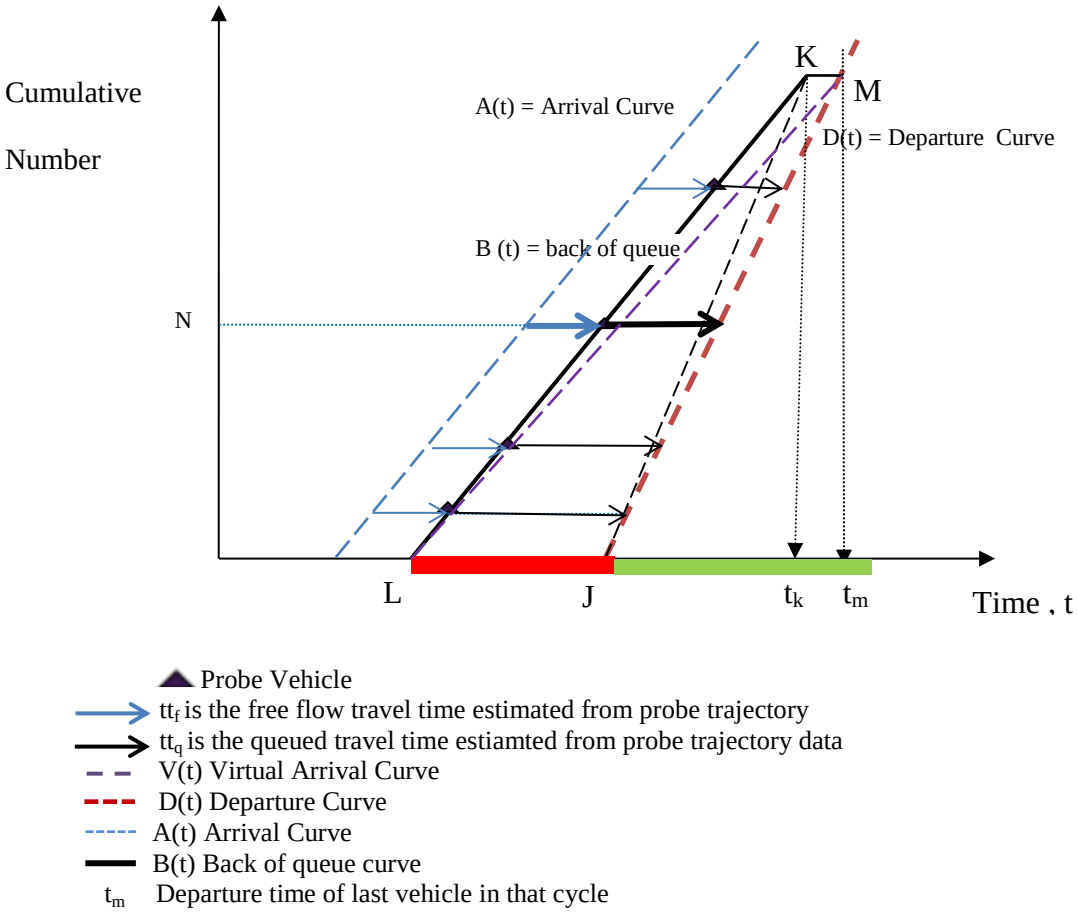

Figure 3.8: Estimation of Dynamic Back of Queue and Cumulative Count from Prove-Vehicle Trajectory and Input-Output Diagram in an Undersaturated Intersection

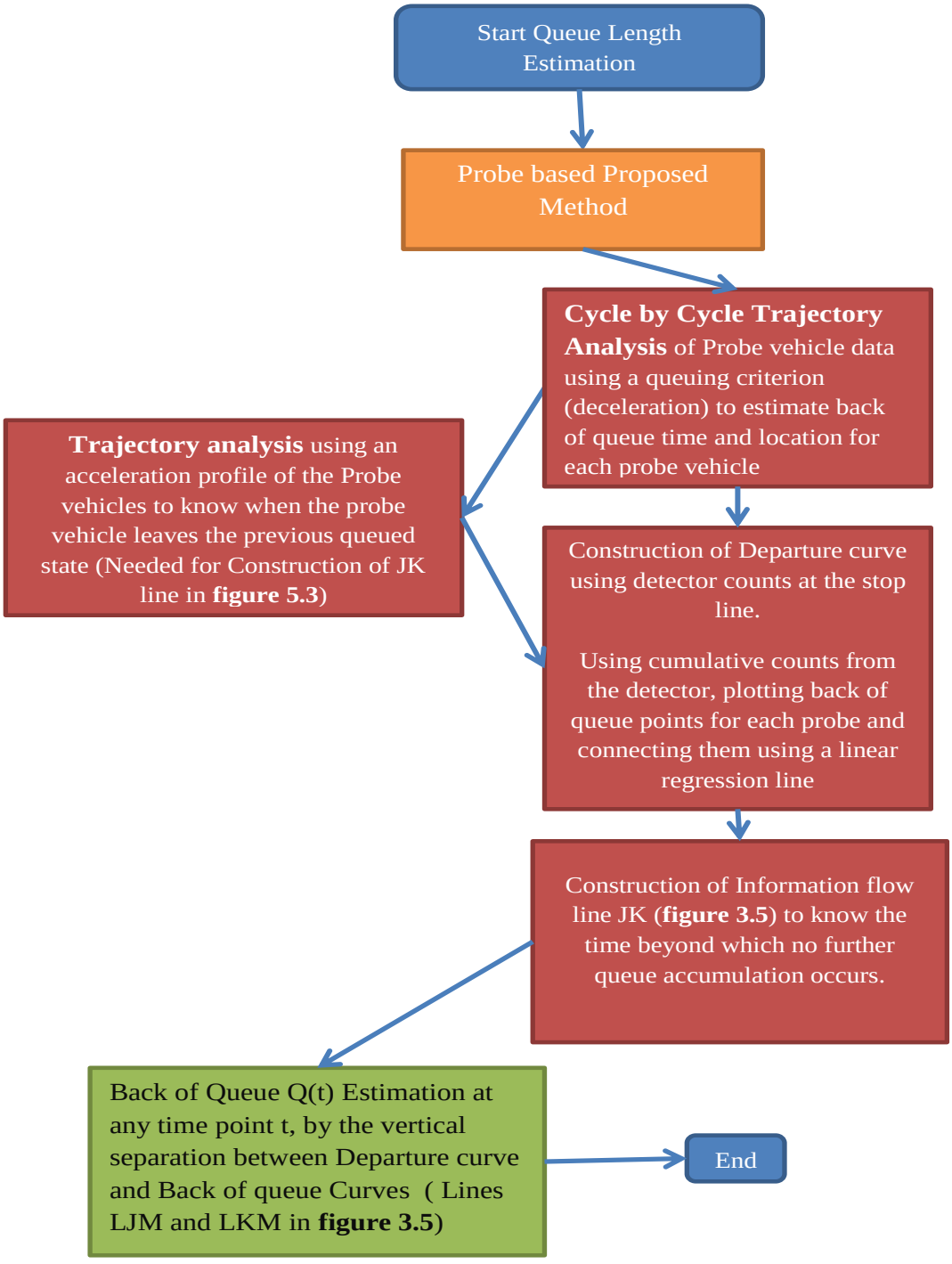

Figure 3.9: Proposed Methodology Flowchart for Case Study 2a (Undersaturated Signal)

3.4.2 Oversaturated Signalized Intersection (Case Study 2b)

By oversaturation we generally mean the demand at a signalized intersection exceeds the available service rate. In other words, when vehicles are stranded during one signal cycle and require one or more additional cycles to clear themselves from the intersection, the phenomenon is called oversaturation, and the intersection is called oversaturated. In the previous section, the queue estimation technique for an undersaturated signalized intersection has been proposed only using probe trajectory data and detector-based departure vehicle counting. A similar methodology can be employed for oversaturated conditions to estimate BOQ in number of vehicles.

Figure 3.10 illustrates a typical time-space diagram of probe vehicles in an oversaturated intersection with a few signal cycles. Unlike the undersaturated condition, some probe vehicles (such as probe *N* in Figure 3.10) in an oversaturated intersection face at least two queued states with two notable deceleration points (B_{N1} and B_{N2} for probe *N*) in their trajectory. The estimation methodology of the queue cessation point (point K) for each cycle is similar to that of the under saturated condition mentioned in the previous section. Points K_1 and K_2 are the two queue cessation points for the two consecutive signal cycle, as shown in Figure 3.10.

Figure 3.11 is the cumulative input-output diagram for an oversaturated condition. The corresponding time-space diagram is Figure 3.10. The departure curve is known from the detector counts at the stop line and is shown as a red line. For each probe vehicle, as the queued travel time, tt_q, is known from the trajectory data of each individual probe vehicle, the BOQ point can be found working from right to left in the cumulative diagram. When point *K* and corresponding time, t_k, for an individual cycle is determined from probe trajectory data, *K* marks

the cessation of queue accumulation for that particular signal cycle; therefore, the BOQ curve, *B(t)*, remains horizontal until the next green phase starts.

Finally, *B(t)* for each particular cycle can easily be estimated by the linear regression of the estimated BOQ points. It is expected that the greater the percentage of probe vehicles in the traffic stream, the greater the accuracy of the estimation of point *K* and, thus, queue propagation. The vertical separation between *B(t)* and departure curve *D(t)* in the cumulative diagram estimates the queue.

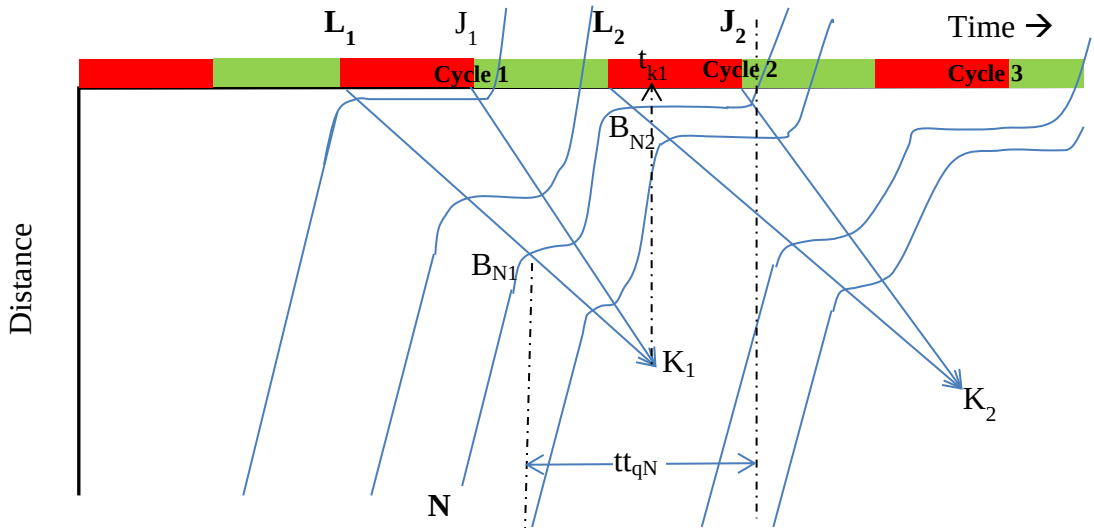

K = K_1,K_2 = point of queue cessation for cycle 1 and 2 respectively

Figure 3.10: Time-Space Diagram in an Oversatured Intersection

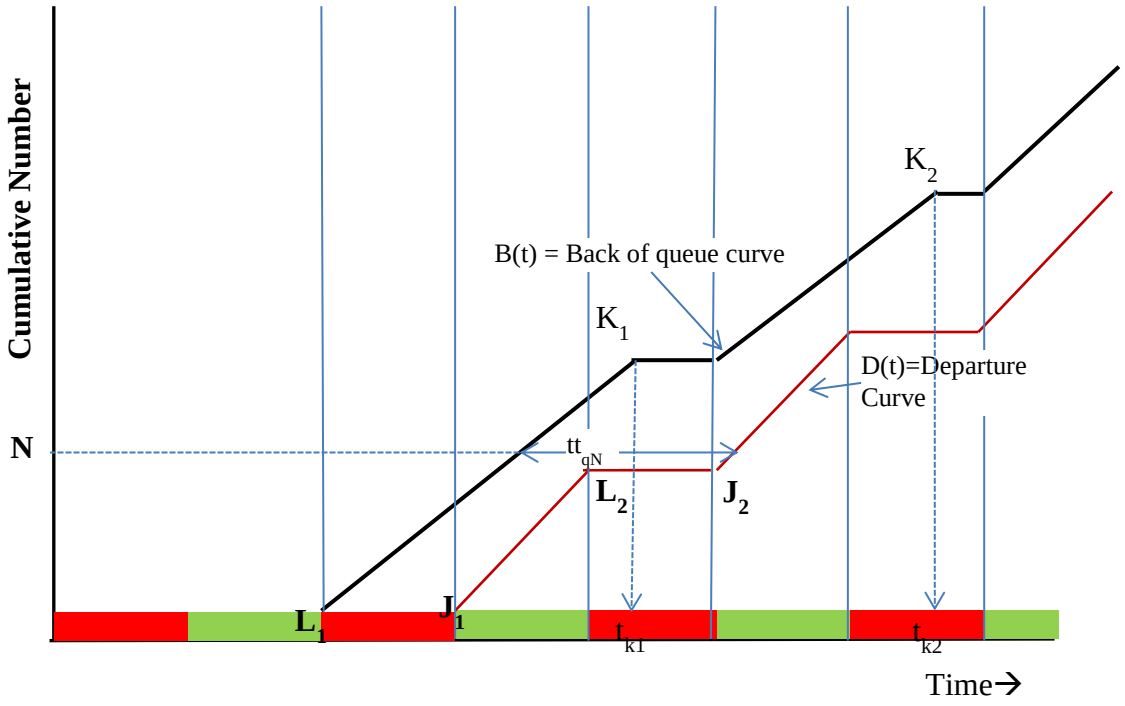

Figure 3.11: Back of Queue Estimation from Probe-Vehicle Trajectory and Detector Data

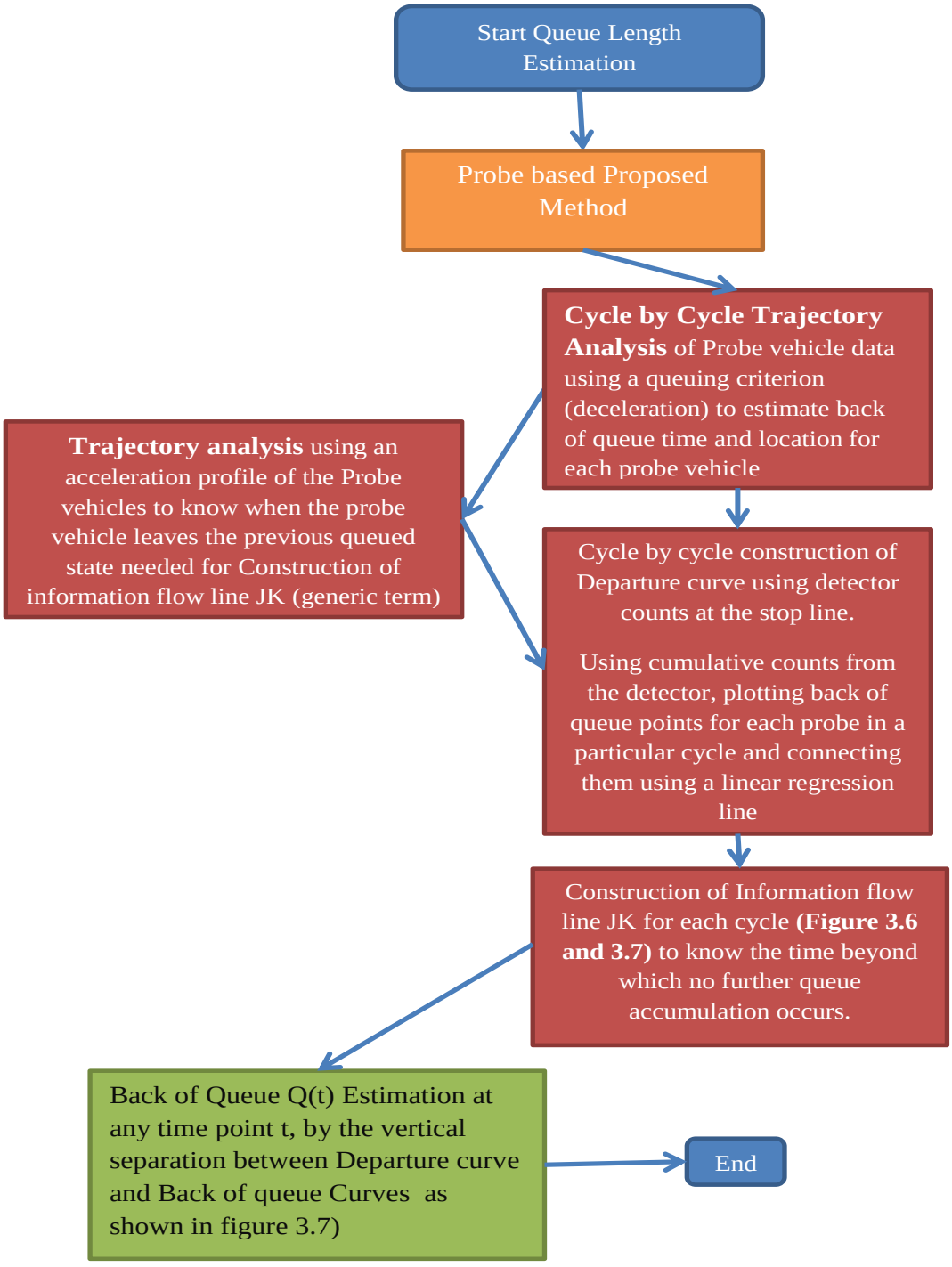

Figure 3.12: Proposed Methodology Flowchart for Case Study 2a (Oversaturated Signal)

3.5 Summary

This chapter proposes simple dynamic approaches for different congestion scenarios and an extension of the method of Lawson et al. (1996) to identify the BOQ in cases of roadway bottlenecks. All of the methods can easily be implemented on a simple spreadsheet. The next chapter describes the design and application of the proposed frameworks to several case studies in a microsimulation environment. In addition, the performance of the proposed probe-based approach was tested for various percentages of probe-vehicle penetration rates and compared with the BOQ estimated through the Lawson et al. method.

Chapter Four: Simulation Modelling and Results Analyses of Case Studies

4.1 Introduction

This chapter describes the case studies designed in Quadstone Paramics simulation software (Version 6.9). Two main experiments were designed: 1) a bottleneck scenario, and 2) a signalized intersection scenario. The bottleneck scenario considered two cases:

1. Case Study 1a: Queue on a main link due to a bottleneck induced by a merging lane/ramp; and,
2. Case Study 1b: Queue on a two-lane roadway due to a 15-minute lane closure resulting from an accident.

For the signalized intersection scenario, two separate case studies were also examined:

1. Case Study 2a: Queue length in an undersaturated signalized intersection; and,
2. Case Study 2b: Queue length in an oversaturated signalized intersection.

The methodologies presented in Chapter 3 were applied; and, the related data analysis and results are presented. For each case study, the methodologies described in Chapter 3 for each roadway scenario were examined and compared to the model of Lawson et al. (1996). The statistical errors showing the difference between the estimated and actual observed queues were also obtained, in order to examine the estimation robustness of the developed models.

4.2 Description of the Simulated Bottleneck Scenarios

4.2.1 Simulation Network Design: Case Study 1a

The network for this scenario consisted of a one-way single-lane roadway and a merging ramp. Vehicles were assumed to move eastbound (Figure 4.1). The horizontal roadway link carried the major flow, and the merging link created an active bottleneck and, thus, a growing upstream queue. Detector 1 was placed just upstream of the bottleneck region on the horizontal lane, in order to count departures from the queue created on the horizontal lane. Detector 3 measured the ramp flow, and Detector 2 measured the combined flow of the horizontal lane and the ramp needed for the fundamental flow-density (q-k) diagram construction. The roadway geometry, road traffic and driver behaviour parameters considered in the simulation are listed in Table 4.1:

Table 4.1: Parameters Considered for the Simulation Network Design of Case Study 1a

Horizontal Link Length	2045 metres
Speed Limit on Horizontal Lane	80 km/hr
Speed Limit on Merging Ramp	50 km/hr
Mean Target Headway	2 seconds
Mean Driver Reaction Time	1.5 seconds
Minimum Gap	2 metres
Lane Width	3.7 metres
Link Category	Urban
O-D (Origin-Destination) Demand (Zone 1 to Zone 2)	1800 veh/hr/lane
O-D Demand (Zone 3 to Zone 2)	720 veh/hr/lane
Average Driver Familiarity	90 percent

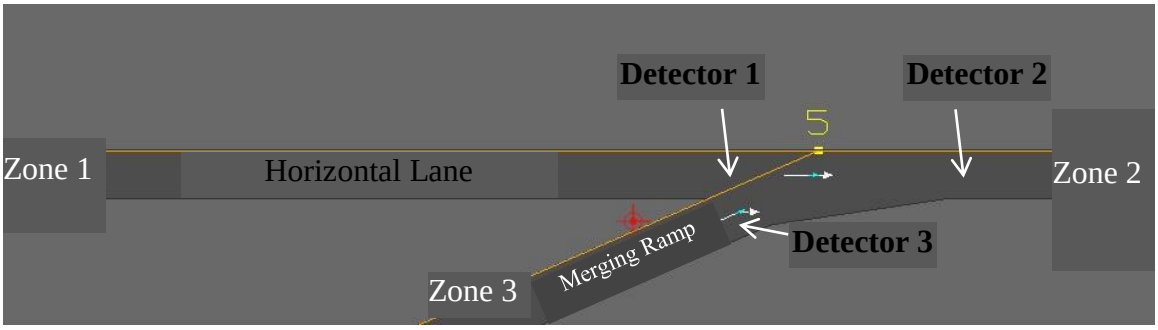

Figure 4.1: Simulation Network for Bottleneck Case Study 1a

4.2.2 Simulation Network Design: Case Study 1b

The queue estimation conducted in this section considered the case of two lanes (Figure 4.2). Lane 1 remained closed for 15 minutes, due to an accident, and gained normal two-lane service after that 15-minute period, as shown in Figure 4.3. White arrow lines in Figures 4.2 and 4.3 show the direction of vehicular movement in the network. To maintain a FIFO (first-in, first-out) state, lane changing was restricted. Vehicles in lane 1 could change lanes just before the lane closure location (yellow lines), thereby maintaining a FIFO traffic state. Both lanes were equipped with detectors at the same downstream location, as shown in Figure 4.3. All other road traffic and driver behaviour parameters are listed in Table 4.2.

Table 4.2: Parameters Considered for the Simulation Network Design of Case Studies 1b and 1c

Link Length (Both Lanes)	2045 metres
Speed Limit on the Link	80 km/hr
Mean Target Headway	2 seconds
Mean Driver Reaction Time	1.5 seconds
Minimum Gap	2 metres
Lane Width for Each Lane	3.7 metres
Link Category	Urban
O-D Demand	3600 veh/hr
Average Driver Familiarity	90 percent

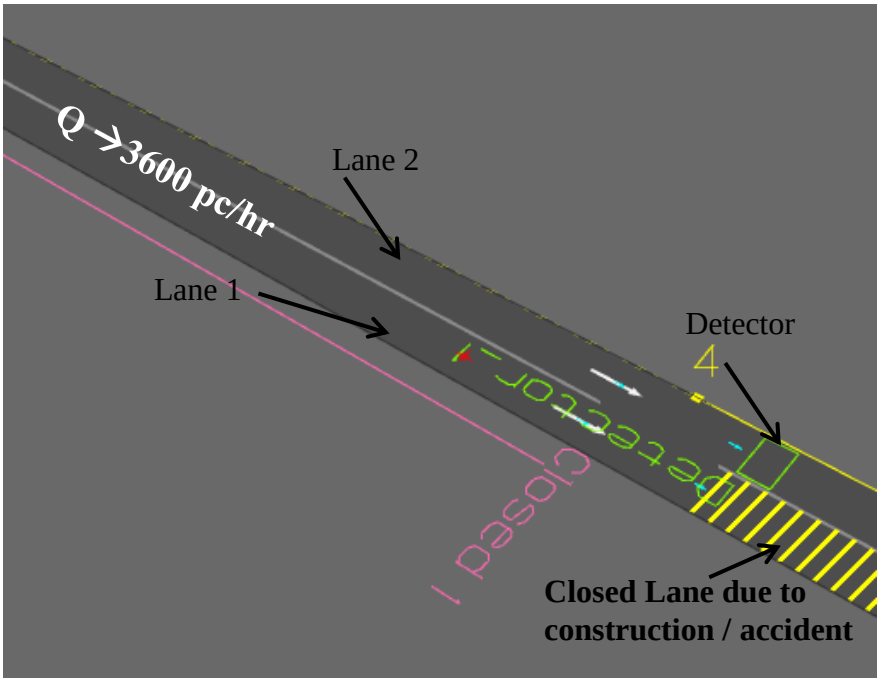

Figure 4.2: Simulation Network for Bottleneck Case Study 1b

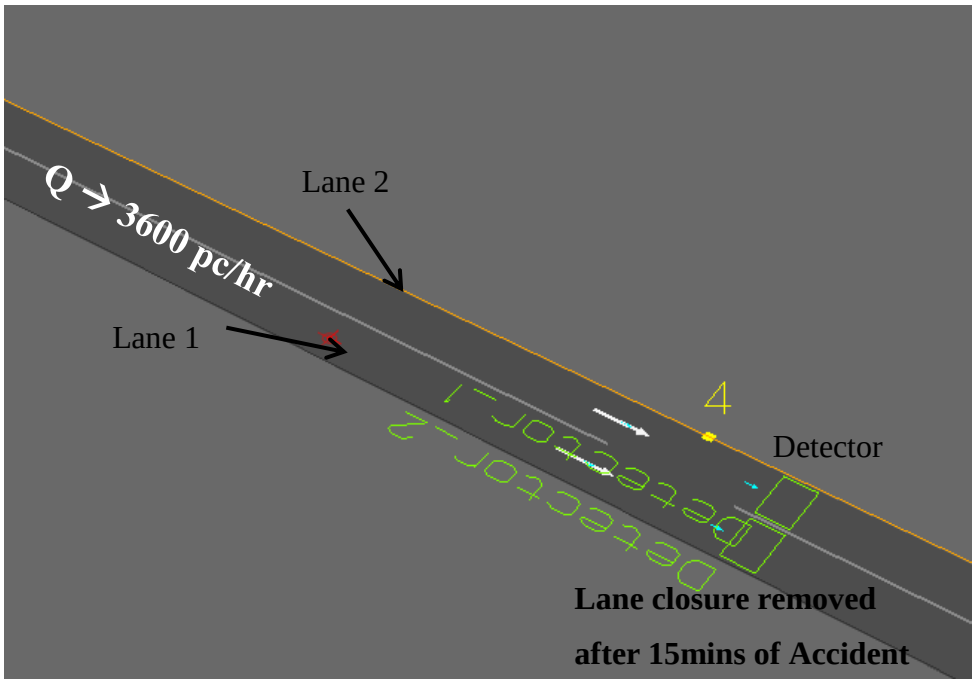

Figure 4.3: Simulation Network for Bottleneck Case Study 1b (Lane Closure Removed)

4.2.3 Simulation Runs: Case Studies 1a and 1b

For Case Studies 1a and 1b, a one-hour long simulation collected temporal and spatial measures of all vehicles going from zone 1 to zone 2 (Figure 4.1) at one-second intervals. The simulation for all case studies considered probe-vehicle penetration rates of 10, 20, 30 and 40%. For each probe percentage, ten runs corresponding to ten different seed values were considered; therefore, for each probe percentage scenario, ten different simulation trials were carried out for data acquisition. It is to be noted that, if the same seed value was used across multiple runs, the results would remain exactly the same; therefore, random seed values have been used, and averaged queue and error estimates were obtained at the end of the analysis after applying the proposed methods. Table 4.3 summarizes the design of the simulation runs for Case Studies 1a and 1b.

Table 4.3: Design of Simulation Runs for the Bottleneck Scenarios

Probe Percentages	10%, 20%, 30%, 40%
Simulation Trials for Each Probe Percentage	10 runs (using 10 random seeds)
Simulation Period for Case Study 1a	1 hour
Simulation Period for Case Study 1b	1 hour
Warm-Up Period	15 minutes
Lane Closure due to Accident	15 minutes
Data Obtained	• Lane-by-lane trajectory data of all probe vehicles • Detector data (vehicle count) at departures

4.2.4 Simulation Data for Bottleneck Scenarios: Case Studies 1a and 1b

The simulation data obtained for analysis contains spatial and temporal data of probe vehicles with known penetration rates and detector counts at the departure point. Time and speed data collection for a portion of the whole vehicle population was possible for vehicles equipped with modern devices, such as GPS (Global Positioning System) units and on-board cellphones with location services enabled (Cheng et al., 2011; Ban et al., 2011). These vehicles can act as probes and reflect the speed of the traffic stream.

Such probe vehicles were simulated in Paramics simulation software, defining a specific vehicle type (passenger cars). In other words, probe-vehicle data were a subset of the main database of all vehicles in the simulation and could be separated by assigning a particular vehicle type number for the probes (passenger cars in this study). Figures 4.4 and 4.5 shows two three-

dimensional snapshots taken from the Paramics simulation software for two scenarios of queue estimation upstream of a bottleneck, where probe vehicles are represented as green cubes.

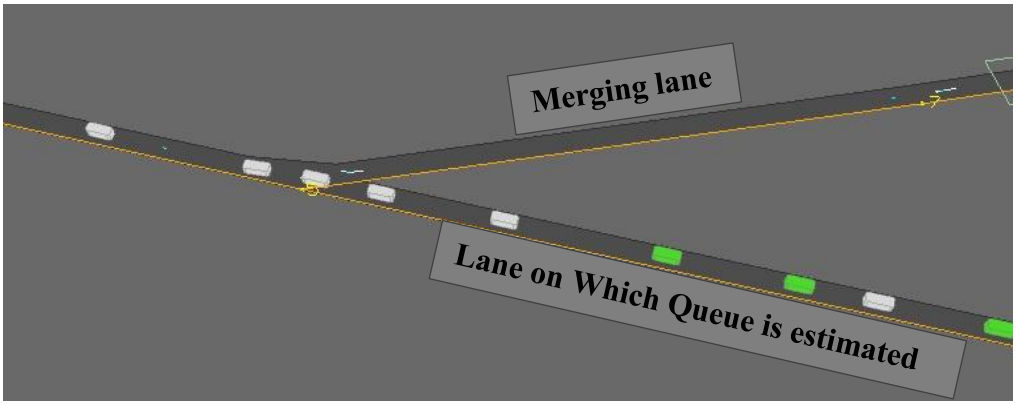

Figure 4.4: Roadway Bottleneck Scenario and Associated Queue (Partial) in the Simulation Network for Case Study 1a

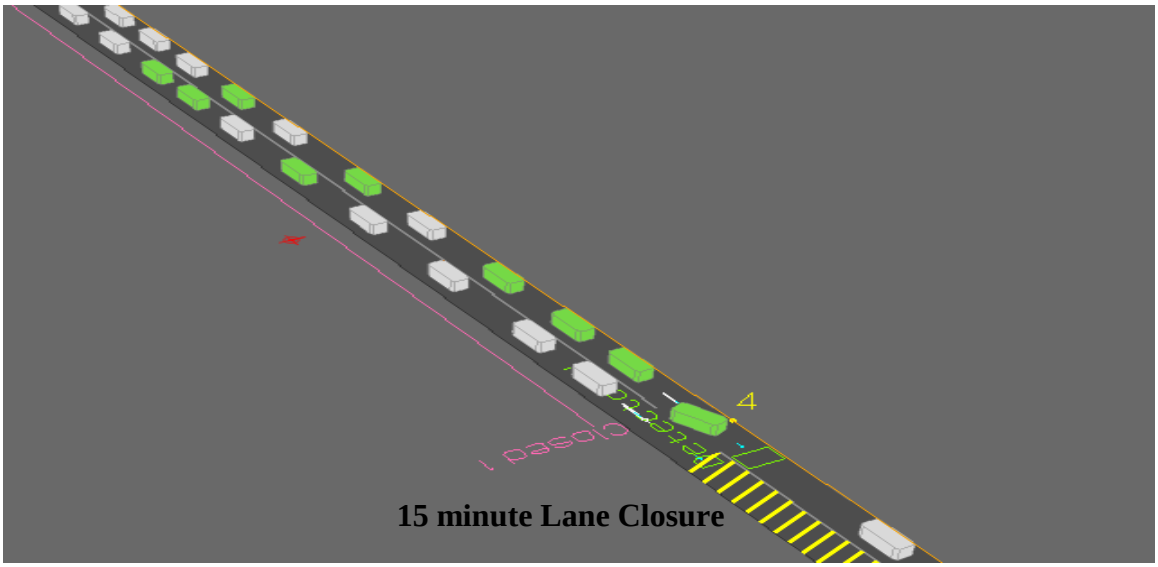

Figure 4.5: Roadway Bottleneck Scenario and Associated Queue (Partial) in the Simulation Network for Case Study 1b

4.3 Analysis Results of the Freeway Bottleneck Scenarios

The results of the two bottleneck case studies were examined separately as a bottleneck on the main link, due to a merging link, and a bottleneck over a two-lane roadway, due to a lane closure for 15 minutes.

4.3.1 Case Study 1a: Bottleneck on the Main Link due to a Merging Ramp

To estimate the queue three different techniques are used: the proposed models outlined in chapter 3 and the original Lawson's et al. (1996) model. Queue estimates of each of these models are compared with the observed queue to estimate the accuracy of each model.

4.3.1.1 The Model of Lawson et al.

The method of Lawson et al. (1996) was applied to the simulated data. It was used as a base of comparison. It was assumed that the arrival time of each vehicle was known during the one-hour analysis period. Necessary parameters, such as free-flow speed and queued speed, were estimated from a basic triangular flow-density diagram that was calibrated based on data collected from simulation trials.

To apply the Lawson et al. method of queue estimation, it was necessary to construct a fundamental diagram. Figure 4.6 shows a fundamental diagram constructed using randomly sampled flow and density data from simulation using concepts from previous research done by Dervisoglu et al. (2009). The steps to construct the triangular fundamental diagram and obtain necessary parameters in this research were:

1. A horizontal line (blue line in Figure 4.6) was drawn through the maximum possible flow point/points (1680 veh/hr/lane), which can also be defined as the capacity point according to Highway Capacity Manual (HCM 2010) definition of capacity.
2. Based on the speed limit of the link (80 km/hr for case study 1a), it was possible to fix upon an initial critical density of 21 veh/km/lane (1680/80).
3. A linear regression line (green line in Figure 4.6**)** was plotted for the uncongested points with density value less than 21 veh/km/lane, constrained to pass through the origin to resemble a triangular fundamental diagram. The intersection point of the blue and green lines in Figure 4.6 was termed as $Q_{capacity}$ on the vertical axis; and, the same point, when projected down on the horizontal axis, defined the actual critical density (k_{crit} = 21 veh/km/lane).
4. The free-flow speed, V_f, could be found averaging the speed of all the sample points with density values of less than k_{crit} (21 veh/km/lane).
5. Assuming that a vehicle consumes 9 m of space in a highly congested queue, a jam density (kj) value could be fixed at 110 veh/km/lane. Finally, both k_j and $Q_{capacity}$ were connected with a line (purple line in Figure 4.6**)** to finalize a triangular flow-density diagram necessary for the Lawson et. al. back of queue (BOQ) estimation process.
6. The queue departure rate from the main lane was found by subtracting the ramp flow from the bottleneck capacity. Accordingly, as shown in the fundamental diagram in Figure 4.6**,** the density of the queue could be found as the density corresponding to the queue departure rate. Thus, the queued speed, V_μ, could be calculated bt dividing queued departures by density of the queue (Figure 4.6).

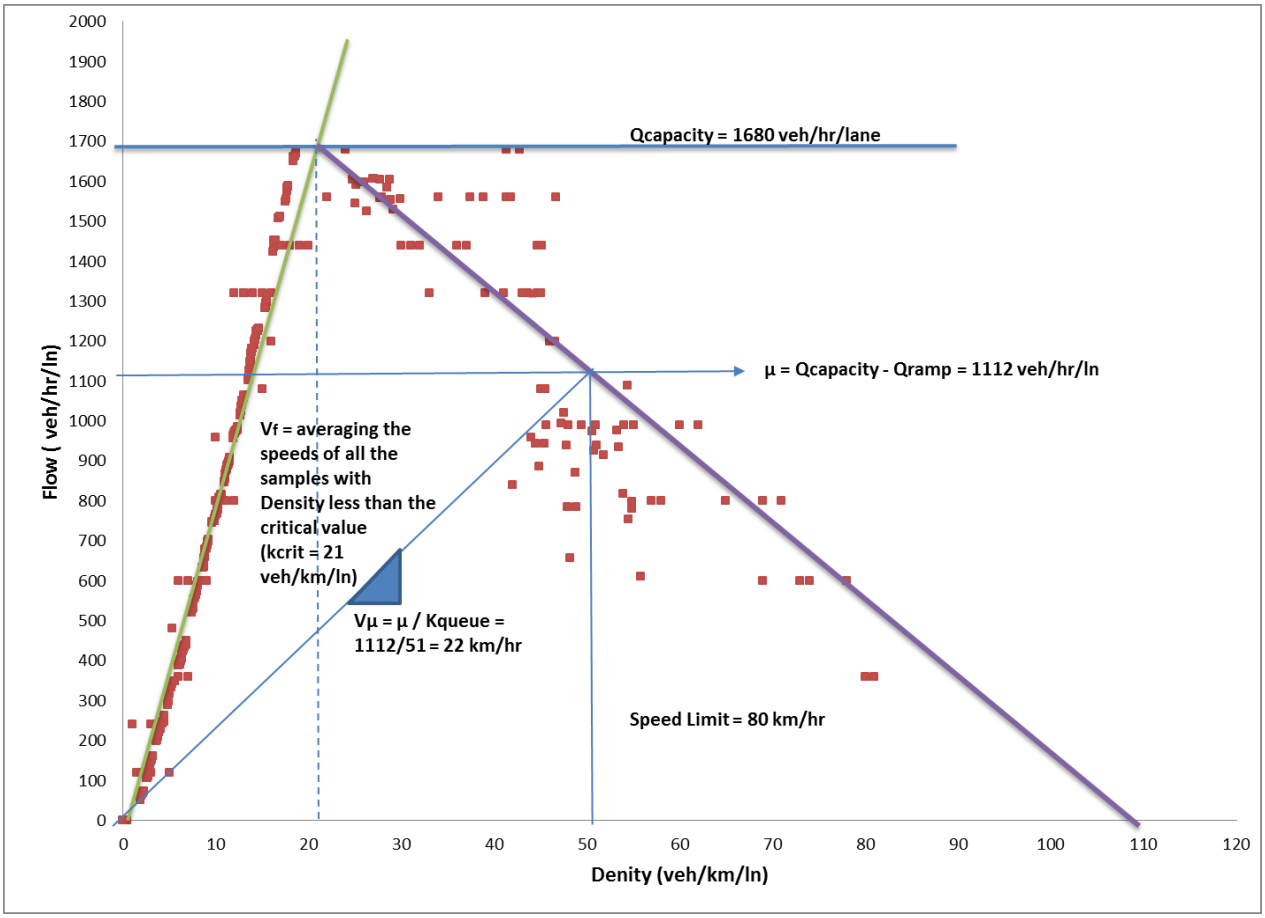

Figure 4.6: Triangular Fundamental Diagram for the Method of Lawson et al.

The necessary parameters for queue estimation needed by the Lawson et al. method from the fundamental diagram shown in Figure 4.6 are summarized in Table 4.3.1.

It is to be noted that Dervisoglu et al. (2009) fitted the congested branch of the fundamental diagram by an approximate quantile regression of the flow-density points on the higher end of their distribution, constrained to pass through the capacity point. This procedure also yielded a linear line skewed outward from the congested flow-density points, confirming the validity of the congested branch constructed for this research using the steps mentioned above.

Table 4.3.1: Parameters from the Fundamental Diagram for the Method of Lawson et al. for Case Study 1a

Parameters	Values
Free-flow speed, V_f	80 km/hr
Queued speed, V_μ	22 km/hr
Departure rate from queue, μ	1112 veh/hr/lane
Jam density	110 veh/km/lane

The theoretical methodology of Lawson et al. is thoroughly discussed in Chapter 2, Section 2.8.1.The free-flow travel time could be calculated as t_f = link length / free-flow speed = 2045 m / 80 km/hr ≈ 92 seconds. The known arrival curve was shifted toward right by t_f for each vehicle in the cumulative diagram to get a virtual arrival curve, *V(t).* Delay w was then calculated for each vehicle, which was the horizontal separation between line *D(t)* and *V(t).* The time each vehicle joined the BOQ could be calculated using the following equation by Lawson et al.:

$$t_{q.n} = \frac{w_n}{1-\frac{V_\mu}{V_f}} = \frac{w_n}{1-\frac{22}{80}} = w_n * 1.38 \ldots. (5)$$

where *n* is the cumulative vehicle number for an individual vehicle in the input-output diagram.

These t_q times were worked backward (toward left) from *D(t)* to get the BOQ curve, *B(t),* as shown in Figure 4.7. The vertical separation of the *D(t)* and *B(t)* curves from the time when the reference vehicle left the queue (i.e. 7:30 am) estimated the BOQ in number of vehicles. The estimated queue evolution diagram is shown in the results section for this case study (Section 4.3.1.4).

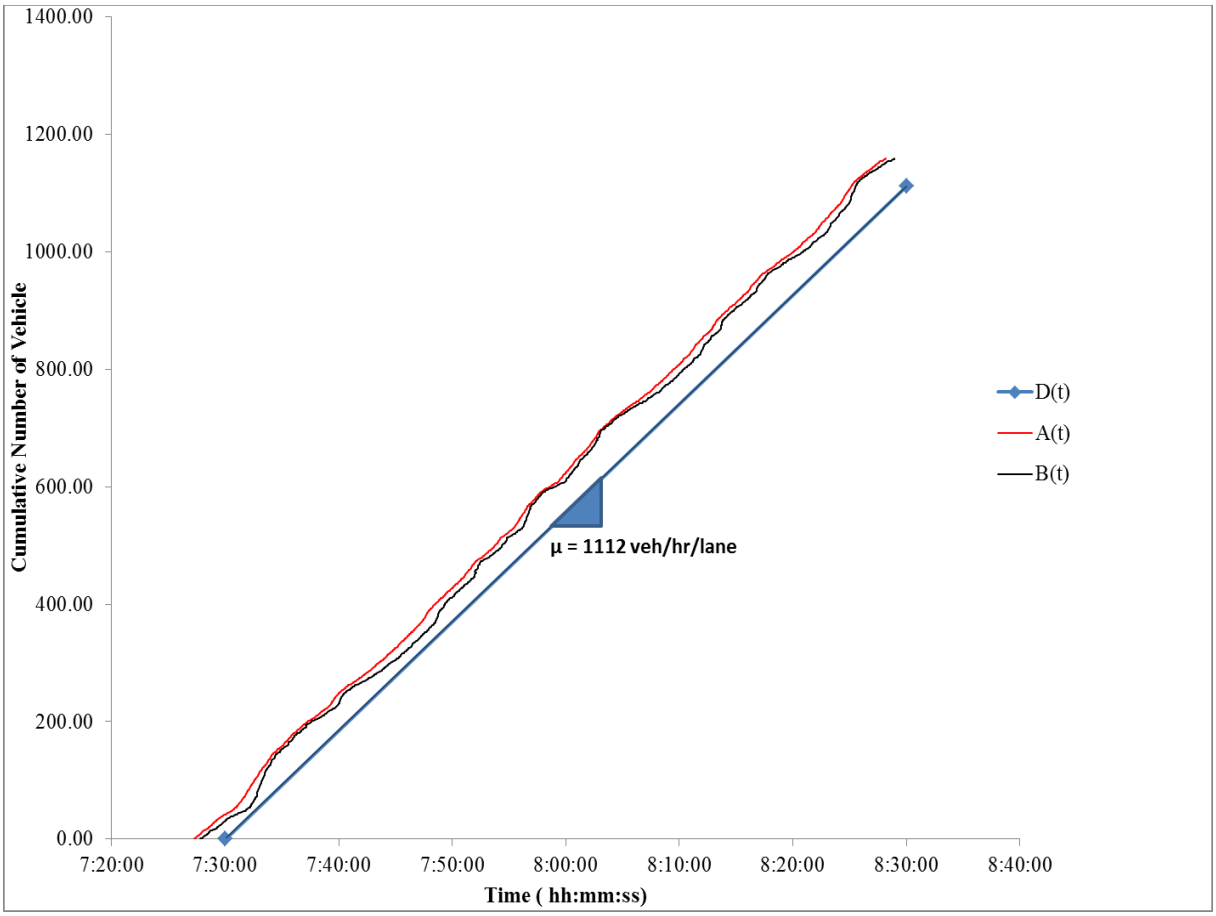

Figure 4.7: Cumulative Input-Output Diagram for the Model of Lawson et al.

4.3.1.2 Extension of the Method of Lawson et al.

An extension of the Lawson et al. (1996) method is proposed to deal with a more realistic departure rate from the queue and the corresponding queued speed that would reflect a more realistic occurrence of the capacity drop formula. The free-flow speed was measured from the fundamental diagram in an usual manner, as explained in the previous section. The fundamental diagram shown in Figure 4.8 represents a bottleneck capacity drop. The dropped capacity was measured from the downstream detector (detector 2 as shown in Figure 4.1) located on the main lane (the lane where queue was estimated) and plotted in the fundamental diagram. The

departure rate from the queue, μ, was thus calculated by subtracting the ramp flow from this dropped capacity of the bottleneck.

Assuming a jam density of 110 veh/km on the horizontal axis, it was possible to construct a straight line between the dropped capacity point and the jam density point to finalize the flow-density diagram on the congested portion. Tracing the density value on the horizontal axis for the corresponding queue departure rate, μ, the queued speed, V_μ, could also be estimated.

It is to be noted that the percentage of capacity drop was about 5.11%; and, according to Brilon et al. (2008), Dervisoglu et al. (2009) and Cassidy et al. (1999), the capacity of a roadway with a bottleneck can be 2 to 24% lower than the capacity measured prior to the congestion or with no congestion. Therefore, the capacity drop found here can be considered logical.

The calculated parameters for the proposed extension of the Lawson et al. method are summarized in Table 4.4. The rest of the methodology was exactly the same as the original Lawson et al. method, which yielded a cumulative diagram as in Figure 4.9. The vertical separation of *D(t)* and *B(t)* curve from the time when the reference vehicle leaves the queue (i.e at 7.30 am) , estimates the back of queue in number of vehicles. The estimated queue evolution diagram has been shown in the results section for this case study.

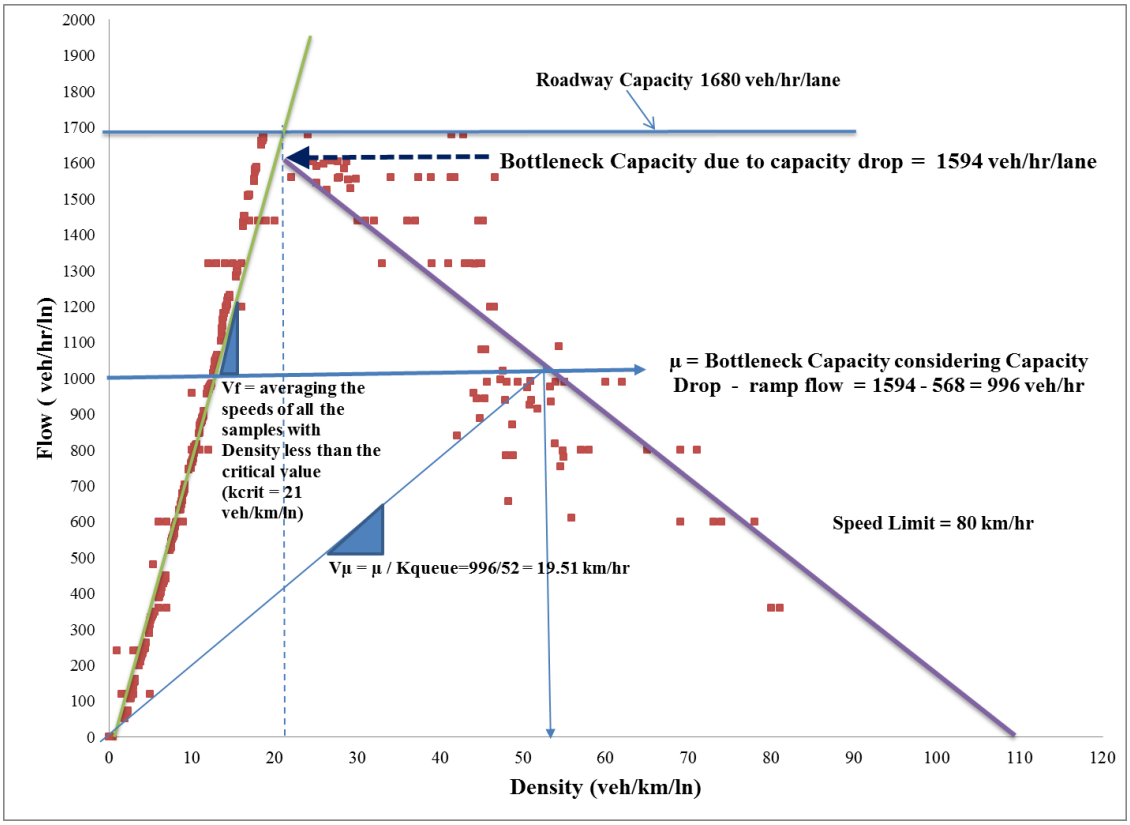

Figure 4.8: Fundamental Diagram for the Extended Method of Lawson et al.

Table 4.4: Parameters from the Fundamental Diagram for the Extend Method of Lawson et al.

Parameters	Values
Free-flow speed, V_f	80 km/hr
Queued speed, V_μ	19.51 km/hr
Departure rate from queue, μ	996 veh/hr/lane
Jam density	110 veh/km/lane

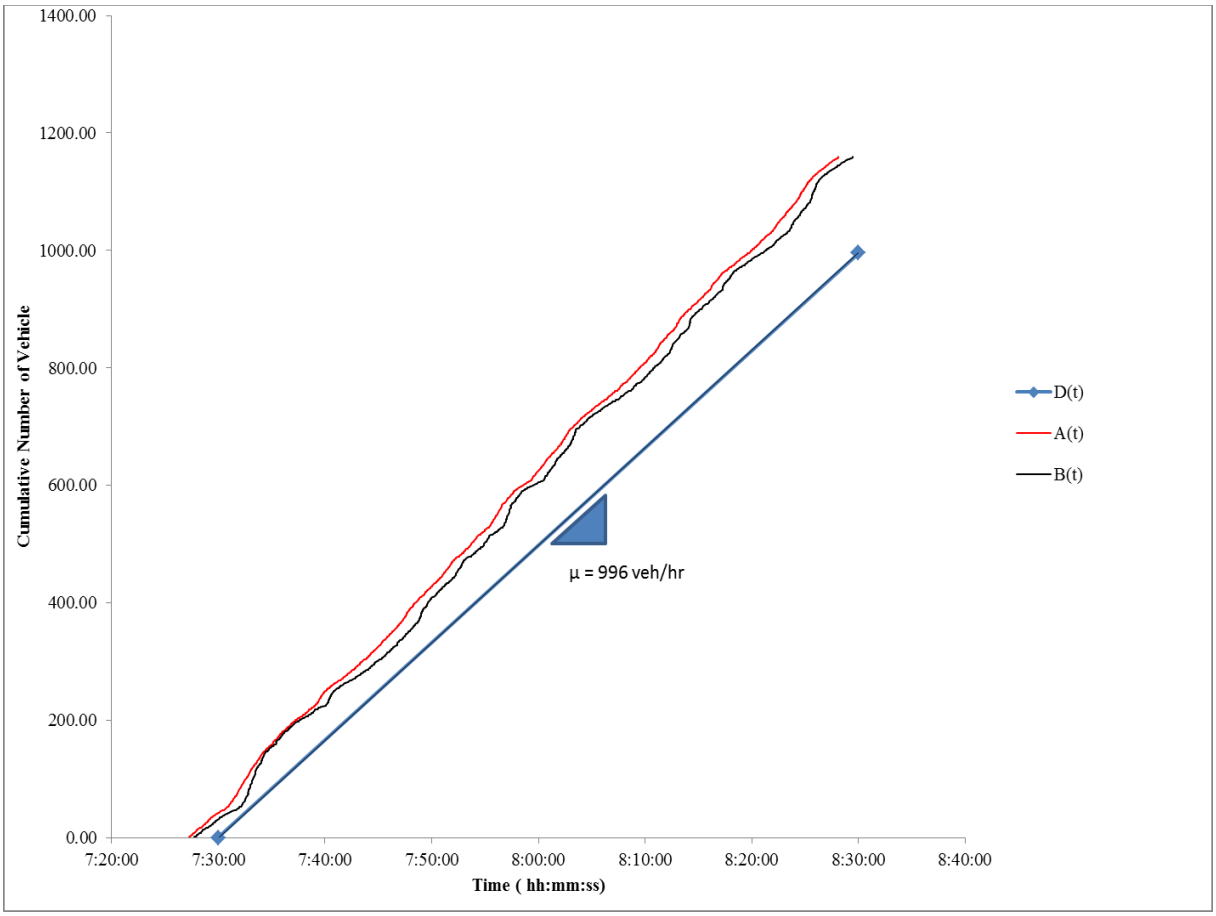

Figure 4.9: Cumulative Input-Output Diagram using the Proposed Extension of Lawson et al.

4.3.1.3 Method based on Probe Trajectory Data and Detector Count

The theoretical framework of this method is explained in Chapter 3. This method employs probe-vehicle trajectory data and a detector (Detector 1) count of the departed vehicles just downstream of the bottleneck to estimate the BOQ. Figure 4.10 shows a time-space diagram for a few probe vehicles. As the vehicle maintained a FIFO condition, probe vehicles were assigned separate serial numbers based on their departures. BOQ location and time for each probe could be identified over their trajectory using queuing criteria. We assumed the vehicles reached the BOQ after sustaining a massive deceleration greater than or equal to $3m/s^2$ for at least 2 seconds. This

is the queuing criteria based upon which the trajectory for each vehicle was analyzed and the BOQ location for each queued vehicle was identified, as shown in Figure 4.10 as a black dotted line. Consequently, the travel times in the free-flow region, tt_f, and queued region, tt_q, for each probe could be extracted directly from their trajectory plot.

For example, for a probe with the serial number 6 shown in Figure 4.10, the BOQ location and relevant time could be identified using the queuing criteria mentioned above; and, the relevant tt_q and tt_f could also be measured. These two quantities for all probe vehicles were used together with the known *D(t)* curve in the cumulative plot in Figure 4.11 to get the BOQ and arrival points on the cumulative diagram.

The known *B(t)* and arrival points, *A(t)*, were connected using a simple linear regression between the consecutive points and *B(t)*, and the *A(t)* curve were estimated. The vertical difference between the *B(t)* and *D(t)* curves at any time instant is the desired queue length in number of vehicles. It is important to note that, in this method, arrival curve *A(t)* can also be estimated and reconstructed without the need of a detector upstream of the queue.

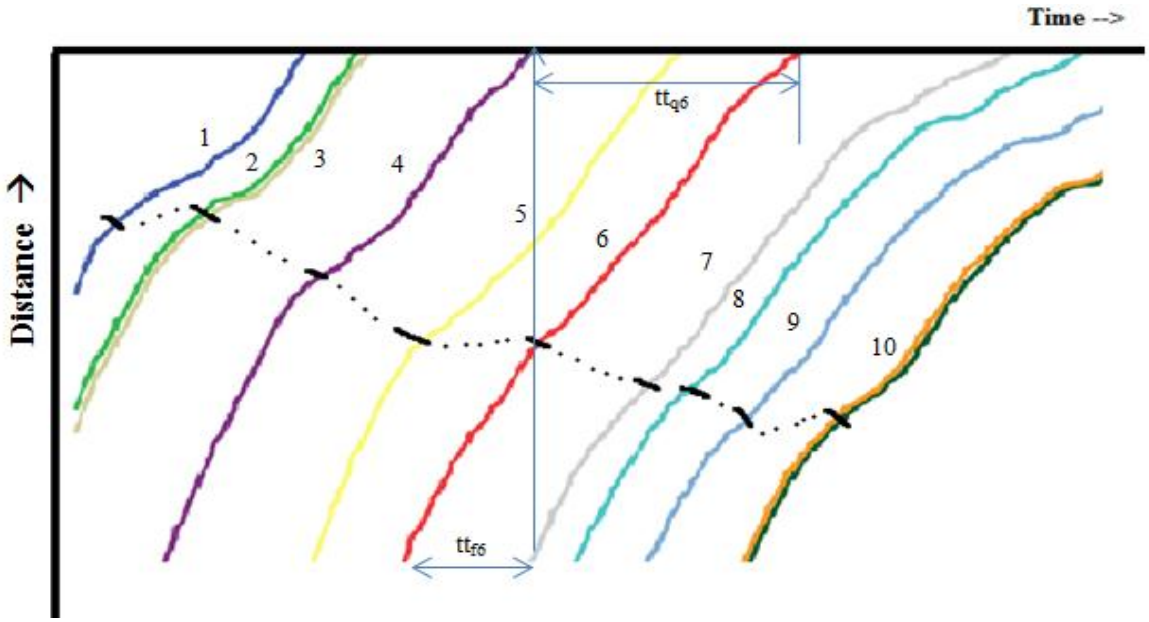

Figure 4.10: Probe-Vehicle Trajectory for Analysis

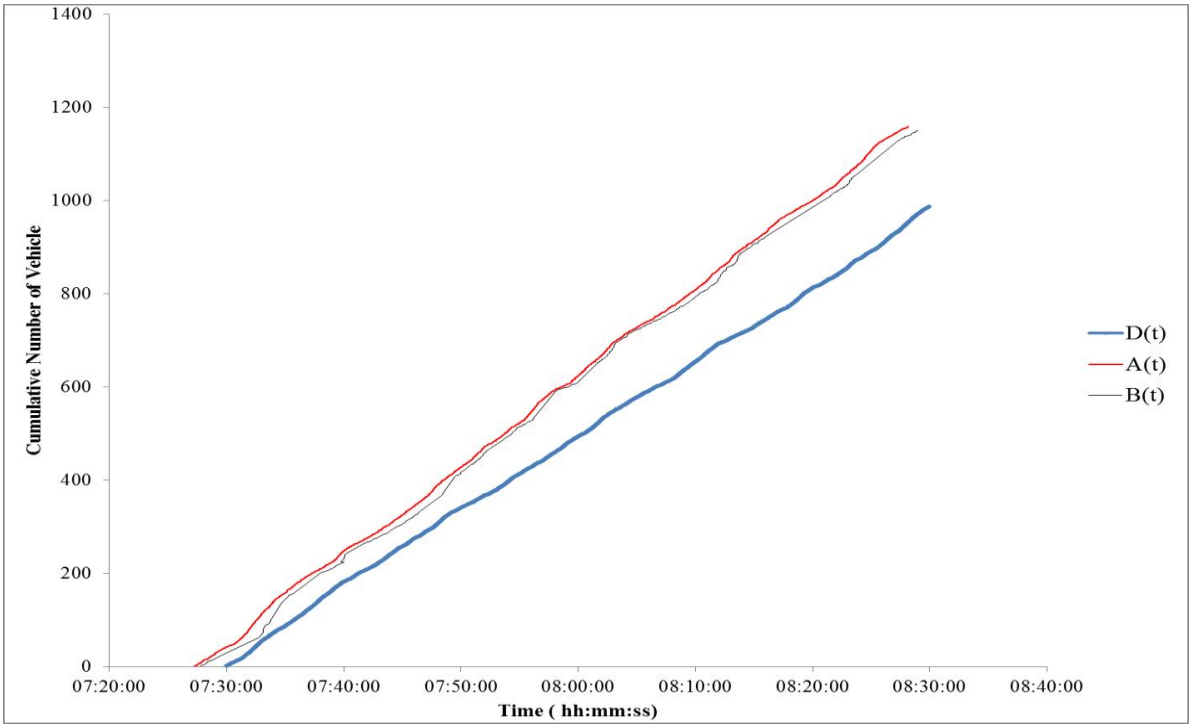

Figure 4.11: Reconstructed Cumulative Diagram using Probe-Vehicle Data

4.3.1.4 Results and Error Estimation for Case Study 1a

This section consists of the data analysis results (estimated queue lengths) with the application the different models discussed in the previous sections. Error estimations and related sensitivity analyses to check accuracy of various models are also explained in this section.

It is quite obvious that the accuracy of estimation of the BOQ curve, *B(t)*, for all the probe-based methods depends on the percentage of probe penetration in the traffic stream. The greater the probe percentage penetration rate, the better the estimated result. Figure 4.12 shows the averaged estimated queues of ten simulation trial for the estimation methods and the observed (actual) queue during a one-hour period. The observed queue length that expresses the BOQ in number of vehicles was found by directly analyzing trajectories of all vehicles in the simulation. The queue growth pattern of the observed queue and all the estimation methods were quite similar; however, it is clear from Figure 4.12 that the Lawson et al. method vastly underestimated the estimated queue and the underestimation accumulated as time passed.

To better describe the accuracy of each model, it was necessary to estimate relative errors of each queue estimation method with respect to the observed queue. The root mean squared error (RMSE) is considered to be one of the best statistical measures to evaluate the accuracy of different methods of queue estimation (Wu J. et al., 2008; Qian et al., 2012; Ban et al., 2011). RMSE measures the average magnitude of error, which ranges between zero and positive infinity. Obviously, the smaller the RMSE value, the better the estimation of queue. As the errors are squared before they are averaged, which gives a relatively high weight to large errors, the RMSE is most useful when large errors are particularly undesirable, which is the case in queue length estimation.

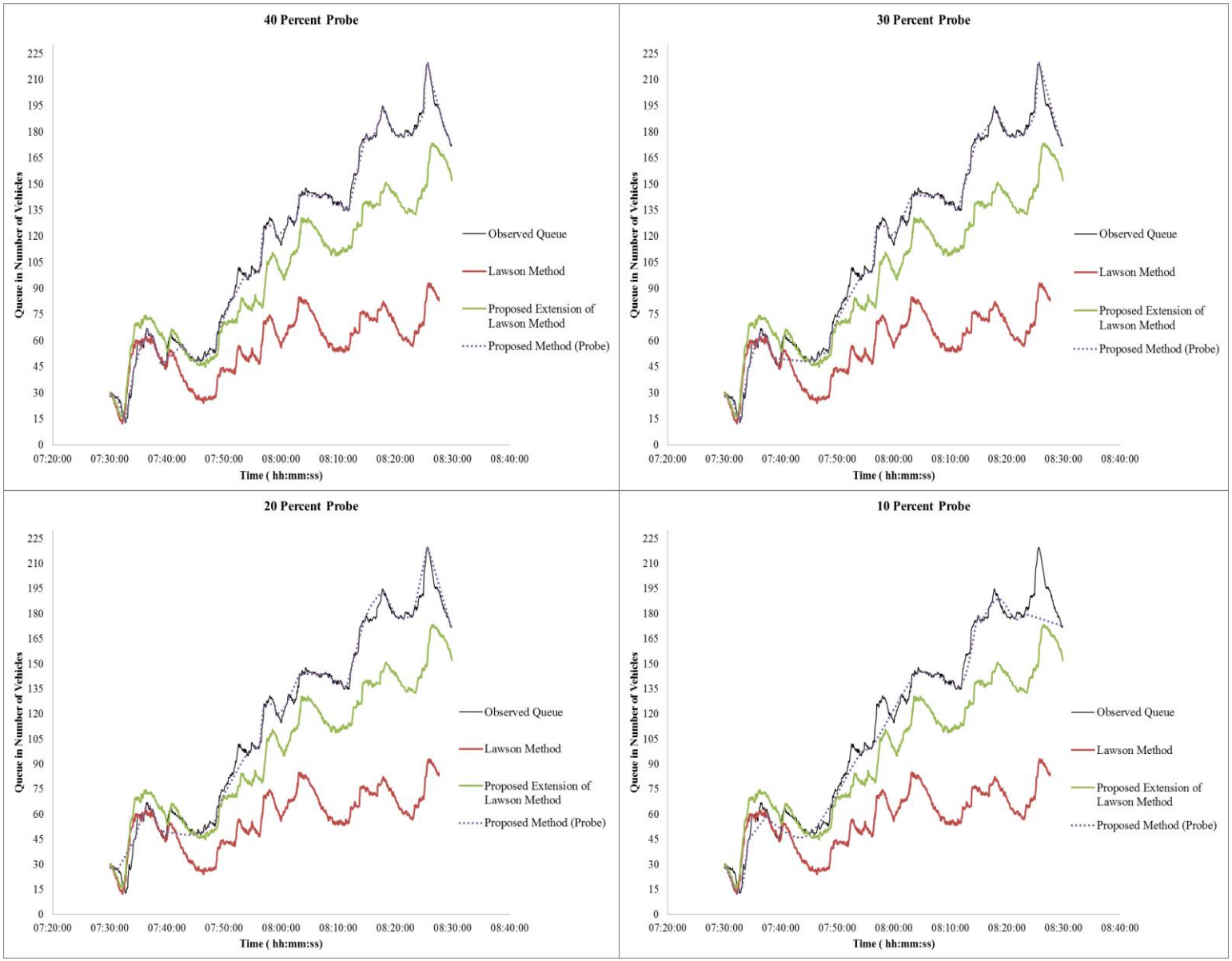

Figure 4.12: Estimated and Observed Queue Evolution Diagrams (Case Study 1a)

Another measure of accuracy used to complement RMSE is the mean absolute percentage error (MAPE). Similar to RMSE, the lower the MAPE value, the better the estimate. RMSE and MAPE can be calculated using the following formulas for different methods of queue estimation:

$$\text{RMSE} = \sqrt{\frac{1}{n}\sum_{t=1}^{n}(Q_{t\ Observed} - Q_{t\ Estimated})^2} \quad \ldots.(6)$$

$$\text{MAPE} = \frac{100\%}{n}\sum_{t=1}^{n}\left|\frac{Q_{t\ Observed} - Q_{t\ Estimated}}{Q_{t\ Observed}}\right| \ldots.(7)$$

Where $Q(t)_{Observed}$ is the actual/observed BOQ length in number of Vehicles at time *t*; $Q(t)_{Estimated}$ is the estimated BOQ length in number of vehicles at time *t*; and, *n* is the number of time points when the queue is estimated.

Figures 4.13 and 4.14 show the calculated average (10-run average) RMSE and MAPE at different probe percentages for the different queue estimation methods. The method of Lawson et al. and its extension do not use probe data; therefore, both the RMSE and MAPE values for these methods remained almost constant. The shown variations were due to the stochastic nature of the Paramics simulation runs. This slight variation was not statistically significant. The figures show that the extension of the Lawson et al. method significantly increased the estimation accuracy when compared to the original theoretical methodology of Lawson et al. However, both of these methods still underestimated the actual BOQ length.

Referring to the RMSE and MAPE plots in **Figures 4.13 and figure 4.14**, it can be said that the accuracy of the proposed probe-based method depends on the available percentage of probes during the analysis period. An analysis of variance (ANOVA) test and related post-hoc tests,

such as Tukey's test (shown in Appendix A) were also performed to see if the error estimates at different probe percentage scenarios were significantly different. The results indicate that, at a 5-percent level of significance, for both RMSE and MAPE, the mean error estimates for different probe percentage scenarios were significantly different from one another. This again proves that the higher the percentage of probe vehicles in the traffic stream, the better the queue estimation.

We can, therefore, conclude that, for accurate or near-accurate queue estimation (error of 1 vehicle or less), the probe-based method should be adopted with preferably a higher percentage of probe penetration in the traffic stream. The probe-based method for this case study outperformed those of the original and extended Lawson et al. methods, even with a minimum probe penetration rate of 10 percent (as seen in Figures 4.13 and 4.14).

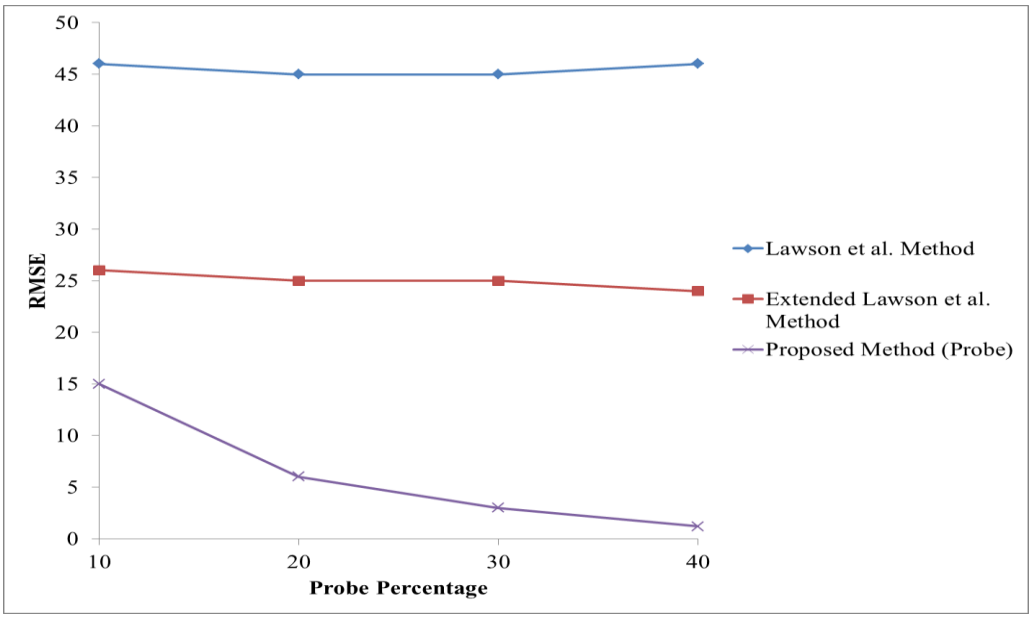

Figure 4.13: RMSE vs. Probe Percentage for Different Methods of Queue Estimation at a Bottleneck Induced by a Merging Lane (Case Study 1a)

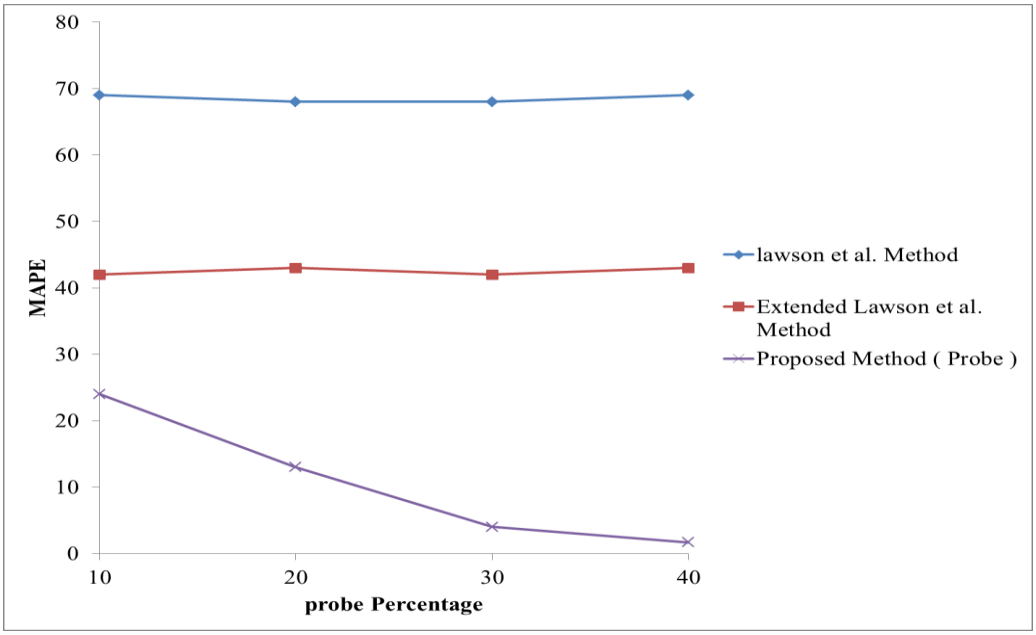

Figure 4.14: MAPE vs. Probe Percentage for Different Methods of Queue Estimation at a Bottleneck Induced by a Merging Lane (Case Study 1a)

4.3.2 Case Study 1b: Bottleneck due to a Lane Closure for 15 Minutes Induced by an Accident

In this case study, queue estimation was carried out for a bottleneck resulting from a 15-minute lane closure. The design of and data acquisition from the simulation model for this case study is discussed in Section 4.2.2 through 4.2.4. It was assumed that passenger cars start to flow freely at 8:00 am through two lanes in the simulation model and that, at 8:10 am, a lane was closed for 15 minutes due to an accident. As a result, a bottleneck formed upstream from the accident site. At 8:25 am, the closed lane was reopened allowing normal flow and causing queue cessation. It was also assumed that:

1. Vehicles did not change lanes prior to the incident site.
2. Vehicles travelling in the accident lane could change lanes right before the location of lane closure to pass the incident, thereby maintaining FIFO characteristics.

3. Analysis was carried out for each lane separately. In other words, it was assumed that the lanes on which probe vehicles were travelling over the link were also known and that the queue estimates were separate for the two lanes. It was also assumed that the departure rate for each lane was equal to the half of the detector count located over lane 2 during the 15-minute lane closure period.
4. Passenger cars were the only vehicles in the entire vehicle population.

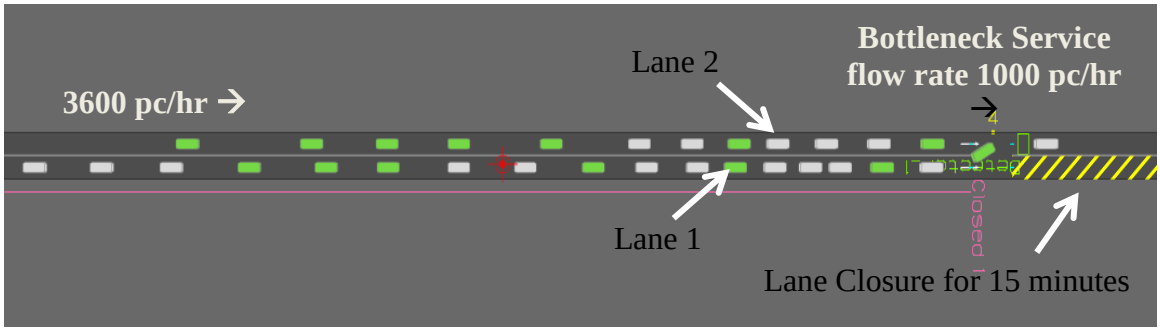

(a)

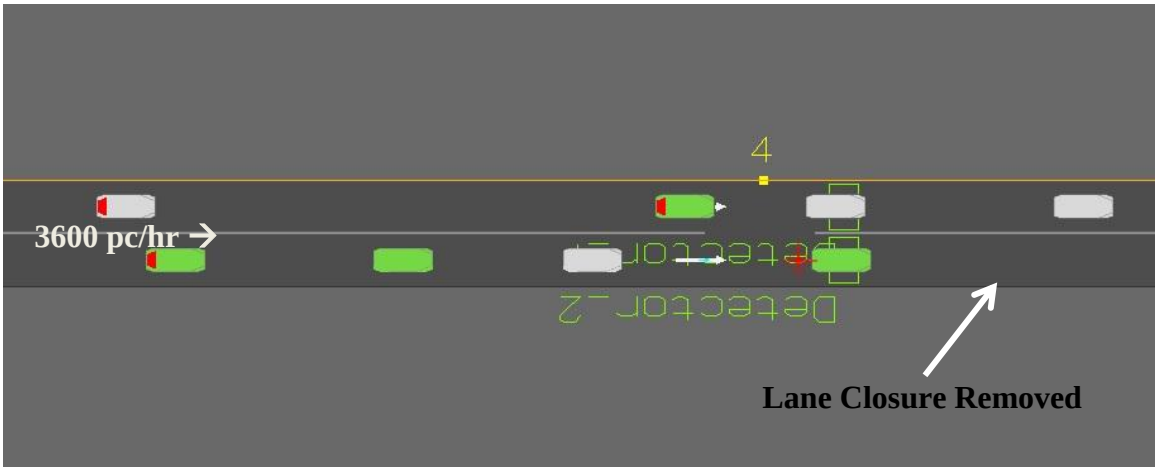

(b)

Figure 4.15: Simulation Model for Queue Estimation: (a) Upstream of a Lane Closure, (b) After the Lane Closure is Removed

Three estimation methodologies adopted for queue evaluation in this scenario were 1) the theoretical model of Lawson et al. (1996), which is based on a triangular-flow density relationship; 2) the extended Lawson et al. method, adopting a fundamental diagram that considers a bottleneck capacity drop; and, 3) the methodology based on probe-vehicle trajectory analysis.

4.3.2.1 Method of Lawson et al.

This theoretical model can estimate queues using a triangular flow-density relationship, which helps to determine necessary parameters, such as queued speeds, $V_{\mu 1}$ and $V_{\mu 2}$, corresponding to two flow conditions (during lane 2 closure and after reopening of lane 2) and free-flow speed, V_f

Figure 4.16 shows a triangular flow-density diagram for this case study, which was constructed following similar steps as mentioned in Section 4.3.1.1, from which two queued speeds for two bottleneck departure rates, μ_1 and μ_2 (one after lane closure and another one after the lane closure is removed), were determined. The free-flow speed was estimated by averaging the speeds calculated for the uncongested flow-density points left of density $k_{critical}$ in Figure 4.16.

It was assumed that, just after the lane closure, the departure rate, μ_1, was one half of the capacity and that μ_2 was the total capacity, which is shown as 1680 veh/hr/lane in Figure 4.16. Table 4.5 presents the values for the free-flow speed, two queued speeds and related departure rates. The separate lanes were analyzed for queue estimation using the theoretical methodology of Lawson et al., as explained in Chapter 2, Section 2.8.2.

Referring to Table 4.5**,** it is clear that the free-flow speed, V_f, and the queued speed at capacity, $V_{\mu 2}$, were almost identical. Therefore, BOQ curve $B_2(t)$ corresponding to $\mu_2 = Q_{capacity}$ became a horizontal line for the last queued vehicle. The vehicle with equal departure time and virtual arrival time was considered to be the last queued vehicle. In other words, in the cumulative diagram, when the $V(t)$ and $D(t)$ curves touch each other (at point *C* in Figure 4.17), the corresponding cumulative number on the vertical axis is the last queued vehicle.

The free-flow travel time could be calculated as t_f = link length / free-flow speed = 2045 m / 80 km/hr ≈ 92 seconds. The known arrival curve was shifted toward the right by time t_f for each vehicle in the cumulative diagram, in order to obtain the virtual arrival curve, $V(t)$. Delay *w* was calculated from the horizontal separation between $D_1(t)$ and $V(t)$, until $V(t)$ touched the $D_2(t)$ line. The time corresponding to each vehicle joining the BOQ could be calculated using the following equation by Lawson et al.:

$$t_{q.n} = \frac{w_n}{1-\frac{V_\mu}{V_f}} = \frac{w_n}{1-\frac{13.3}{80}} = w_n * 1.19 \ldots.(8)$$

where *n* is the cumulative vehicle number for an individual vehicle in the input-output diagram.

These t_q times were worked backward (towards the left) from the $D_1(t)$ line to obtain the BOQ line, $B_1(t)$, as shown in Figure 4.17. The vertical separation between line ADC and line ABC from the time when the reference vehicle left the queue (i.e. at 8.10 am) estimated the BOQ in number of vehicles.

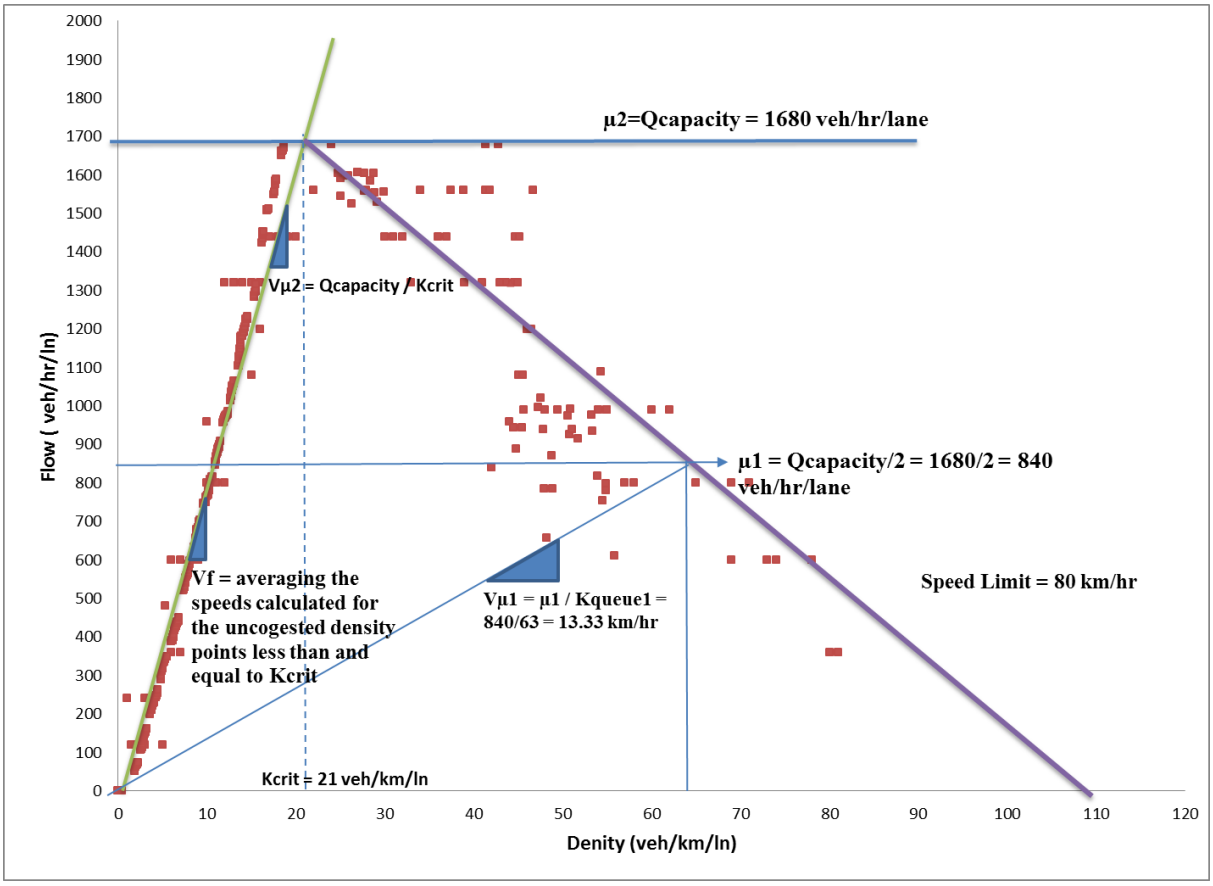

Figure 4.16: Flow-Density Diagram in Case Study 1b for the Method of Lawson et al.

Table 4.5: Parameters from the Fundamental Diagram for the Method of Lawson et. al for Case Study 1b

Parameters	Values
Free-flow speed, V_f	80 km/hr
Queued speed, $V_{\mu 1}$	13.3 km/hr
Queued speed, $V_{\mu 2}$	80 km/hr
Departure rate from queue, μ_1	840 veh/hr/lane
Departure rate from queue, $\mu_2 = Q_{capacity}$	1680 veh/hr/lane
Jam density	110 veh/km/lane

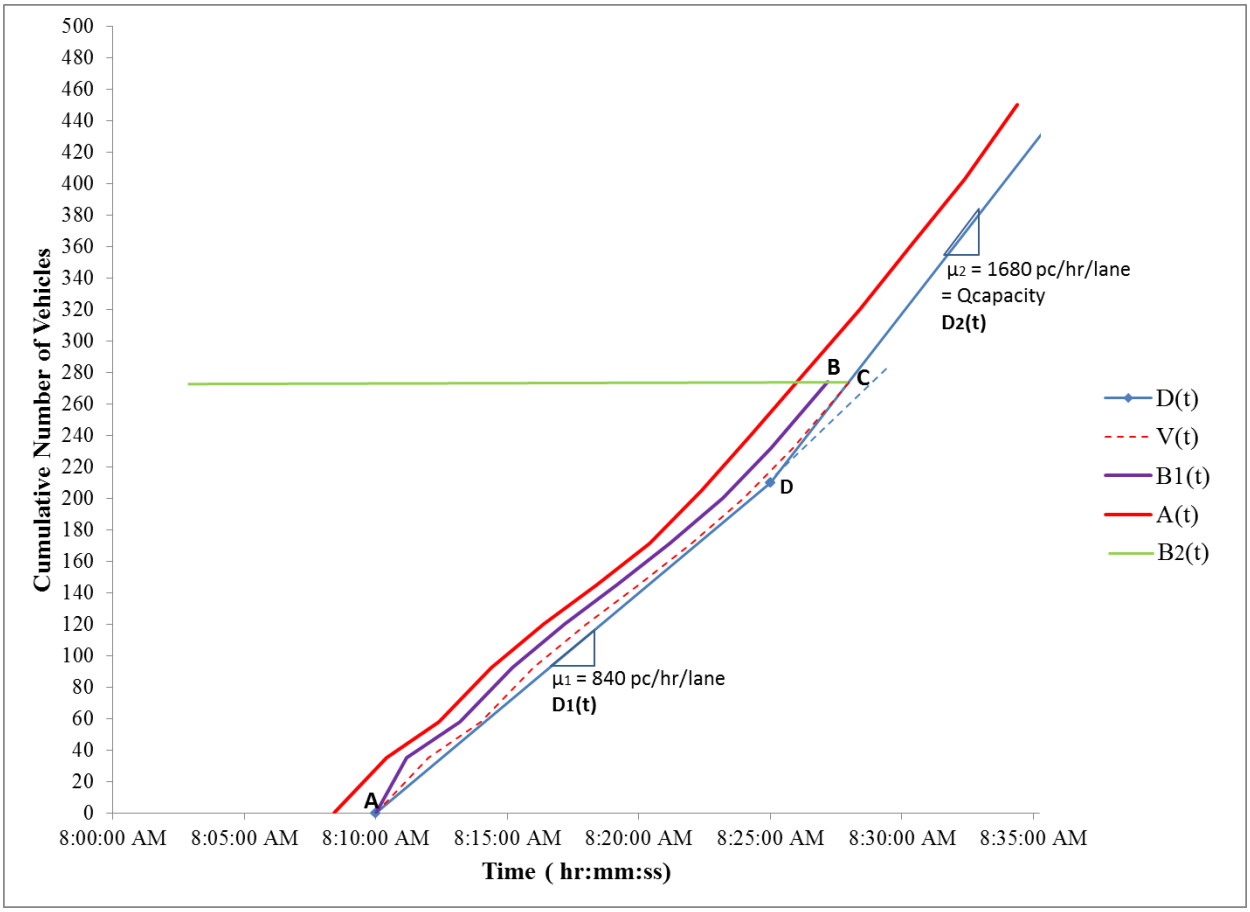

Figure 4.17: Cumulative Input-Output Diagram for Lane 1 (Lawson et al. Method)

4.3.2.2 Extended Lawson et al. method

This procedure follows the Lawson et al. method, but considers the occurrence of a capacity drop due to the formation of an active bottleneck. In other words, the perfect triangular flow-density diagram used by Lawson et al. method was not used, rather a more realistic fundamental diagram, such as the one in Figure 4.18, was used to estimate the free-flow speed, V_f, and two queued speeds, $V_{\mu 1}$ and $V_{\mu 2}$, corresponding to the two queue departure flow rates (μ_1 and μ_2, respectively), one during the lane closure and the other when the closed lane was reopened, but the bottleneck was still active. The departure rates were found directly from the simulation runs,

and the speeds were calculated using the corresponding density values on the horizontal axis of the fundamental diagram (Figure 4.18).

It is to be noted that the percentage of capacity drop was about 6.54%; and, according to Brilon et al. (2008), Dervisoglu et al. (2009) and Cassidy et al. (1999), the capacity of a roadway with a bottleneck can be 2 to 24% lower than the capacity measured prior to the congestion or with no congestion. Therefore, the capacity drop found here using the simulation data can be considered logical.

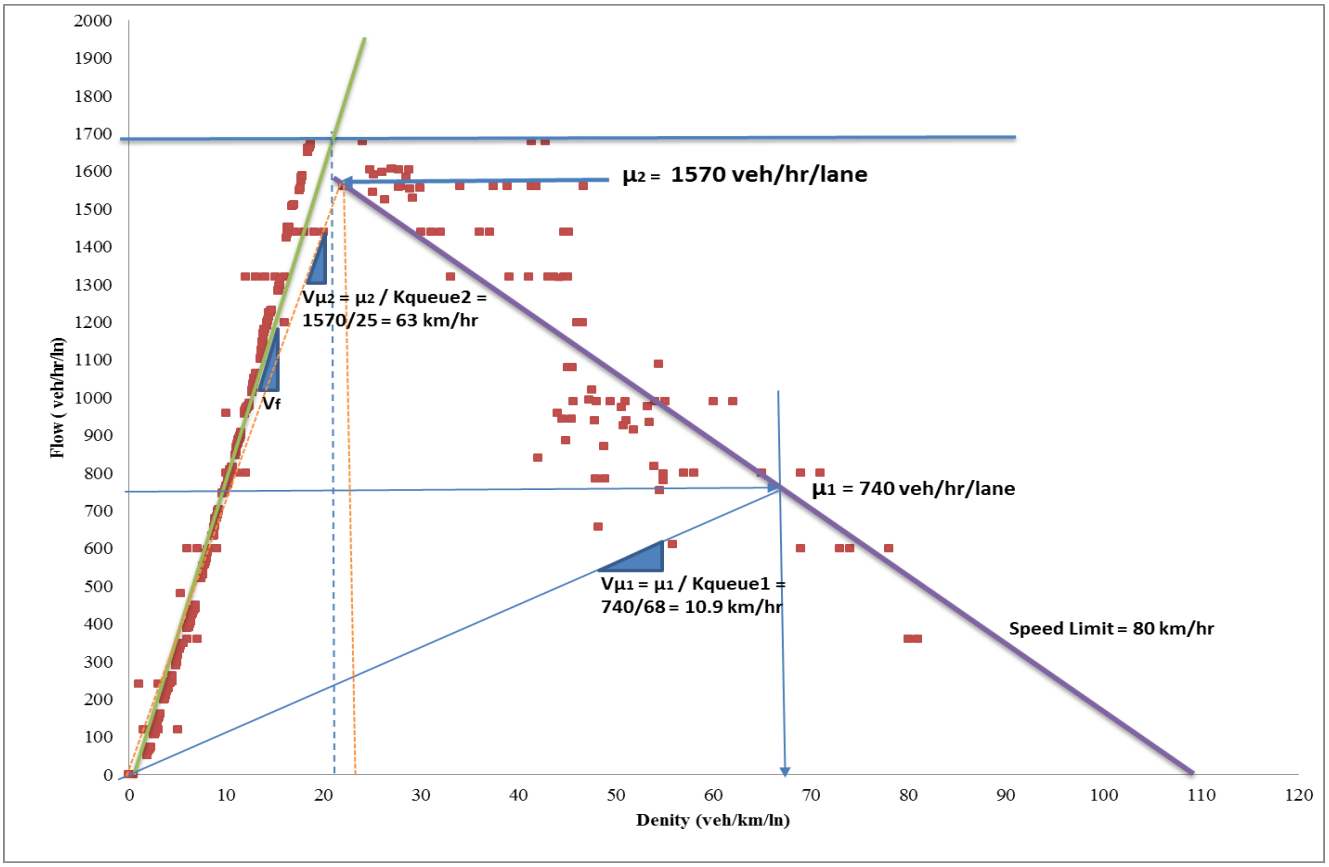

Figure 4.18: Flow-Density Diagram in Case Study 1b for the Extended Lawson et al. Method

Table 4.6: Parameters from the Fundamental Diagram for the Extended Lawson et. al Method for the Case Study 1b

Parameters	Values
Free-flow speed, V_f	80 km/hr
Queued speed, $V_{\mu 1}$	10.9 km/hr
Queued speed, $V_{\mu 2}$	63 km/hr
Departure Rate from Queue , μ_1	740 veh/hr/lane
Departure Rate from Queue , μ_2	1570 veh/hr/lane
Jam density	110 veh/km/lane

Figure 4.19 shows a cumulative diagram that was built based on the extended Lawson et al. method for lane 1. $B_1(t)$ and $B_2(t)$ are the BOQ curves that correspond to the bottleneck departure rates, μ_1 and μ_2, respectively. These two lines intersected at point *B* and developed the *B(t)* curve (line ABC) needed for queue estimation. The vertical separation between lines ABC and ADC (departure curve) at any time *t* was the queue in number of vehicles at time *t*, *Q(t)*.

4.3.2.3 Probe-Based Methodology

The probe-based methodology uses a lane-by-lane probe-vehicle trajectory data analysis based on the queuing criterion to detect the BOQ, and the departure curve, *D(t)*, was plotted in real time using the detector counts. The queuing criterion was assumed to be a deceleration value greater or equal to 3 m/s^2 sustained by a vehicle at least for 2 seconds before it joined the BOQ. It was also assumed that a vehicle joining the BOQ remained in the queued state until it departed from the bottleneck. The time instant when each probe vehicle joined the back of queue was stored, and the corresponding cumulative number was assigned to each probe vehicle found with the detector to plot them in the cumulative diagram. The *B(t)* curve was found using linear

regression of the consecutive known probe-vehicle data points on the cumulative diagram, as shown in Figure 4.20.

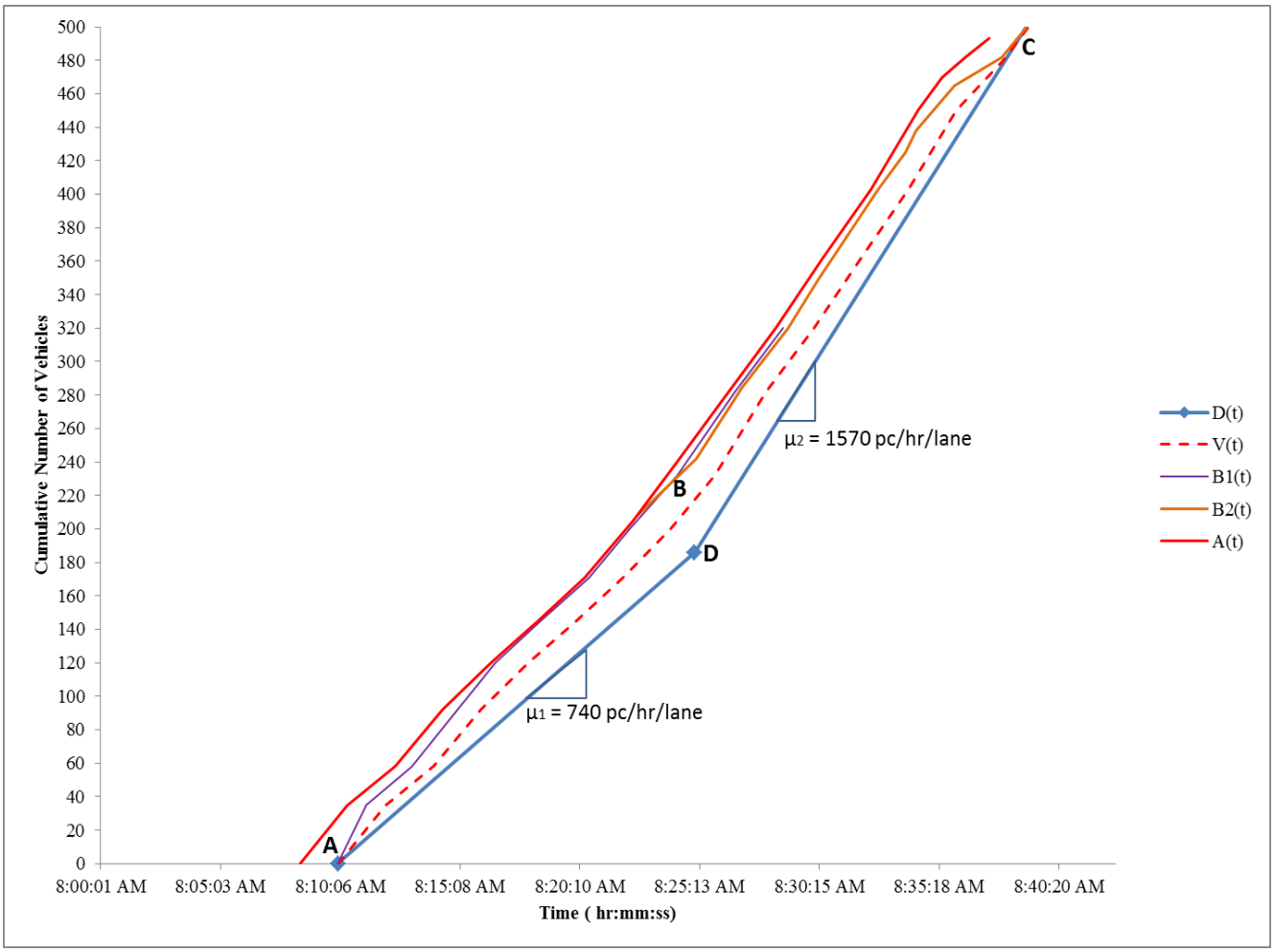

Figure 4.19: Cumulative Input-Output Diagram for Lane 1 (Extended Lawson et al. Method)

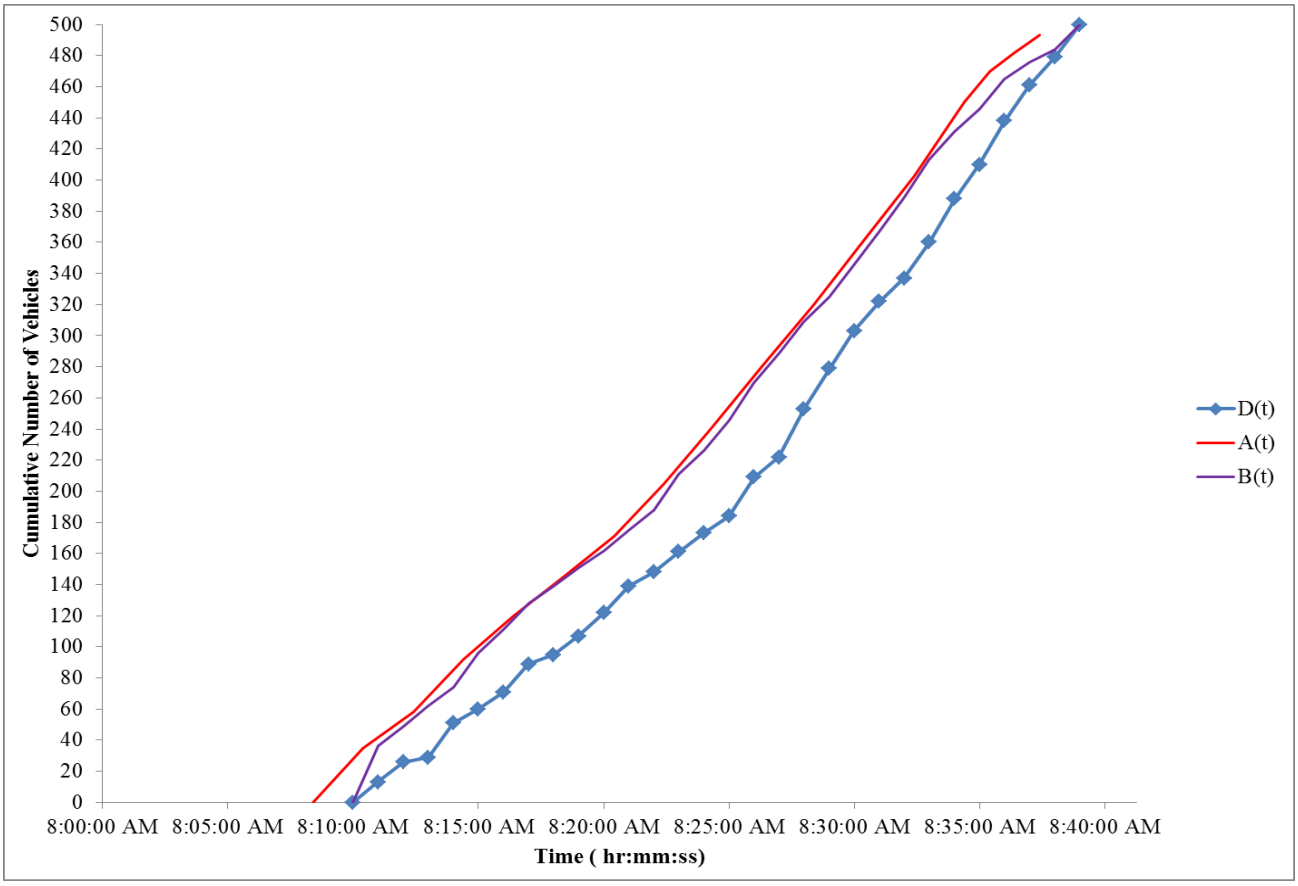

Figure 4.20: Cumulative Diagram using Probe-Based Proposed Methodology for Lane 1

4.3.2.4 Results and Error Estimations (Case Study 1b)

This section presents the data analysis results (estimated queue length) with the application of the different models discussed in the previous sections for Case Study 1b. Error estimations and related sensitivity analyses to check accuracy of various models are also explained in this section. It is quite obvious that the accuracy of estimation of the BOQ curve, *B(t)*, for all the probe-based methods depends on the percentage of probe penetration in the traffic stream. As expected, the greater the probe percentage penetration rate, the better the estimated result.

Figures 4.21 and 4.22 show the observed (actual) queues and the averaged estimated queues of ten random simulation trials for the estimation methods for lanes 1 and 2, respectively. The observed queue length expressed as the BOQ in number of vehicles was found by directly analyzing the trajectories of all vehicles in the Paramics simulation. The growth and dissipation patterns of the observed queue and all the estimation methods were quite similar, but it was quite evident from both the queue evolution diagrams that the Lawson et al. method vastly underestimated the queue length. A logical may be that the use of a triangular flow-density diagram, which overestimates the departure capacity, leads to a lower BOQ estimation.

A notable observation from Figure 4.21 is that the extended Lawson et al. method performs well in the estimation of the queue accumulation. However, its performance was poor during queue dissipation. During the one-hour analysis period, after 10 minutes of warm-up, the queue accumulation occurred for 15 minutes, due to the lane closure; and, the remaining 35 minutes was considered as the period of queue dissipation, although the real queue completely dissipated well before 35 minutes. The average departure rate during the first 15 minutes of lane closure and the last 35 minutes of queue dissipation were used to construct the *D(t)* curve. Thus, Lawson

et al. method does not consider the variation of departures during that period. This explains why the extended Lawson fails to perform well during queue dissipation compared to the one during queue accumulation. On the other hand, the probe-based method uses real-time departure rate data from detectors and probes and, thus, is capable of representing the queue dissipation more closely.

Comparing figure 4.21 and 4.22 , it is clear that lane 1, on which the lane closure was induced, suffered a longer queue compared to lane 2. This can be attributed to the fact that the vehicles in lane 1 waited for a safe gap to change lanes just upstream of the lane closure, in order to pass out of the bottleneck, leading to the greater queue length in lane 1.

RMSE and MAPE values were used to measure the accuracy of the different models with respect to the observed BOQ length. Figures 4.23 and 4.24 show the RMSE and MAPE plots, respectively, at different probe penetration percentages.

It is to be noted that the extended Lawson et al. method performed better than the original Lawson et al. method in this case study and for both lanes, due the consideration of a legitimate capacity drop at the bottleneck, significantly improving the estimation accuracy, as shown in Figures 4.23 and 4.24.

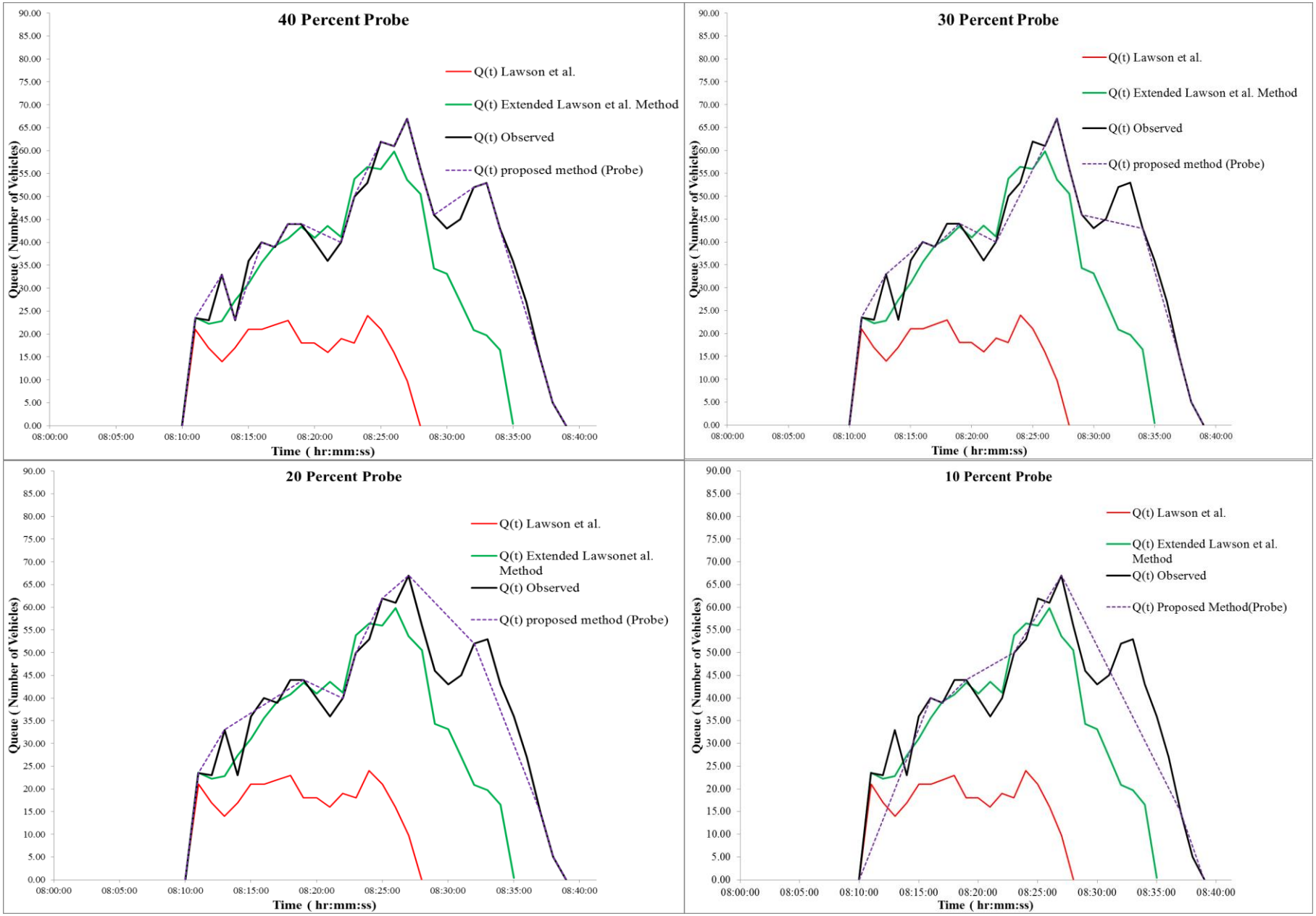

Figure 4.21: Queue Evolution Diagram for Lane 1 (Case Study 1b)

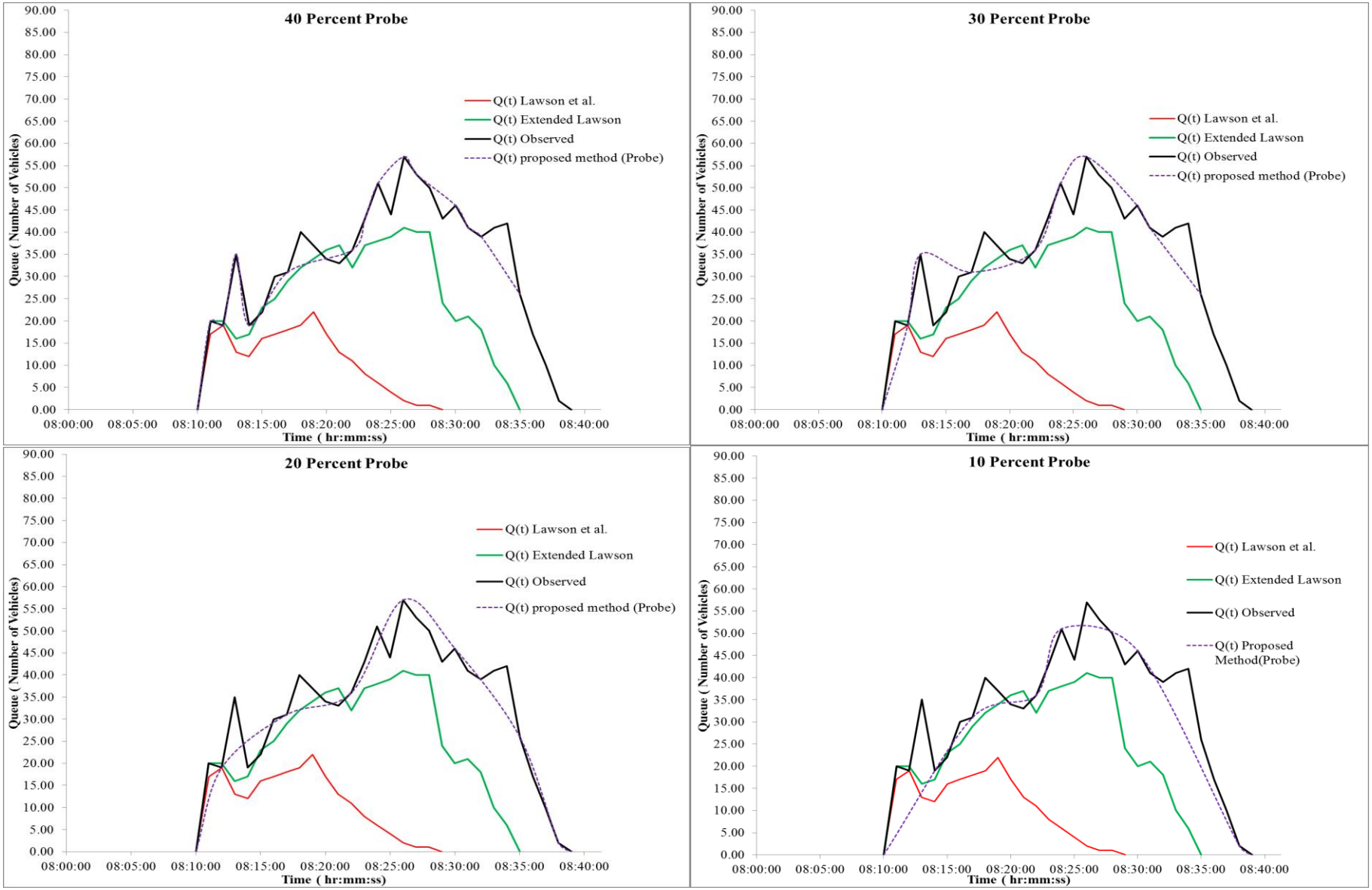

Figure 4.22: Queue Evolution Diagram for Lane 2 (Case Study 1b)

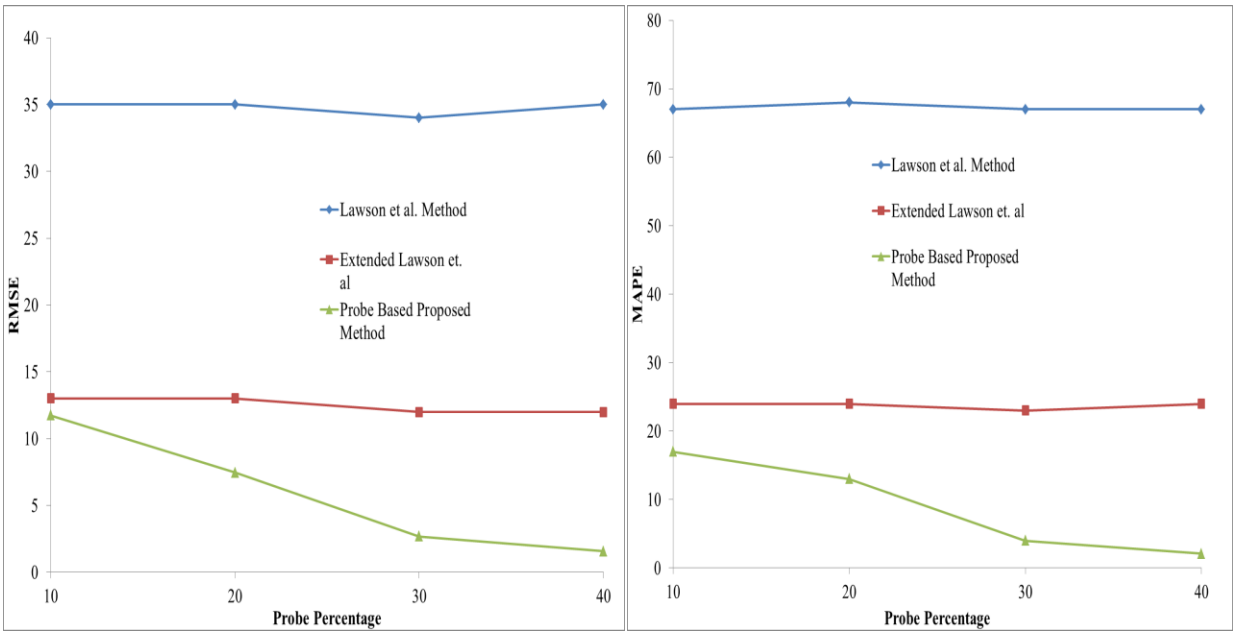

Figure 4.23: RMSE and MAPE Values at Different Probe Penetration Percentages for Lane 1 (Case Study 1b)

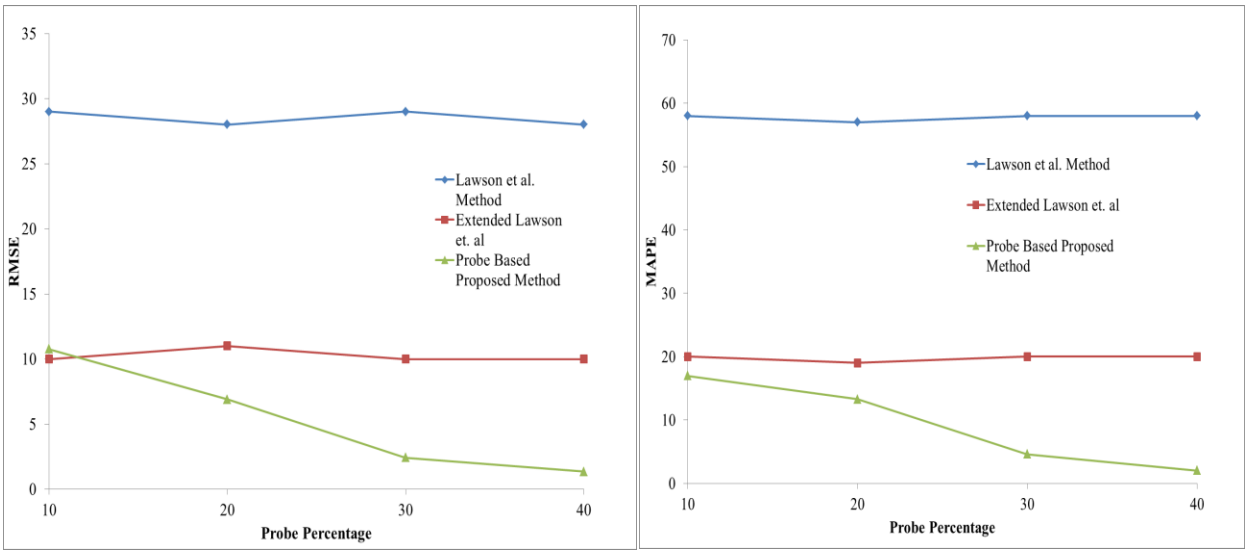

Figure 4.24: RMSE and MAPE Values at Different Probe Penetration Percentages for Lane 2 (Case Study 1b)

Referring to the RMSE and MAPE plots, it is obvious that the accuracy of the probe-based method was highly sensitive to the percentage of probe market share. A single-factor ANOVA test with a related post-hoc test, such as Tukey's test, were conducted for different probe percentages using RMSE and MAPE as dependent variables (Appendix B). It was found that a significant difference existed among errors at different probe percentage scenarios at a five-percent level of significance, which in turn implied that a higher probe percentage yielded better queue estimates.

4.4 Signalized Intersection Scenarios

4.4.1 Simulation Network Design (Case Studies 2a and 2b)

In signalized intersection scenarios, the one-lane urban roadway (Figure 4.25) in the simulation consisted of an isolated intersection with fixed signal timing for an undersaturated (Case Study 2a) intersection and an oversaturated (Case Study 2b) intersection. It was assumed that all vehicles passed through the intersection and that there were no driveways resulting in the addition or loss of vehicles inside the link, except from the downstream intersection at the end of the link. The simulation could trace probe-vehicle location and time inside the link where queue estimation was to be carried out.

The fixed signal was a one minute long cycle with two phases in (Figure 4.26). In the phase 1 split of the signal cycle, vehicles moved from left to right over the horizontal link, as shown in Figure 4.25. The all-red phase time was considered to be 2 seconds, and the standard yellow/amber interval was considered to be 3 seconds. The proposed horizontal link carried a high number of vehicles; therefore, the amount of green time allocated to it was higher (29 seconds). Vehicles also tended to move in the amber period, and this time was usually 2 of the 3

seconds of amber time (Mehran et al., 2012). Therefore, during the data analysis, vehicles were seen to pass the stop line up to the first 31 seconds of each cycle in the proposed link. Table 4.7 summarizes the roadway geometric, road traffic and driver behaviour parameters needed for the signalized simulation network design.

Table 4.7: Parameters Considered for Simulation Network Design for Signalized Intersection Scenarios (Case Studies 2a and 2b)

Horizontal Link Length	1300 metres
Speed Limit on Horizontal Link	50 km/hr
Mean Target Headway	2 seconds
Mean Driver Reaction Time	1.5 seconds
Minimum Gap	2 metres
Lane Width	3.7 metres
Link Category	Urban
All Red Time	2 seconds (each phase)
Amber Time	3 seconds
Average Driver Familiarity	90%

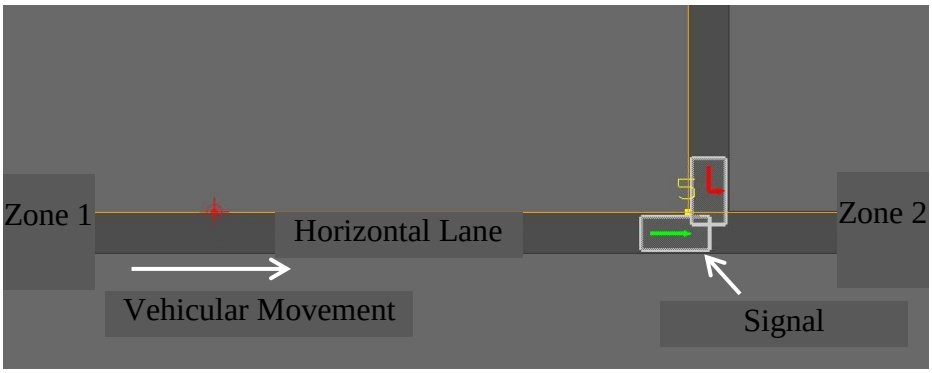

Figure 4.25: Simulation Network for Signalized Intersection Scenarios

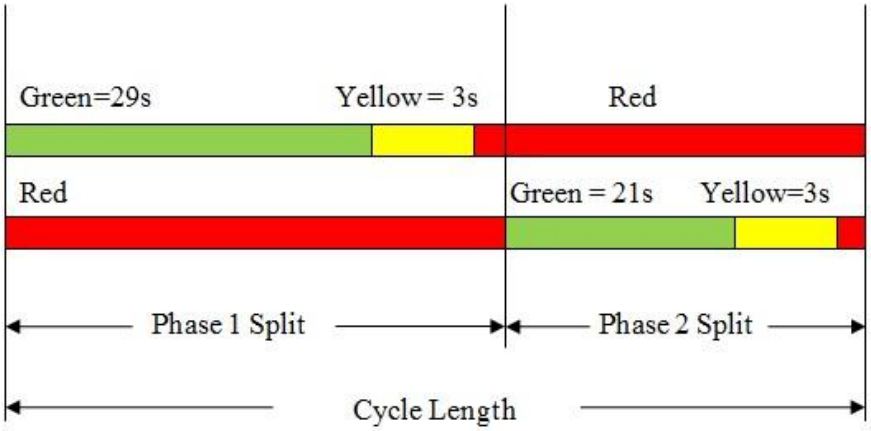

Figure 4.26: Fixed Signal Operation

4.4.2 Simulation Runs (Case Studies 2a and 2b)

One-hour long simulation runs were conducted for the signalized intersection scenarios with two different demand levels. In this thesis, the data analysis was done for each individual signal cycle of 60 seconds throughout the entire simulation period.

Similar to the bottleneck scenarios, 10, 20, 30 and 40% penetration rates of probe vehicles were examined. Ten random seeds were also used to replicate the simulation process. In total, 40 runs were conducted, and separate data analyses were performed for each probe penetration case. Table 4.8 summarizes the design of the simulation runs.

Table 4.8: Design of Simulation Runs for the Signalized Intersection Scenarios

Probe Percentages	10%, 20%, 30% and 40%
Simulation Trials for Each Probe Percentage	Ten (using ten random seeds)
Simulation Period	7:20 am – 8:30 am
Simulation Warm-Up Period	10 minutes
Simulation Data Acquisition	7:30 am – 8:30 am
Demand in Undersaturated Signal Case (from Zone 1 to Zone 2, as shown in Figure 4.25)	1800 veh/hr/lane
Demand in Oversaturated Signal Case (from Zone 1to Zone 2, as shown in Figure 4.25)	2200 veh/hr/lane
Data Obtained	• Trajectory data of all probe vehicles inside the horizontal link • Detector count at the stop line

4.4.3 Simulation Data for Signalized Intersection Scenarios

For both of the signalized intersection queue estimation scenarios, probe and detector data at the stop line were collected from the simulation runs to analyze and estimate queues. Probe-vehicle data were a subset of the main database of all vehicles in the simulation and could be separated by assigning a particular vehicle type number to the probes (passenger cars - vehicle type 2 - in

this study). Figures 4.27 and 4.28 show two three-dimensional snapshots taken from the simulation software for the queue estimation of the two signalized intersection scenarios. Probe vehicles are shown in green.

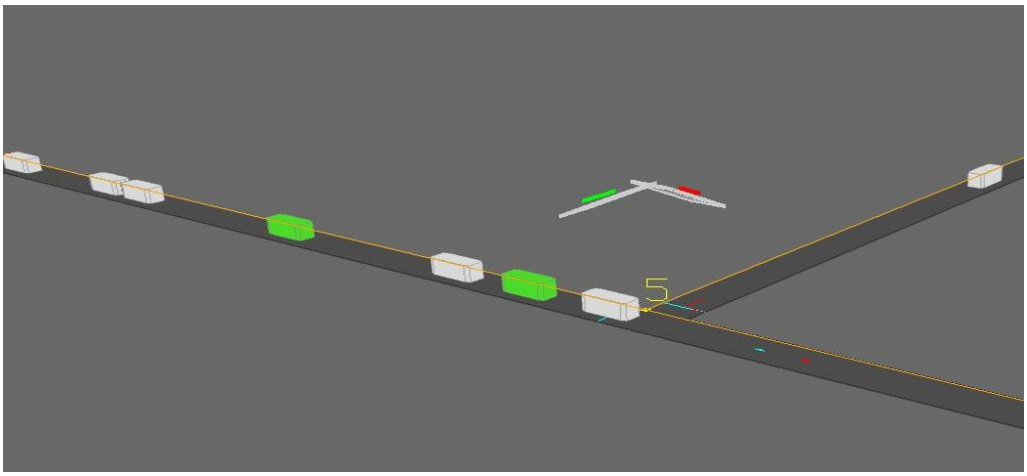

Figure 4.27: Undersaturated Isolated Signalized Intersection and Associated Queue (Partial) in the Simulation Network

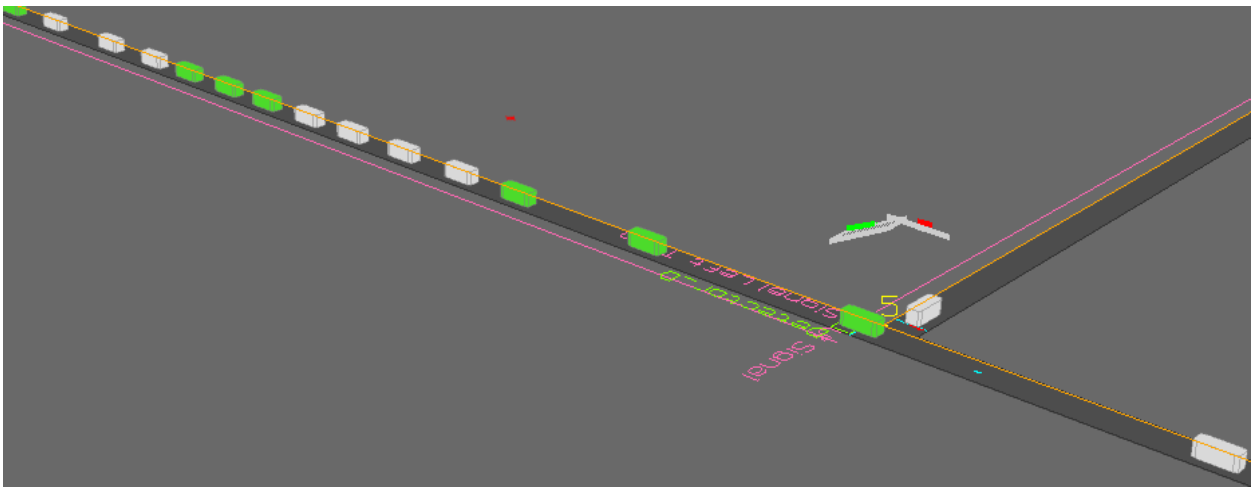

Figure 4.28: Oversaturated Isolated Signalized Intersection and Associated Queue (Partial) in the Simulation Network

4.5 Analysis Results of the Signalized Intersection Scenarios

4.5.1 Case Study 2a: Undersaturated Signalized Intersection

In this section, a cycle-by-cycle analysis procedure is presented for the estimation of the queue length at an undersaturated signalized intersection. The queue length was estimated using two different methods. The first method used all vehicle data and tried to replicate the theoretical method of Lawson et al. The second method was the proposed method of estimation, which used trajectory analysis to estimate the BOQs. The accuracies of these methods were compared with respect to the observed queue length using two measures of accuracy (RMSE and MAPE).

4.5.1.1 Model of Lawson et al.

The method of Lawson et al. (1996), the explanation of which is given in Chapter 2, Section 2.8.2, was used for estimating the BOQ in the signalized intersection scenarios. Some of the necessary parameters, such as V_f, k_j and $Q_{capacity}$ (saturation flow rate), during the green interval were found from a triangular flow-density diagram constructed using simulation data.

To apply the Lawson et al. queue estimation method, it was necessary to construct a fundamental diagram for isolated signalized intersection scenarios. Figure 4.29 shows a fundamental diagram constructed using randomly sampled flow and density data from simulation, using concepts from research done by Dervisoglu et al. (2009). The steps to construct the triangular fundamental diagram and obtain the necessary parameters in this research were:

1. A horizontal line (blue line in Figure 4.29) was drawn through the maximum possible flow point/points (1610 veh/hr/lane), which can also be defined as capacity or saturation flow from the signalized intersection according to the HCM.

2. Based on the speed limit of the link (50 km/hr for Case Study 2a), it was possible to fix upon an initial critical density of 32 veh/km/lane (1610/50).
3. A linear regression line (black line in Figure 4.29**)** was plotted for the uncongested points with density values of less than 32 veh/km/lane, constrained to pass through the origin to resemble a triangular fundamental diagram. The intersection point of the blue and black lines in Figure 4.29 was considered $Q_{capacity}$ on the vertical axis; and, the same point, when projected down on the horizontal axis, defined the actual critical density (k_{crit} = 30 veh/km/lane).
4. The free-flow speed, V_f, could then be found, averaging the speed of all the sample points with density values of less than the k_{crit} (30 veh/km/lane).
5. Assuming that a vehicle consumes 9 m space in a highly congested queue, a jam density (k_j) value could be fixed at 110 veh/km/lane. Both k_j and $Q_{capacity}$ were connected with a purple line in Figure 4.29 to finalize the triangular flow-density diagram necessary for Lawson et al. BOQ estimation process.
6. Parameters such as V_f „k_j and $Q_{capacity} = \mu$ could then be readily found from this fundamental diagram for construction of the input-output (I/O) diagram **(**Figure 4.30**)** using the Lawson et al. method, as explained in Section 2.8.3 of Chapter 2.

It is to be noted that Dervisoglu et al. (2009) fitted the congested branch of the fundamental diagram by an approximate quantile regression of the flow-density points on the higher end of their distribution, constrained to pass through the capacity point. This procedure also yielded a linear line skewed outward from the congested flow-density points, confirming the validity of the congested branch constructed for this research in Figure 4.29 using the steps mentioned above.

Table 4.9: Parameters and Associated Values for the Method of Lawson et al.

Parameters	Values
V_f	54 km/hr
k_j	110 veh/km/lane
$Q_{capacity}$ (i.e. saturation flow rate, μ, during the green interval)	1610 veh/hr/lane

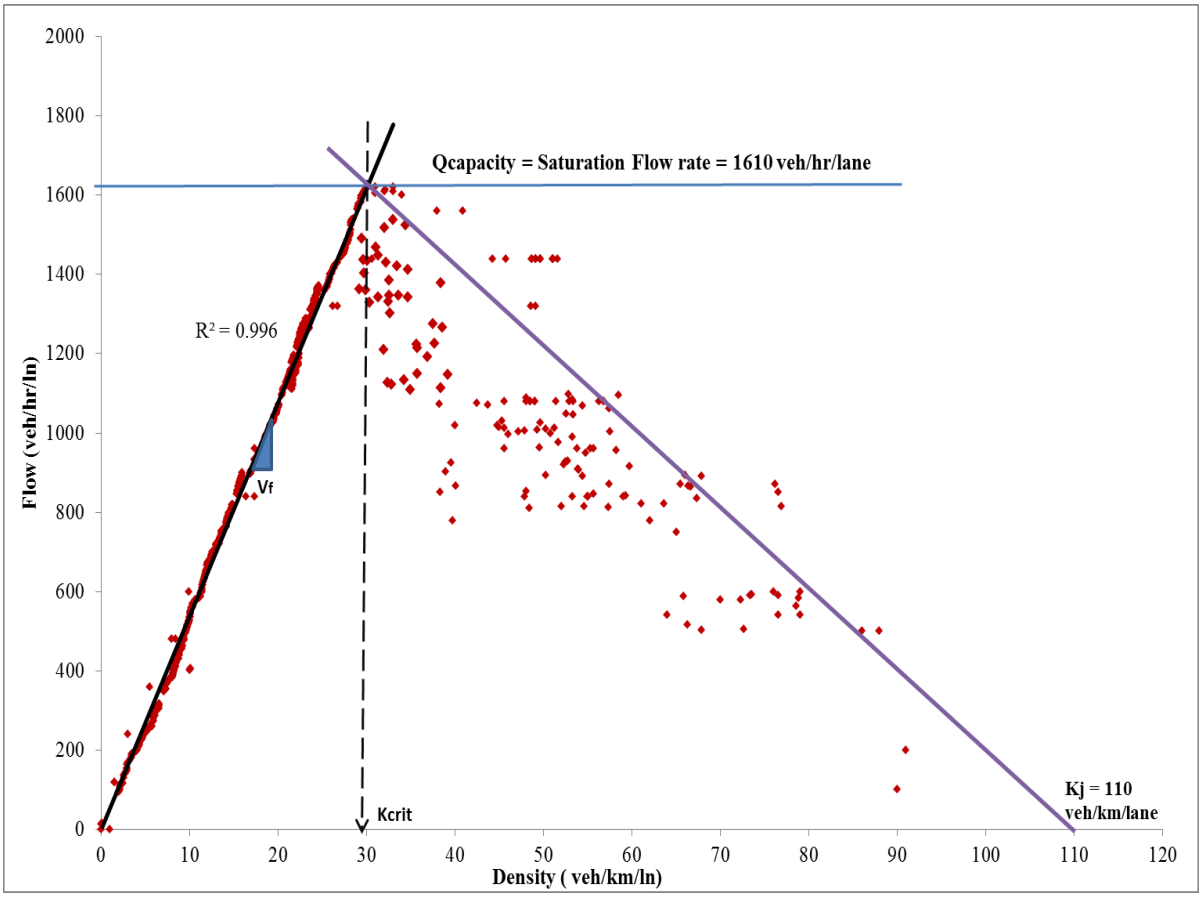

Figure 4.29: Fundamental Flow-Density Diagram for Signalized Intersection Scenarios

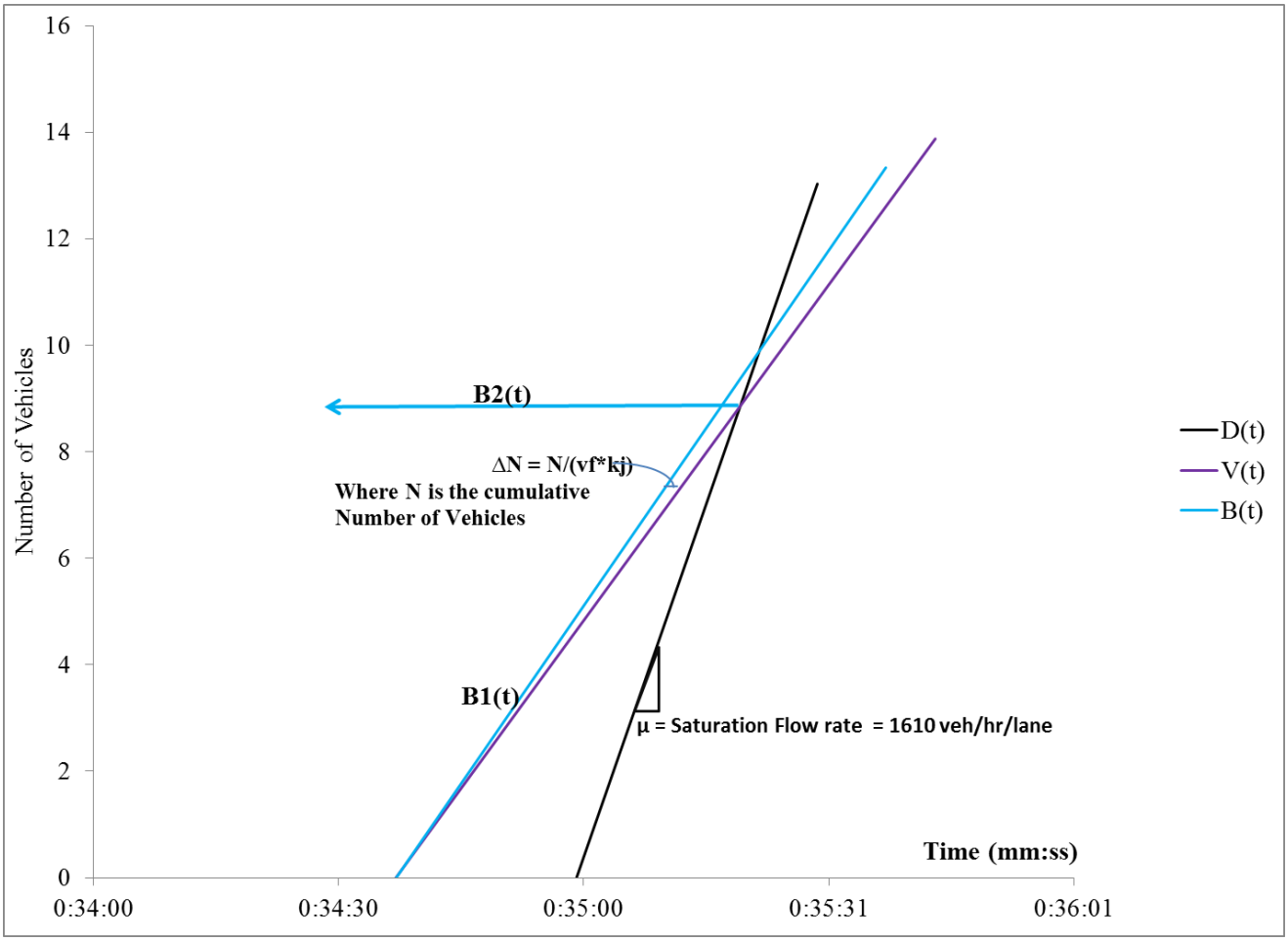

Figure 4.30: Cumulative Diagram using Lawson et al. Method (Single Cycle)

4.5.1.2 Probe-Based Method taking Probe-Vehicle Trajectory and Detector Count Data in Combination with an Input-Output Technique

This method relies mainly on the true trajectory data of individual probe vehicles to estimate the BOQ location and time for the probes and, consequently, the BOQ curve, *B(t)*.

As a FIFO state was maintained, the cumulative number, *N*, for probes in the cumulative diagram could be determined using detector counts at the stop line. A probe trajectory analysis that applied queuing criteria enabled us to find the BOQ location and time for each probe.

From observation of the actual trajectory data of probes in Figure 4.31, it was confirmed that a BOQ point (when and where a vehicle joins the BOQ) could be detected out of the trajectory data of the probes using the following queuing criteria:

1. Speed at the BOQ must be much smaller than the free-flow speed and must also be greater than or equal to zero.
2. The vehicle sustains deceleration or zero acceleration at the BOQ.
3. A sustained speed reduction from free-flow speed for a couple of seconds (minimum 2 seconds) at a deceleration rate above 3 m/s^2 when the vehicle comes toward the stop line.
4. No BOQ can be found for vehicles that travel the link at a speed at or near V_f and are not regarded to cause a queue.

Another important parameter that was needed for successful queue estimation is the time when queue accumulation ceases. Queue accumulation ceases when lines *JK* and *LK* intersect with each other, as shown in Figure 4.32 and we get time t_k and the cumulative vehicle number on the same figure, corresponding to the intersection of the two lines mentioned above. *LK* is the BOQ line, which was found by applying the BOQ criteria for each probe vehicle and by running a least square regression line through the known probe vehicles' BOQ points. *JK* is the information line, which travels backwards from the stop line, as shown in Figure 4.31 and reconstructed for probe vehicles in Figure 4.32, when they started to accelerate during the green phase.

These two regression lines intersected at point *K*; and, the time instant, t_k, when they intersect marked the cessation of queue accumulation (i.e. growth). As time point t_k was known, the cumulative number of the last queued vehicle could be calculated from the input-output diagram.

Also the departure time of last queued vehicle (vertical projection of point *M*) was known from the detector data. The BOQ could be estimated by the vertical separation between lines *LKM* and *JM*, shown in the cumulative input-output diagram of Figure 4.32.

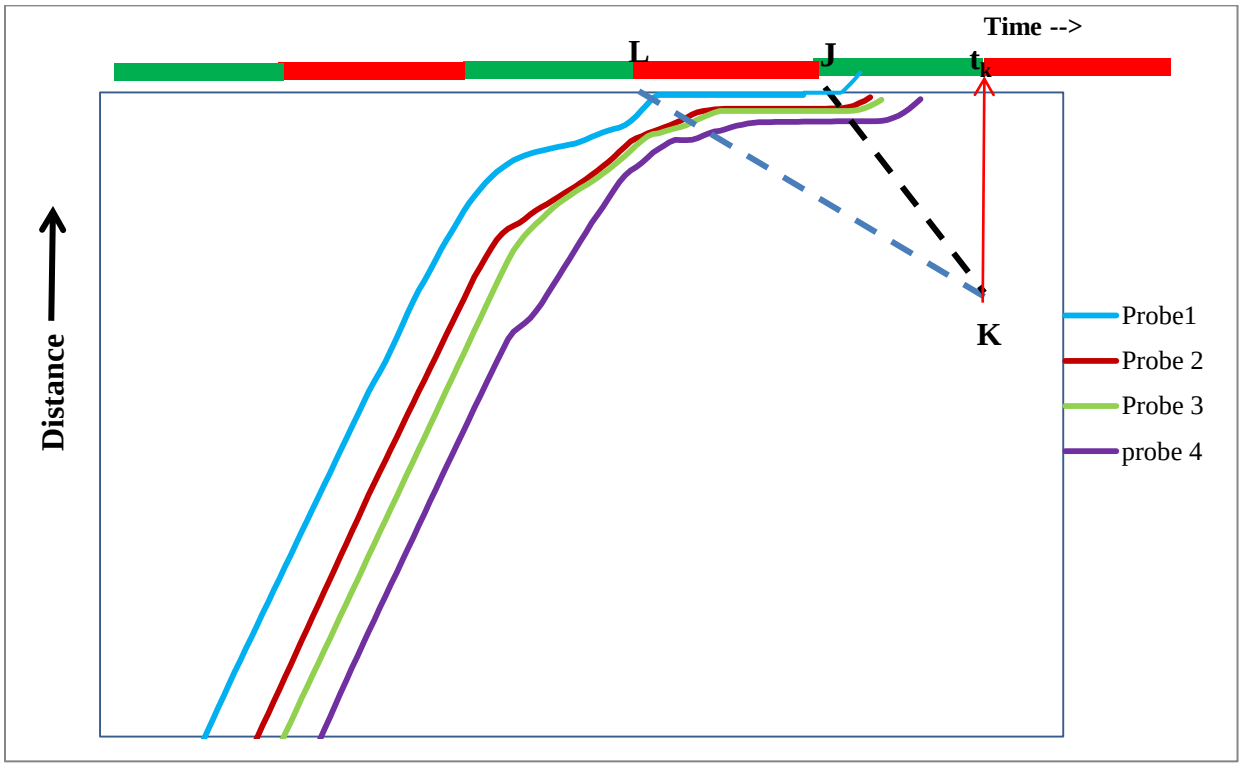

Figure 4.31: Analysis of Probe Trajectories to Determine the Back of Queue Line *LK* and Information Flow Line *JK*

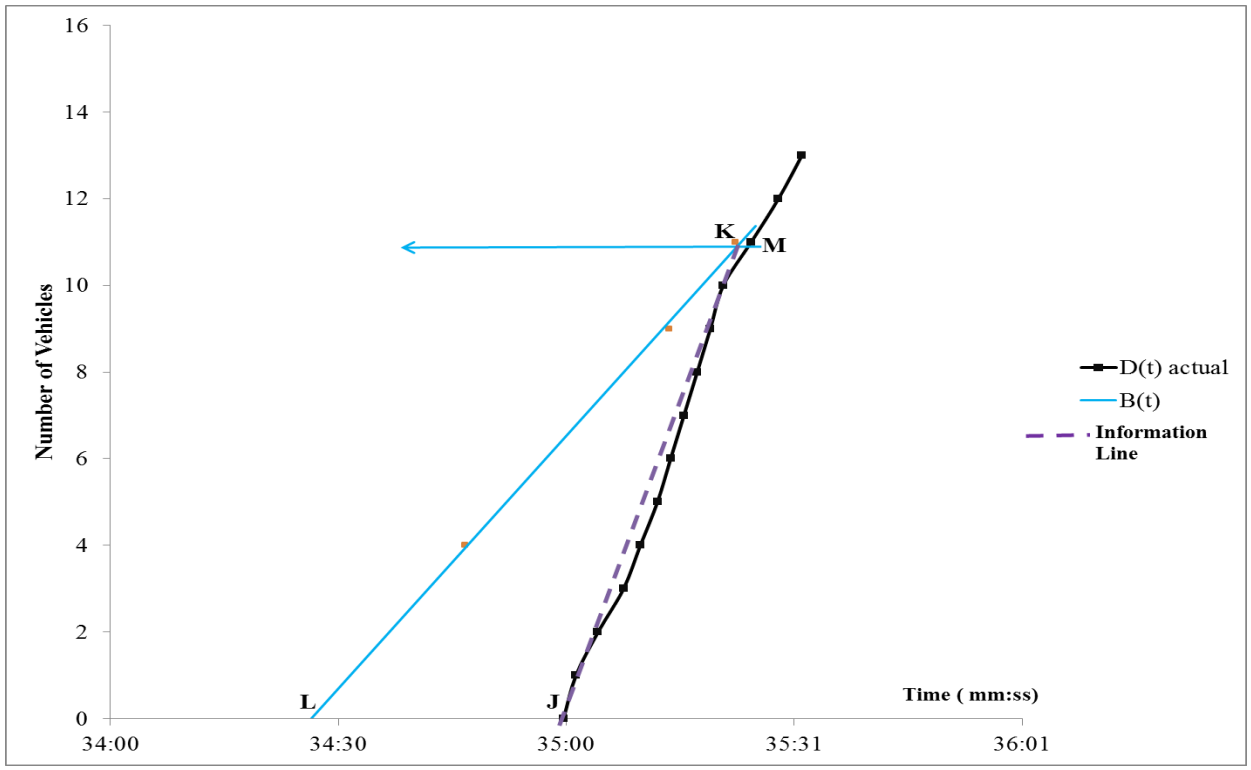

Figure 4.32: Analysis of Probe Trajectories to Determine the Back of Queue Line *LK* and Information Flow Line *JK* (Single Cycle)

4.5.1.3 Results and Accuracy Estimates of Models

The queue value at the signalized intersection was estimated in number of vehicles using the approaches mentioned in the previous sections. Figure 4.33 shows the estimated BOQ using the Lawson et al. method and the proposed method at different probe penetration percentages. The accuracy of the methods, which can best be described by RMSE and MAPE values, are shown in Figures 4.34 and 4.35, respectively.

Referring to Figures 4.34 and 4.35, it is quite evident that the RMSE and MAPE values for the Lawson et al. method were identical (around 1.0 and 1.9, respectively) at all probe penetration percentages, because this method has no sensitivity with respect to probe percentages. For the proposed probe-based method, it is clear that the queue estimation error reduced with increases in probe market share, outperforming the Lawson et al. method at least above a probe market share of 30 percent.

Ban et al. (2011) estimated queue length at a signalized intersection using sampled travel times from probe vehicles with a penetration rate of 30 percent. The corresponding MAPE value was about 16 percent; whereas, in this research, the MAPE value at 30 percent probe market shares was about 2 percent for the undersaturated signalized intersection scenario (Case Study 2a). Therefore, the estimation accuracy of queue length of the probe-based method proposed in this thesis can be deemed promising.

The analyses were done on a per cycle basis and low probe penetration percentages (e.g. 10 or 20%) left only a few probe vehicle data points (i.e. around only 3 to 4 data points per cycle) for the trajectory analysis and for the construction of the cumulative BOQ curve, *B(t)*. This can

explain the lower performance of the probe-based method compared to the Lawson et al. method, which considers all vehicle data points during each cycle.

From the RMSE plot in Figure 4.34, it is clear that the error reached well below 1 vehicle error at a 40 percent probe penetration rate for the probe-based method. A separate single-factor ANOVA test with a related post-hoc test, such as Tukey's test (Appendix C), was conducted with RMSE and MAPE values as dependent variables at different probe penetration percentages. At a five-percent level of significance, it was found that a significant difference existed among errors at different probe market shares, which, in other words, means that queue estimation accuracy is highly sensitive to the probe penetration percentages.

Another important finding from the queue evolution diagram in Figure 33 is the underestimation of queue length by the Lawson et al. method. This underestimation may have been due to some strict assumptions of the Lawson et al. method, such as the inclusion of only zero speed vehicles as queued vehicles and simultaneous speed changes directly from free-flow to zero speed and vice versa.

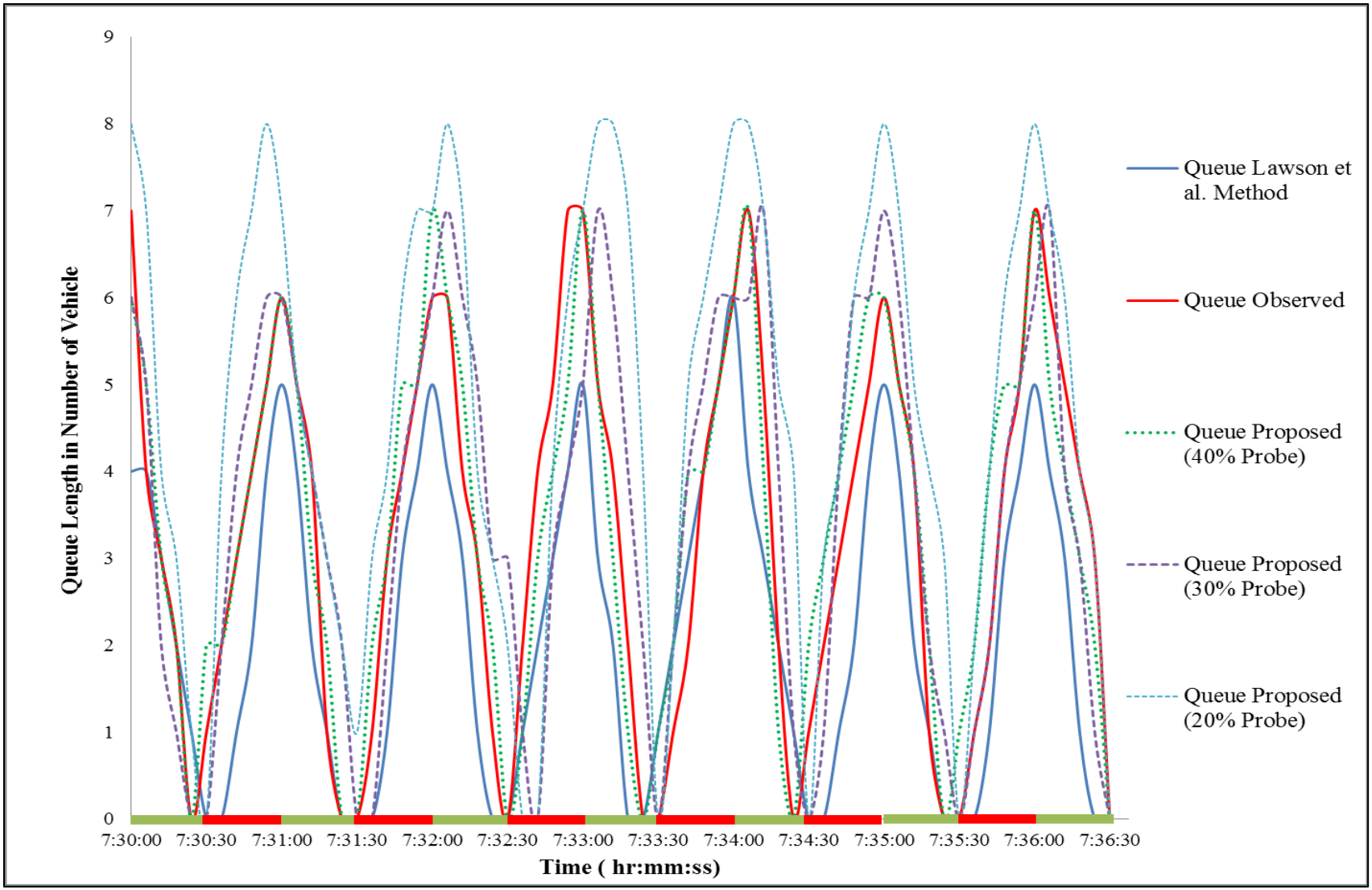

Figure 4.33: Sample Queue Estimation Result using Different Methods (Five Cycles)

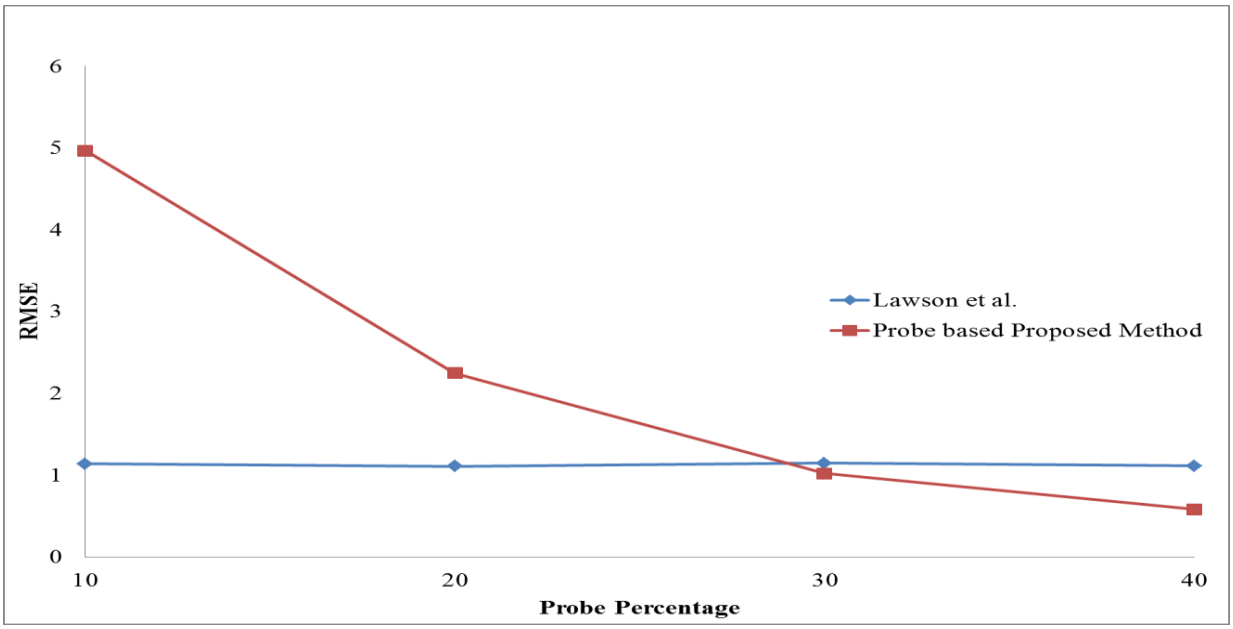

Figure 4.34: RMSE vs. Probe Penetration Percentage for Different Queue Estimation Methods of at Signalized Intersections

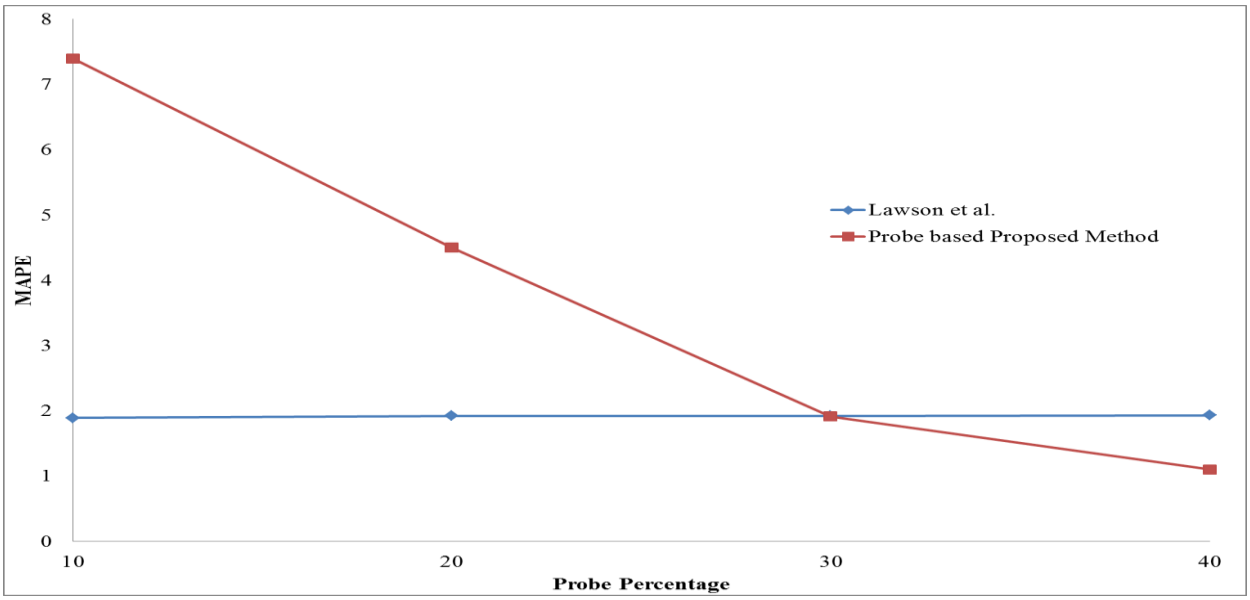

Figure 4.35: MAPE vs. Probe Penetration Percentage for Different Queue Estimation Methods at Signalized Intersections

4.5.2 Case Study 2b: Oversaturated Signalized Intersection

The proposed methodology could be extended to estimate queue lengths for oversaturated situations. The assumptions related to the input-output technique, such as a FIFO state, were maintained over the same one-lane link. Another assumption was that there is no interference or impact of nearby intersection signals on the intersection where queue is being estimated. In other words, the estimation is carried out for an isolated intersection. The signal was again assumed to maintain the same fixed phase splits (60 second cycle) as in the undersaturated signalized intersection scenario discussed in previous sections.

Figure 4.37 shows a sample time-space diagram of probe vehicles facing oversaturation. Applying the proposed method, it was possible to construct the cumulative BOQ line, *B(t)* (black line), as shown in Figure 4.38. The relevant queue lengths in number of vehicles (Figure 4.40) could be found by measuring the vertical separation between the *B(t)* and *D(t)* lines. It was also possible to estimate the delay encountered by each vehicle and compare it with the HCM 2010 delay formula. According to HCM 2010, the delay for a given lane group is computed by using the following equation:

$$d = d_1 + d_2 + d_3 \ldots. (9)$$

where,

d = control delay (s/veh)

d_1 = uniform delay (s/veh) = $\frac{.5\, C\, (1-{}^{g}/_{C})^{2}}{1-[\min(1,X){}^{g}/_{C}]}$ …… (10)

d_2 = incremental delay (s/veh) = Overflow delay = $900T[(X-1)+\sqrt{(X-1)^2+\frac{8kIX}{cT}}]$ …. (11)

d_3 = initial queue delay (s/veh) = assumed to be zero at the start of the analysis period

X = volume to capacity ratio of lane group ≈ 1.2

C = traffic signal cycle length (sec) = 60 sec

c = capacity of lane group (veh/h) = 1610 veh/hr

g = effective green time for lane group (sec) = 30 sec

k = incremental delay factor dependent on signal controller setting (0.50 for pre-timed signals; vary from 0.04 to 0.50 for actuated controllers) = assumed to be 0.5

I = upstream filtering/metering adjustment factor = adjusts for the effect of an upstream signal on the randomness of the arrival pattern = 1 (1.0 for an isolated intersection)

T = analysis period (hours) = each cycle time = 1 hr

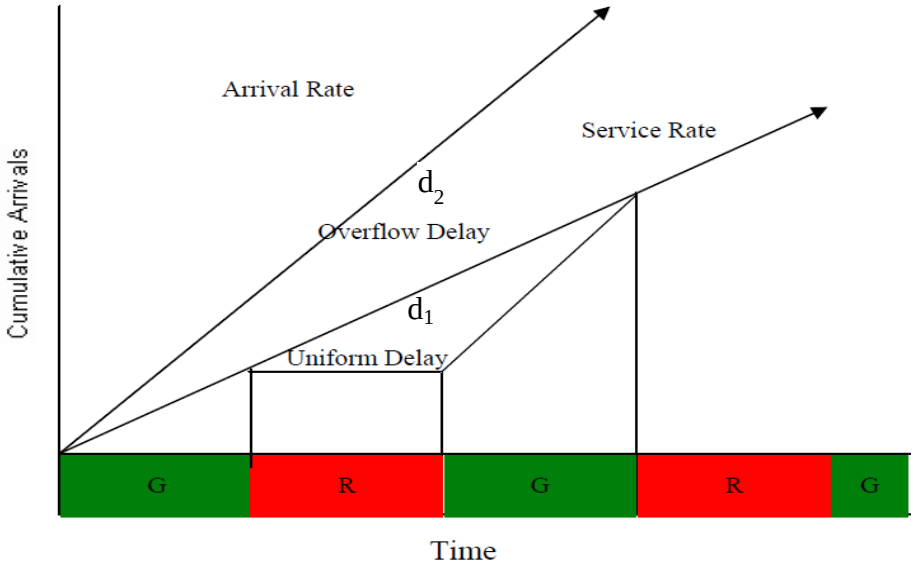

Figure 4.36: Delay Components in Cumulative Diagram (Assumed Initial Queue d_3 = 0 seconds)

Assuming a zero initial queue delay (d_3= 0 sec) at the beginning of the one-hour analysis period, the average delay per vehicle in seconds can easily be computed using the HCM 2010 delay

estimation equations with the necessary parameters values mentioned above. Figure 4.39 shows the estimated delay and average HCM delay per vehicle for the cumulative diagram of Figure 4.38. From this figure, it is clear that the HCM 2010 estimated a very high average delay per vehicle compared to the probe-based method.

Another important finding from the delay graph in Figure 4.39 is that the probe-based method can identify delays for individual probe vehicles, whereas the HCM 2010 delay model can only estimate the average delay of vehicles during the analysis period. Therefore, we can conclude that HCM delay formulas cannot be used when real-time vehicle specific microscopic delay is required for analysis.

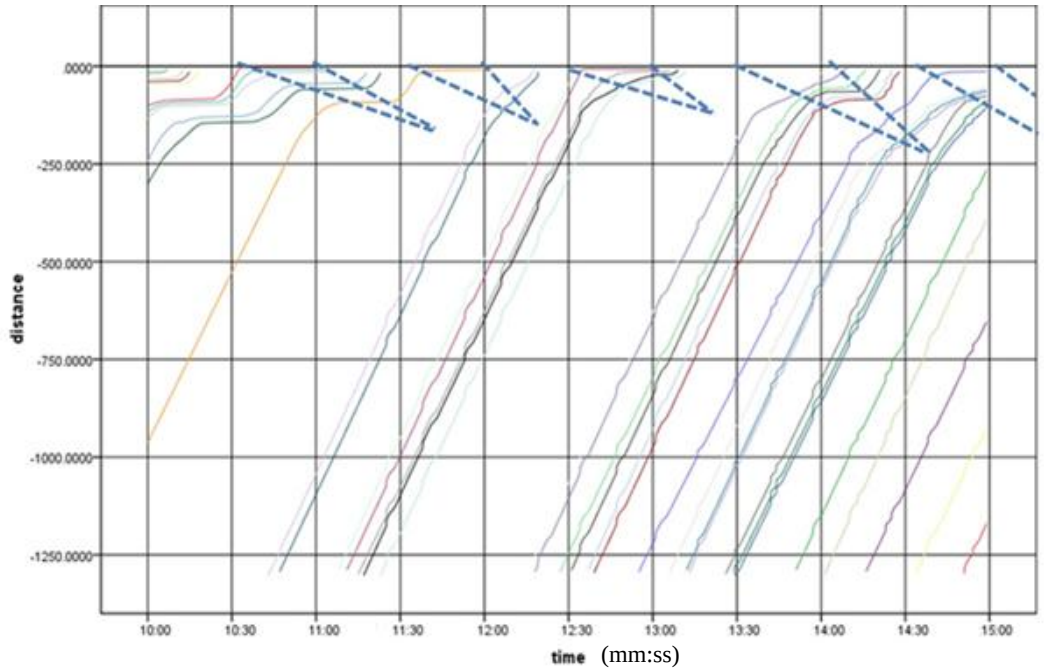

Figure 4.37: Sample Probe Trajectory (40% Penetration, Run 3)

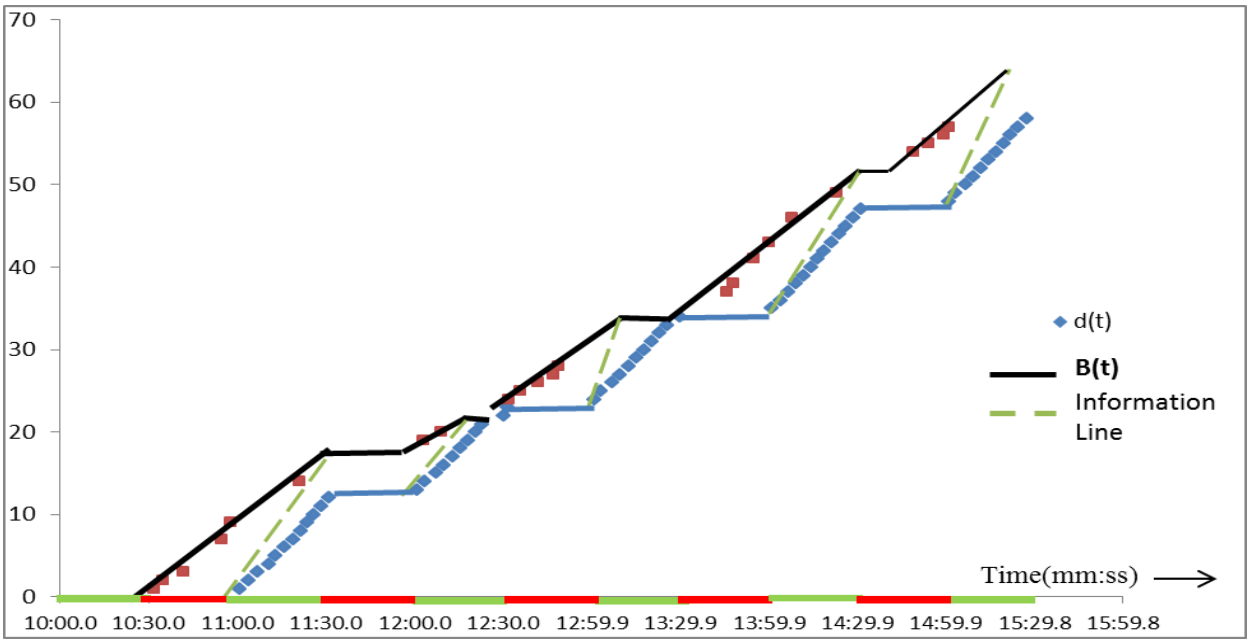

Figure 4.38: Sample Cumulative Diagram (40% Penetration, Run 3)

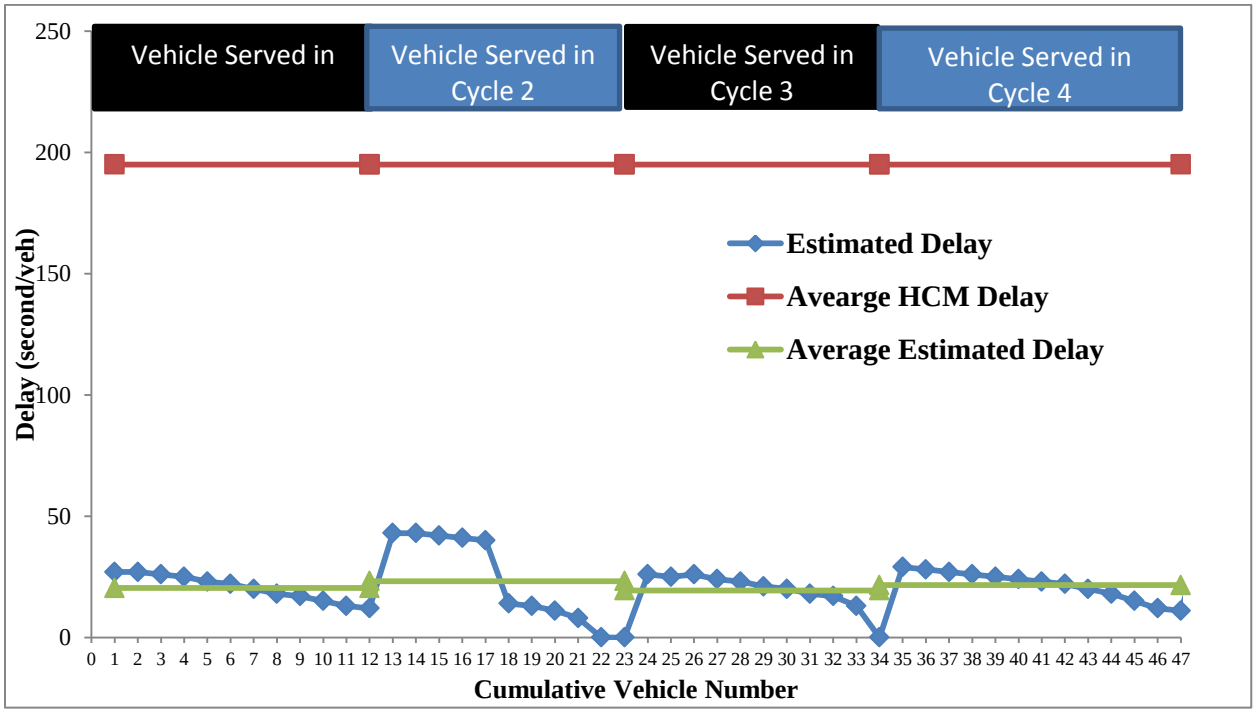

Figure 4.39: Estimated Delay for Each Vehicle and the HCM 2010 Average Delay (40% Penetration)

4.5.2.1 Data Analysis Results and Error Estimates

The only method adopted to estimate queue was the probe-based method, which uses probe trajectory data and stop line detector counts to directly estimate queues. Figure 4.40 presents a sample queue evolution, which shows the estimated and actual queue lengths during a five-cycle period, where the actual queue length was the outcome of all vehicle trajectory analyses.

From Figure 4.40, it can be said that the estimated queue closely matched the observed BOQ length, defined as the last number of the vehicle that undergoes significant deceleration (more than 3 m/s^2) due to the queue in front of it at time *t*. If the probe penetration percentage can be increased in the traffic stream, the estimation would become significantly more accurate. The RMSE and MAPE plots in Figure 4.41 clearly shows that a higher percentage of probe penetration increased the accuracy of the estimation of queue length and that a 30% probe market share was quite enough to achieve an estimated BOQ with an RMSE of ±1 vehicle and an an MAPE of about 4%. In Ban et al. (2011), estimated queue lengths at a signalized intersection using sampled travel times from probe vehicles with a penetration rate of 30 percent yielded a higher MAPE (around 16%). Therefore, the estimation accuracy of queue length for the probe-based method proposed in this thesis can be deemed as promising.

An ANOVA test with a related post-hoc test, such as Tukey's test in Appendix D, illustrated that the accuracy of the methodology at different percentages of probe penetration varied significantly, which in turn verified that the higher the probe percentage in the estimation process, the better the queue estimates.

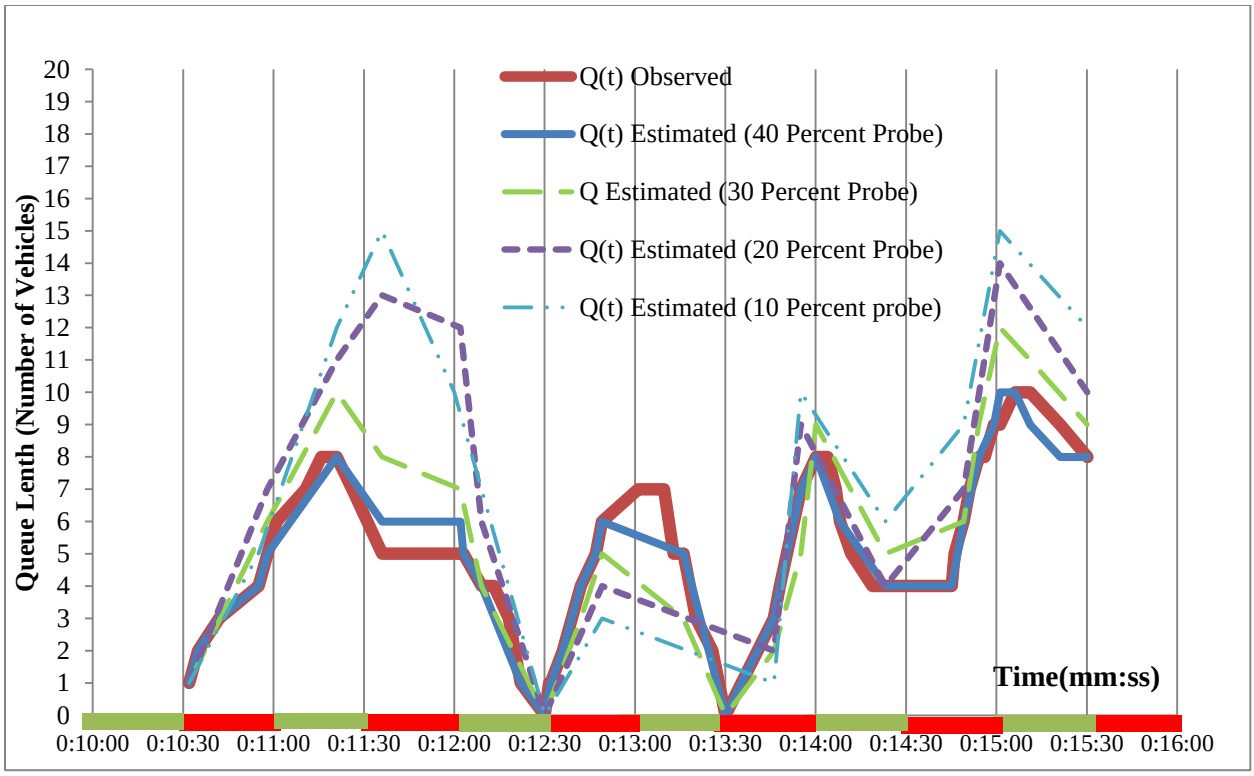

Figure 4.40: Queue Evolution in an Oversatured Signalized Intersection (Five Cycles)

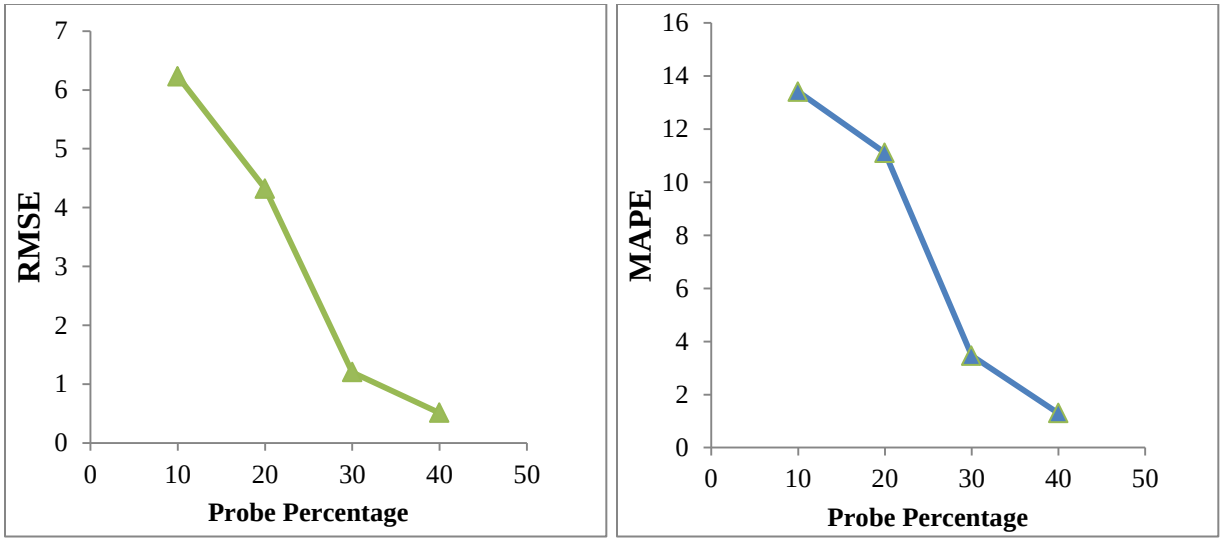

Figure 4.41: RMSE and MAPE Plots of the Probe-Based Method with respect to the Observed Queue

4.6 Summary

This chapter presents applications of the proposed methodology outlined in Chapter 3 for queue estimation based on an input-output model, probe-vehicle trajectory data and the Lawson et al. theoretical model (explained in Chapter 2). The estimated queue in this thesis is the back of queue, which is defined as the queue in number of vehicles (cumulative), including the vehicles that join the queue after the beginning of the green phase or a moving queue in a bottleneck situation. In order to know whether the vehicles are in the back of queue or not, BOQ criteria have been devised, using the micro traffic feature of the probe-vehicle data (trajectory data analysis) for the probe-based method. Estimations were also carried out for different probe penetration percentages.

The queue estimates from different methods were compared with the observed or actual queue length, so that the robustness of different methods at varying probe penetration rates could be analyzed. It was found that the probe-based method for both the bottleneck and signalized intersection scenarios estimated the BOQ with a relatively high accuracy. Therefore, we can conclude that the use of only probe-vehicle information in combination with an input-output technique can yield better estimation results of the vehicle queue than the other methods.

Chapter Five: Summary and Conclusions

This chapter mainly focuses on the outcomes, contributions and further development aspects of the research conducted in the development of this thesis. Section 5.1 briefly explains the whole research effort, explaining the implications and worthwhile contributions of the research for traffic engineering, which requires queue estimation processes for situations like urban bottleneck scenarios and at signalized intersections. Finally, the author's recommendations toward future research and development of methods based on this thesis are also laid out in Section 5.2.

5.1 Research Summary and Contributions

The main focus of the research is the estimation of the back of queue (BOQ) length from the available probe data in a controlled simulation environment, where several assumptions were strictly maintained in the simulation runs as conducted with Quadstone Paramics traffic simulation software package. Such assumptions were related to designated driver behaviour and car following theories to maintain a first-in, first-out (FIFO) condition.

To the best of the author's knowledge, this research is the first attempt for real-time queue estimation using probe-vehicle trajectory data in conjunction with an input-output technique. The estimation procedures were designed so that they can be employed in mainly two different queuing scenarios: 1) urban bottlenecks that generate queues, and 2) at signalized intersections, which are the most common cases of queue generation. Queue estimation in these two situations is important due to their implication on roadway measures of effectiveness, such as delays, wait times, travel times and fuel consumption.

The main findings from this research are outlined below.

1. The probe-based method was found to be highly sensitive to the penetration percentage of probe vehicles in the traffic stream. The greater the probe percentage, the better the BOQ estimates.
2. The theoretical Lawson et al. method of BOQ estimation was outperformed by the developed probe-based method at any probe penetration percentage in bottleneck scenarios.
3. An absolute vehicle error of less than 1 can be achieved with the use the probe-based method, when the probe vehicle penetration rate is in the range of 30 to 40%/
4. In queue estimation for signalized intersections, a probe market share of at least 30 percent is needed to outperform the Lawson et al. method. This can be explained by the fact that the Lawson et al. method uses all vehicle information regarding arrivals and departures. However, with a probe penetration rate of at least 30%, the probe-based method is able to outperform the Lawson et al. method without any information on cumulative arrivals.
5. The extension of the Lawson et al. method always performed better than the original Lawson et al. method, due to the reasonable and logical consideration of capacity drops at bottlenecks.

The main contributions of the thesis are:

- Development of a BOQ estimation approach based on individual probe-vehicle trajectory data analysis in combination with an input-output model.

- Improvement of the theoretical Lawson et al. (1996) model, by taking into consideration capacity drops.
- Fewer detectors are needed for the estimation of cumulative arrivals with the probe-based method, as there is no need for an upstream detector.
- Sensitivity analyses with several bottleneck scenarios and at different probe penetration rates have been conducted.
- Traditionally, probe data are only used to estimate travel times. However, probe data carry detailed trajectory data, including speed, location, acceleration and deceleration. Travel times estimated from probe data may depend on the probe vehicle type (e.g. passenger car, bus, taxi). However, the location of a probe vehicle within a queue does not depend on the vehicle type. In this research, the position of a probe vehicle within the queue was considered as one of the main inputs; and, as a result, the methodology was less dependent on probe-vehicle type (or probe sensor type).

5.2 Further Research Scope and Recommendations

The research presented in this thesis had some limitations, which may lay the foundation of further research based on this study. Several future research guidelines are proposed.

- The application of the methodology is currently restricted to lane-by-lane analysis. with no passing permitted to maintain a FIFO condition. A possible extension to the current research would be to develop a way to implement an input-output technique without maintaining FIFO.

- In this research, only one type of vehicle (i.e. passenger cars) acted as probe vehicles. In future work, different types of vehicles, such as taxis, trucks, SUVs and transit bus, can also be considered to get better estimates of the queue length.
- Only two case studies related to bottleneck scenarios were examined. Some other bottleneck situations and related queues created due to off-ramps, complex weaving behaviours and lane changing also need to be considered in queue estimation.
- No turning movements were allowed in the proposed queue estimation algorithm for signalized intersections. As future work, this can be addressed by considering the presence of incoming/outgoing vehicles that can be generated midblock of the examined link.
- GPS (Global Positioning System) sensors are prone to estimation errors in cases such as urban canyons. In such situations, other non-intrusive complementary sensor data, such as WiFi, Bluetooth and mobile signal triangulation, can be fused with the onboard GPS sensor data to minimize estimation errors.
- The developed algorithm can be tested with real data. One of the limitations of this study was the use of simulation data as the basis for analysis. Future research should consider testing the algorithm with real data.

References

Akcelik, R. (1988) “The Highway Capacity Manual Delay Formula for Signalized Intersections” ITE Journal 58 (3), pp. 23-27.

Akçelik, R. (2001). HCM 2000 back of queue model for signalised intersections. Akcelik and Associates Pty Ltd., Melbourne Australia.

Al-Deek, H., A. Garib, and A. E. Radwan. 1995. New Method for Estimating Freeway Incident Congestion. In Transportation Research Record 1474, TRB, National Research Council, Washington D.C, pp. 30–39Akcelik, R., 1999. A Queue Model for HCM 2000. ARRB Transportation Research Ltd., Vermont South, Australia

Balke, K. N., Charara, H. A., & Parker, R. (2005). Development of a traffic signal performance measurement system (TSPMS) (No. FHWA/TX-05/0-4422-2). Texas Transportation Institute, Texas A&M University System

Ban, X., Hao, P., & Sun, Z. (2011). Real time queue length estimation for signalized intersections using travel times from mobile sensors. Transportation Research Part C: Emerging Technologies, 19(6), 1133-1156. doi: 10.1016/j.trc.2011.01.002

Brilon, W., T.J. Geistefeld and M. Regler, 2008. Reliability of freeway traffic flow: A stochastic concept of capacity. Proceedings of the 16th International Symposium on Transportation and Traffic Theory, July 2005, College Park, MD., USA., pp: 125-144.

Cassidy, M. J., & Bertini, R. L. (1999). Some traffic features at freeway bottlenecks. Transportation Research Part B: Methodological, 33(1), 25-42.

Catling I. (1977) A time-dependent approach to junction delays. Traffic Engineering & Control 18, 520-526.

Cayford, R., J. Colson and K. Guthrie (2008). Accuracy of Traffic Information Generated by an Anonymous Cell Phone Tracking System. 87th Annual Meeting of the Transportation Research Board. Washington, D.C.

Cetin, M. & Comert, G. (2007). Estimating queues at signalized intersections: Value of location and time data from instrumented vehicles. Intelligent Vehicles Symposium, 2007 IEEE, 1138-1143.

Chang, T. H. & Lin, J. T. (2000). Optimal signal timing for an oversaturated intersection. Transportation Research Part B: Methodological, 34(6), 471-491.

Cheek, M. T. (2007). Improvements to a queue and delay estimation algorithm utilized in video imaging vehicle detection systems (Doctoral dissertation, Texas A&M University).

Cheng, Y., Qin, X., Jin, J., Ran, B., & Anderson, J. (2011). Cycle-by-cycle queue length estimation for signalized intersections using sampled trajectory data. Transportation Research Record: Journal of the Transportation Research Board, 2257(-1), 87-94.

Comert, G. & Cetin, M. (2009). Queue length estimation from probe vehicle location and the impacts of sample size. European Journal of Operational Research, 197(1), 196-202.

Constantin, H. (2011). Markov chains and queueing theory.

Cronje, W. (1983). Analysis of Existing Formulas for Delay, Overflow, and Stops,

Cronje, W. (1983). Derivation of Equations for Queue Length, Stops, and Delay for Fixed-Time Traffic Signals,

Dervisoglu, G., Gomes, G., Kwon, J., Horowitz, R., & Varaiya, P. (2009, January). Automatic calibration of the fundamental diagram and empirical observations on capacity. In Transportation Research Board 88th Annual Meeting (No. 09-3159).

Felsburg Holt & Ullevig.(2008). Performance Measures for Traffic Signal Operations, Final report prepared for Denver Regional Council of Governments.

Friedrich, B., Matschke, I., Almasri, E., & Mück, J. (2003). Data fusion techniques for adaptive traffic signal control. Proceedings of the 10th IFAC Symposium on Control in Transportation Systems, 85-86.

Gazis, D. C. (1964). Optimum control of a system of oversaturated intersections. Operations Research, 12(6), 815-831.

Gazis, D.C., 1974. Traffic Science. Wiley Interscience, New York.

Geroliminis, N. & Skabardonis, A. (2005). Prediction of arrival profiles and queue lengths along signalized arterials by using a markov decision process. Transportation Research Record: Journal of the Transportation Research Board, 1934(-1), 116-124.

Green, D.H., 1968. Control of oversaturated intersections. Operational Research Quarterly 18 (2), 161–173.

Hao, P. & Ban, X. J. Estimating vehicle position in a queue at signalized intersections using sample travel times from mobile sensors.

Hao, P. & Sun, Z. (2011). Real time queue length estimation for signalized intersections using travel times from mobile sensors. Transportation Research Part C: Emerging Technologies, 19(6), 1133-1156.

Hellinga, B., & Gudapati, R. (2000). Estimating link travel times for advanced traveler information systems. Proceedings of the Canadian Society of Civil Engineers, 3rd Transportation Specialty Conference,

Herring, R., Hofleitner, A., Abbeel, P., & Bayen, A. (2010). Estimating arterial traffic conditions using sparse probe data. Proceedings of the 13th International IEEE Conference on Intelligent Transportation Systems, Madeira, Portugal, 929-936.

John M. Noble.(2009). NMAC22: Markov Chains and Queueing Theory. Complied notes. Mathematiska institutionen, Linköpings universitet,58183 LINKÖPING, Sweden.

Kimber, R. M. and Hollis, E. M. (1979) Traffic Queues and Delays at Road Junctions.

LR 909, Transportation Road Research Laboratory, Crowthorne.

Kong, Q. J., Li, Z., Chen, Y., & Liu, Y. (2009). An approach to urban traffic state estimation by fusing multisource information. Intelligent Transportation Systems, IEEE Transactions on, 10(3), 499-511.

Kwong, K., Kavaler, R., Rajagopal, R., & Varaiya, P. (2009). Arterial travel time estimation based on vehicle re-identification using wireless magnetic sensors. Transportation Research Part C: Emerging Technologies, 17(6), 586-606.

Lawson, T. W., Lovell, D. J., & Daganzo, C. F. (1996). Using input-output diagram to determine spatial and temporal extents of a queue upstream of a bottleneck. Transportation Research Record: Journal of the Transportation Research Board, 1572, 140-147.

Lighthill, M. J. & Whitham, G. B. (1955). On kinematic waves. II. A theory of traffic flow on long crowded roads. Proceedings of the Royal Society of London.Series A.Mathematical and Physical Sciences, 229(1178), 317-345.

Liu, H. X. & Ma, W. (2009). A virtual vehicle probe model for time-dependent travel time estimation on signalized arterials. Transportation Research Part C: Emerging Technologies, 17(1), 11-26.

Liu, H. X., Wu, X., Ma, W., & Hu, H. (2009). Real-time queue length estimation for congested signalized intersections. Transportation Research Part C: Emerging Technologies, 17(4), 412-427. doi: DOI: 10.1016/j.trc.2009.02.003

Mannering, F., Kilareski, W., & Washburn, S. (2007). Principles of highway engineering and traffic analysis John Wiley & Sons.

Mehran, B., Kuwahara, M., & Naznin, F. (2012). Implementing kinematic wave theory to reconstruct vehicle trajectories from fixed and probe sensor data. Transportation Research Part C: Emerging Technologies, 20(1), 144-163. doi: 10.1016/j.trc.2011.05.006

Messer, C. J., C. L. Dudek, and J. D. Friebele. (1973). Method for Predicting Travel Time and Other Operational Measures in Real-Time During Freeway Incident Conditions. In Highway Research Record 461, TRB, National Research Council, Washington, D.C., 1973, pp. 1–11.

Michalopoulos, P. G., & Stephanopoulos, G. (1977). Oversaturated signal systems with queue length constraints—I: Single intersection. Transportation Research, 11(6), 413-421.

Michalopoulos, P. G., Stephanopoulos, G., & Stephanopoulos, G. (1981). An application of shock wave theory to traffic signal control. Transportation Research Part B: Methodological, 15(1), 35-51.

Miller, A. J. (1968). The capacity of signalized intersections in Australia.

Morales, M. J. Sept. 1986.Analytical Procedures for Estimating Freeway Traffic Congestion. Public Road, Vol. 50, No. 2.

Mück, J. (2002). Using detectors near the stop-line to estimate traffic flows. Traffic Engineering & Control, 43(11), 429-434.

Mystkowski, C. & Khan, S. (1999). Estimating queue lengths by using SIGNAL94, SYNCHRO3, TRANSYT-7F, PASSER II-90, and CORSIM. Transportation Research Record: Journal of the Transportation Research Board, 1683, 110-117.

National Research Council (U.S.). (2010). HCM 2010: Highway capacity manual. Washington, D.C: Transportation Research Board.

Newell, G. F. (1965). Approximation methods for queues with application to the fixed-cycle traffic light. SIAM Review, 7(2), 223-240.

Pecherkova, P., Flidr, M., & Dunik, J. (2008). Application of estimation techniques on queue lengths estimation in traffic network. Cybernetic Intelligent Systems, 2008. CIS 2008. 7th IEEE International Conference on, 1-6.

Qian, G., Lee, J., & Chung, E. (2012). A real-time queue estimation algorithm for signalized motorway off-ramps. 91st Transportation Research Board Annual Meeting, 2012, Washington, DC, USA, 12-2046.

Richards, P. I. (1956). Shock waves on the highway. Operations research, 4(1), 42-51.

Robertson, D. I. (1969). TRANSYT: A traffic network study tool.

Rouphail, N. M., Courage, K. G., & Strong, D. W. (2006). New Calculation Method for Existing and Extended Highway Capacity Manual Delay Estimation Procedures. In Transportation Research Board 85th Annual Meeting (No. 06-0106)

Sadegh, A., Radwan, A., and Matthias, J. (1987).A Comparison of Arterial and Network Software Programs. ITE Journal. Vol. 57, No. 8, pp. 35- 39.

SCOOT (2013). http://www.scoot-utc.com. Accessed on : 17 Jan 2013

Sharma, A., Bullock, D. M., & Bonneson, J. A. (2007). Input-output and hybrid techniques for real-time prediction of delay and maximum queue length at signalized intersections. Transportation Research Record: Journal of the Transportation Research Board, 2035, 69-80.

Smith, B. L., R. Venkatanarayana, H. Park, N. Goodall, J. Datesh, et al. 2001.IntelliDrive Traffic Signal Control Algorithms. Final report Prepared for IntelliDriveSM Pooled Fund Study

Stephanopoulos, G., Michalopoulos, P. G., & Stephanopoulos, G. (1979). Modelling and analysis of traffic queue dynamics at signalized intersections. Transportation Research Part A: General, 13(5), 295-307.

Strong, D.W., Nagui M.R, Ken C., 2006. New calculation method for existing and extended HCM delay estimation procedure. Paper #06-0106, Proceedings ofthe 85th annual meeting of the Transportation Research Board, Washington, DC.

Vigos, G., Papageorgiou, M., & Wang, Y. (2006). A ramp queue length estimation algorithm. Intelligent Transportation Systems Conference, 2006. ITSC'06. IEEE, 418-425.

Vigos, G., Papageorgiou, M., & Wang, Y. (2008). Real-time estimation of vehicle-count within signalized links. Transportation Research Part C: Emerging Technologies, 16(1), 18-35.

Viloria, F., Courage, K., & Avery, D. (2000). Comparison of queue-length models at signalized intersections. Transportation Research Record: Journal of the Transportation Research Board, 1710(-1), 222-230.

Viti, F., & Van Zuylen, H. J. (2010). Probabilistic models for queues at fixed control signals. Transportation Research Part B: Methodological, 44(1), 120-135.

Viti, F. & van Zuylen, H. J. (2004). Modeling queues at signalized intersections. Transportation Research Record: Journal of the Transportation Research Board, 1883, 68-77.

Wang, H., Rudy, K., & Ni, D. (2008). Modeling and optimization of link traffic flow. 87th Transportation Research Board Annual Meeting, 08-2129.

Webster, F., 1958. Traffic signal settings. Road Research Technical Paper 39. Road Research Laboratory, Her Majesty's Stationery Office, London,

Webster, F.V. and Cobbe, B. M. (1966). Traffic Signals. Road Research Technical Paper No. 56. HMSO London UK

Welch, G. & Bishop, G. (1995). An Introduction to the Kalman Filter,

Wikipedia 2013. http://en.wikipedia.org/wiki/Markov_chain. Accessed on 17 Jan , 2013

Wirasinghe, C. S. (1978).Determination of Traffic Delays from Shock Wave Analysis. Transportation Research, Vol. 12.

Worthington, D. (2009). Reflections on queue modelling from the last 50 years. Journal of the Operational Research Society, , S83-S92.

Wu, J., Jin, X., & Horowitz, A. J. (2008). Methodologies for estimating vehicle queue length at metered on-ramps. Transportation Research Record: Journal of the Transportation Research Board, 2047, 75-82.

Yi, P., Xin, C., & Zhao, Q. (2001). Implementation and field testing of characteristics-based intersection queue estimation model. Networks and Spatial Economics, 1(1), 205-222.

Zou, N. (2007). Queuing models and analyses of traffic control. (Ph.D., The University of Arizona). ProQuest Dissertations and Theses. (304895568).

Appendix A

Single Factor ANOVA For PROBE Based Proposed Method (Case Study 1a)

Anova: Single Factor RMSE as Dependent variable						
SUMMARY						
Percent of Probe	*Count*	*Sum*	*Average*	*Variance*		
10	10	150.1959	15.01959	0.071785		
20	10	60.26337	6.026337	0.018836		
30	10	27.92782	2.792782	0.06059		
40	10	12.89996	1.289996	0.008329		
ANOVA						
Source of	*SS*	*df*	*MS*	*F*	*P-value*	*F crit*
Between Groups	1135.056	3	378.352	9486.092	3.28E-52<0.05	2.866266
Within Groups	1.435857	36	0.039885			
Total	1136.492	39				

Post Hoc Tests

Multiple Comparisons

RMSE

Tukey HSD

(I) Percentof Probe	(J) Percentof Probe	Mean Difference (I-J)	Std. Error	Sig.	95% Confidence Interval	
					Lower Bound	Upper Bound
10.00	20.00	8.99325*	.08931	.000	8.7527	9.2338
	30.00	12.22681*	.08931	.000	11.9863	12.4674
	40.00	13.72960*	.08931	.000	13.4891	13.9701
20.00	10.00	-8.99325*	.08931	.000	-9.2338	-8.7527
	30.00	3.23355*	.08931	.000	2.9930	3.4741
	40.00	4.73634*	.08931	.000	4.4958	4.9769
30.00	10.00	-12.22681*	.08931	.000	-12.4674	-11.9863
	20.00	-3.23355*	.08931	.000	-3.4741	-2.9930
	40.00	1.50279*	.08931	.000	1.2622	1.7433
40.00	10.00	-13.72960*	.08931	.000	-13.9701	-13.4891
	20.00	-4.73634*	.08931	.000	-4.9769	-4.4958
	30.00	-1.50279*	.08931	.000	-1.7433	-1.2622

*. **The mean difference is significant at the 0.05 level.**

Anova: Single Factor , MAPE as Dependent variable						
SUMMARY						
Groups	*Count*	*Sum*	*Average*	*Variance*		
10	10	240.7951	24.07951	0.053875		
20	10	139.8004	13.98004	0.156361		
30	10	40.3475	4.03475	0.127363		
40	10	15.1869	1.51869	0.027331		
ANOVA						
Source of Variation	*SS*	*df*	*MS*	*F*	*P-value*	*F crit*
Between Groups	3183.268	3	1061.089	11630.6	8.42E-54 < 0.05	2.866266
Within Groups	3.284372	36	0.091233			
Total	3186.552	39				

Post Hoc Tests

Multiple Comparisons

MAPE
Tukey HSD

(I) Percent ofProbe	(J) Percent ofProbe	Mean Difference (I-J)	Std. Error	Sig.	95% Confidence Interval	
					Lower Bound	Upper Bound
10.00	20.00	10.09947*	.13508	.000	9.7357	10.4633
	30.00	20.04476*	.13508	.000	19.6810	20.4086
	40.00	22.56082*	.13508	.000	22.1970	22.9246
20.00	10.00	-10.09947*	.13508	.000	-10.4633	-9.7357
	30.00	9.94529*	.13508	.000	9.5815	10.3091
	40.00	12.46135*	.13508	.000	12.0975	12.8251
30.00	10.00	-20.04476*	.13508	.000	-20.4086	-19.6810
	20.00	-9.94529*	.13508	.000	-10.3091	-9.5815
	40.00	2.51606*	.13508	.000	2.1523	2.8799
40.00	10.00	-22.56082*	.13508	.000	-22.9246	-22.1970
	20.00	-12.46135*	.13508	.000	-12.8251	-12.0975
	30.00	-2.51606*	.13508	.000	-2.8799	-2.1523

*. **The mean difference is significant at the 0.05 level**

Appendix B

Single Factor ANOVA For PROBE Based Proposed Method (Case Study 1B lane 1)

Anova: Single Factor (RMSE as Dependent Variable)						
SUMMARY						
Groups	*Count*	*Sum*	*Average*	*Variance*		
10 Percent	10	116.619606	11.66196	0.012007		
20 Percent	10	75.2566846	7.525668	0.017765		
30 Percent	10	23.3045209	2.330452	0.09956		
40 Percent	10	15.2924879	1.529249	0.003389		
ANOVA						
Source of Variation	*SS*	*df*	*MS*	*F*	*P-value*	*F crit*
Between Groups	676.1176492	3	225.3725	6792.345	1.33E-49	2.866266
Within Groups	1.194493531	36	0.03318			
Total	677.3121428	39				

Post Hoc Tests

Multiple Comparisons

RMSE
Tukey HSD

(I) Percent ofProbe	(J) Percent ofProbe	Mean Difference (I-J)	Std. Error	Sig.	95% Confidence Interval	
					Lower Bound	Upper Bound
10.00	20.00	4.13629*	.08146	.000	3.9169	4.3557
	30.00	9.33151*	.08146	.000	9.1121	9.5509
	40.00	10.13271*	.08146	.000	9.9133	10.3521
20.00	10.00	-4.13629*	.08146	.000	-4.3557	-3.9169
	30.00	5.19522*	.08146	.000	4.9758	5.4146
	40.00	5.99642*	.08146	.000	5.7770	6.2158
30.00	10.00	-9.33151*	.08146	.000	-9.5509	-9.1121
	20.00	-5.19522*	.08146	.000	-5.4146	-4.9758
	40.00	.80120*	.08146	.000	.5818	1.0206
40.00	10.00	-10.13271*	.08146	.000	-10.3521	-9.9133
	20.00	-5.99642*	.08146	.000	-6.2158	-5.7770
	30.00	-.80120*	.08146	.000	-1.0206	-.5818

*. The mean difference is significant at the 0.05 level.

Single Factor ANOVA For PROBE Based Proposed Method (Case Study 1B lane 2)

Anova: Single Factor: RMSE as dependent Variable						
SUMMARY						
Groups	*Count*	*Sum*	*Average*	*Variance*		
10 Percent	10	108.518	10.8518	0.013417		
20 Percent	10	69.0612	6.90612	0.005567		
30 Percent	10	24.61991	2.461991	0.038568		
40 Percent	10	13.90646	1.390646	0.007296		
ANOVA						
Source of Variation	*SS*	*df*	*MS*	*F*	*P-value*	*F crit*
Between Groups	566.9732	3	188.9911	11657.58	8.07E-54	2.866266
Within Groups	0.583627	36	0.016212			
Total	567.5568	39				

Post Hoc Tests

Multiple Comparisons

RMSE
Tukey HSD

(I) Percent ofProbe	(J) Percent ofProbe	Mean Difference (I-J)	Std. Error	Sig.	95% Confidence Interval	
					Lower Bound	Upper Bound
10.00	20.00	3.94568*	.05694	.000	3.7923	4.0990
	30.00	8.38981*	.05694	.000	8.2365	8.5432
	40.00	9.46116*	.05694	.000	9.3078	9.6145
20.00	10.00	-3.94568*	.05694	.000	-4.0990	-3.7923
	30.00	4.44413*	.05694	.000	4.2908	4.5975
	40.00	5.51547*	.05694	.000	5.3621	5.6688
30.00	10.00	-8.38981*	.05694	.000	-8.5432	-8.2365
	20.00	-4.44413*	.05694	.000	-4.5975	-4.2908
	40.00	1.07135*	.05694	.000	.9180	1.2247
40.00	10.00	-9.46116*	.05694	.000	-9.6145	-9.3078
	20.00	-5.51547*	.05694	.000	-5.6688	-5.3621
	30.00	-1.07135*	.05694	.000	-1.2247	-.9180

*. The mean difference is significant at the 0.05 level.

Appendix C

Case study 2a

Anova: Single Factor RMSE as dependent Variable						
SUMMARY						
Groups	*Count*	*Sum*	*Average*	*Variance*		
10	10	50.03066	5.003066	0.015455		
20	10	23.45479	2.345479	0.010055		
30	10	9.512136	0.951214	0.000949		
40	10	5.545864	0.554586	0.009407		
ANOVA						
Source of Variation	*SS*	*df*	*MS*	*F*	*P-value*	*F crit*
Between Groups	121.4446	3	40.48152	4514.735	2.04E-46	2.866266
Within Groups	0.322795	36	0.008967			
Total	121.7674	39				

Post Hoc Tests

Multiple Comparisons

RMSE
Tukey HSD

(I) Percent ofProbe	(J) Percent ofProbe	Mean Difference (I-J)	Std. Error	Sig.	95% Confidence Interval	
					Lower Bound	Upper Bound
10.00	20.00	2.65759*	.04235	.000	2.5435	2.7716
	30.00	4.05185*	.04235	.000	3.9378	4.1659
	40.00	4.44848*	.04235	.000	4.3344	4.5625
20.00	10.00	-2.65759*	.04235	.000	-2.7716	-2.5435
	30.00	1.39427*	.04235	.000	1.2802	1.5083
	40.00	1.79089*	.04235	.000	1.6768	1.9049
30.00	10.00	-4.05185*	.04235	.000	-4.1659	-3.9378
	20.00	-1.39427*	.04235	.000	-1.5083	-1.2802
	40.00	.39663*	.04235	.000	.2826	.5107
40.00	10.00	-4.44848*	.04235	.000	-4.5625	-4.3344
	20.00	-1.79089*	.04235	.000	-1.9049	-1.6768
	30.00	-.39663*	.04235	.000	-.5107	-.2826

*. The mean difference is significant at the 0.05 level.

Anova: Single Factor MAPE as Dependent Variable						
SUMMARY						
Groups	*Count*	*Sum*	*Average*	*Variance*		
10	10	74.37011	7.437011	0.005777		
20	10	45.96646	4.596646	0.032683		
30	10	19.08748	1.908748	0.011404		
40	10	10.32623	1.032623	0.016435		
ANOVA						
Source of Variation	*SS*	*df*	*MS*	*F*	*P-value*	*F crit*
Between Groups	250.8505	3	83.61684	5044.799	2.78E-47	2.866266
Within Groups	0.596695	36	0.016575			
Total	251.4472	39				

Post Hoc Tests

Multiple Comparisons

MAPE
Tukey HSD

(I) Percent ofProbe	(J) Percent ofProbe	Mean Difference (I-J)	Std. Error	Sig.	95% Confidence Interval	
					Lower Bound	Upper Bound
10.00	20.00	2.84036*	.05758	.000	2.6853	2.9954
	30.00	5.52826*	.05758	.000	5.3732	5.6833
	40.00	6.40439*	.05758	.000	6.2493	6.5595
20.00	10.00	-2.84036*	.05758	.000	-2.9954	-2.6853
	30.00	2.68790*	.05758	.000	2.5328	2.8430
	40.00	3.56402*	.05758	.000	3.4090	3.7191
30.00	10.00	-5.52826*	.05758	.000	-5.6833	-5.3732
	20.00	-2.68790*	.05758	.000	-2.8430	-2.5328
	40.00	.87612*	.05758	.000	.7211	1.0312
40.00	10.00	-6.40439*	.05758	.000	-6.5595	-6.2493
	20.00	-3.56402*	.05758	.000	-3.7191	-3.4090
	30.00	-.87612*	.05758	.000	-1.0312	-.7211

*. The mean difference is significant at the 0.05 level.

Appendix D

SINGLE FACTOR ANOVA FOR PROPOSED METHOD OF QUEUE ESTIMATION (CASE STUDY 2B)

Anova: Single Factor using RMSE						
SUMMARY						
Groups	*Count*	*Sum*	*Average*	*Variance*		
10 percent Probe	10	62.334	6.2334	0.021551		
20 percent Probe	10	43.21	4.321	0.008121		
30 percent Probe	10	11.99	1.199	0.009654		
40 percent Probe	10	5.117	0.5117	0.004324		
ANOVA						
Source of Variation	*SS*	*df*	*MS*	*F*	*P-value*	*F crit*
Between Groups	216.1758	3	72.05862	6603.2	2.21E-49	2.866266
Within Groups	0.392857	36	0.010913			
Total	216.5687	39				

Post Hoc Tests

Multiple Comparisons

RMSE
Tukey HSD

(I) Percent ofProbe	(J) Percent ofProbe	Mean Difference (I-J)	Std. Error	Sig.	95% Confidence Interval	
					Lower Bound	Upper Bound
10.00	20.00	1.91240*	.04672	.000	1.7866	2.0382
	30.00	5.03440*	.04672	.000	4.9086	5.1602
	40.00	5.72170*	.04672	.000	5.5959	5.8475
20.00	10.00	-1.91240*	.04672	.000	-2.0382	-1.7866
	30.00	3.12200*	.04672	.000	2.9962	3.2478
	40.00	3.80930*	.04672	.000	3.6835	3.9351
30.00	10.00	-5.03440*	.04672	.000	-5.1602	-4.9086
	20.00	-3.12200*	.04672	.000	-3.2478	-2.9962
	40.00	.68730*	.04672	.000	.5615	.8131
40.00	10.00	-5.72170*	.04672	.000	-5.8475	-5.5959
	20.00	-3.80930*	.04672	.000	-3.9351	-3.6835
	30.00	-.68730*	.04672	.000	-.8131	-.5615

*. The mean difference is significant at the 0.05 level.

Anova: Single Factor using MAPE						
SUMMARY						
Groups	*Count*	*Sum*	*Average*	*Variance*		
10 percent Probe	10	134.01	13.401	0.027321		
20 percent Probe	10	111.17	11.117	0.003468		
30 percent Probe	10	34.62	3.462	0.000818		
40 percent Probe	10	13.016	1.3016	0.023101		
ANOVA						
Source of Variation	*SS*	*df*	*MS*	*F*	*P-value*	*F crit*
Between Groups	1025.011	3	341.6702	24981.45	8.98E-60 <.05	2.866266
Within Groups	0.49237	36	0.013677			
Total	1025.503	39				

Post Hoc Tests

Multiple Comparisons

RMSE
Tukey HSD

(I) Percent ofProbe	(J) Percent ofProbe	Mean Difference (I-J)	Std. Error	Sig.	95% Confidence Interval	
					Lower Bound	Upper Bound
10.00	20.00	2.28400*	.05230	.000	2.1431	2.4249
	30.00	9.93900*	.05230	.000	9.7981	10.0799
	40.00	12.09940*	.05230	.000	11.9585	12.2403
20.00	10.00	-2.28400*	.05230	.000	-2.4249	-2.1431
	30.00	7.65500*	.05230	.000	7.5141	7.7959
	40.00	9.81540*	.05230	.000	9.6745	9.9563
30.00	10.00	-9.93900*	.05230	.000	-10.0799	-9.7981
	20.00	-7.65500*	.05230	.000	-7.7959	-7.5141
	40.00	2.16040*	.05230	.000	2.0195	2.3013
40.00	10.00	-12.09940*	.05230	.000	-12.2403	-11.9585
	20.00	-9.81540*	.05230	.000	-9.9563	-9.6745
	30.00	-2.16040*	.05230	.000	-2.3013	-2.0195

*. The mean difference is significant at the 0.05 level.